Труды Москов. Матем. Общ.
Том 66 (2005)

Trans. Moscow Math. Soc.
2005, Pages 1–83
S 0077-1554(05)00148-2
Article electronically published on October 28, 2005

COMBINATORIAL COMPUTATION OF COMBINATORIAL FORMULAS FOR KNOT INVARIANTS

V. A. VASSILIEV

Abstract. We construct a homology algebraic algorithm for computing combinatorial formulas of all finite degree knot invariants. Its input is an arbitrary *weight system*, i.e., a virtual principal part of a finite degree invariant, and the output is either a proof of the fact that this weight system actually does not correspond to any knot invariant or an effective description of some invariant with this principal part, i.e., a finite collection of easily described singular chains of full dimension in the space of spatial curves such that the value of this invariant on any generic knot is equal to the sum of multiplicities of these chains in a neighborhood of the knot. (In examples calculated by now, the former possibility never occurred.) This algorithm is formally realized over $\mathbb{Z}_2$, but its generalization to the case of arbitrary coefficients is just a technical task. The algorithm is based on the study of a complex of chains in the space of smooth curves in the three-dimensional space with a fixed flag of directions, and also in the discriminant variety of this space of curves.

Introduction

Informally, a combinatorial formula for a knot invariant is a prescription of how to compute the value of the invariant looking at the diagram of the knot in general position and counting (with appropriate coefficients) the configurations of its singular (in an appropriate sense) points. We give a formal definition of a combinatorial formula and consider such formulas for *knot invariants of finite degree* described in [17], [3], [2]. The best known formulas for these invariants are Polyak–Viro arrow diagrams [15], counting for only crossing points of the knot diagram. Any invariant given by Polyak–Viro formulas has a finite degree; by the Goussarov theorem [8] the converse also is true: any finite degree invariant can be expressed by such a formula. There exist also some other combinatorial formulas for some invariants, in particular the ones described in [12], [4], and in the present work (see also [24], [27]).

All previously known algorithms, allowing one to find explicit expressions of all finite degree invariants on any given knot, include drawing the pictures (diagrams of knots and singular knots) and deforming these pictures. Below we propose a *completely combinatorial* algorithm, i.e., one dealing not with planar or spatial pictures but with easily encodable combinatorial objects similar to the chord diagrams. The execution of the algorithm is a chain of linear algebraic operations over these objects, similar to checking the homological 4T- and 1T-conditions (see [17, 2, 3]) for a sum of chord diagrams. In particular, the complexity of this calculation and of its answers can be estimated in terms

2000 *Mathematics Subject Classification.* Primary 57M27, 57M25.

Key words and phrases. Knot, invariant, combinatorial formula, discriminant, combinatorial algorithm, spectral sequence, subalgebraic chain, simplicial resolution.

Supported in part by grants RFBR-01-01-00660, INTAS–00-0259, grant 1972.2003.01 of President of Russia, and Program "Contemporary Mathematics" of the Mathematical division of Russian Ac. Sci.

of the degree of our invariant only, and not of the complexity of arising knot diagrams. Therefore the algorithm is ready for efficient computer realization.

Starting from a proper *weight system* of rank k, i.e., the principal part of a knot invariant of degree k, the algorithm produces a finite collection of subalgebraic chains of full dimension in the space of knots, any of which is defined by at most k standard conditions on the geometrical disposition of knots, so that the value of our invariant on an arbitrary generic knot in $\mathbb{R}^3$ is equal to the multiplicity of the sum of these chains at this knot. This algorithm is based on the study of a complex of chains defined by similar conditions in the resolved *discriminant* space consisting of singular spatial curves; cf. [23].

We demonstrate the work of the algorithm on the simplest knot invariants of degrees 2 and 3, reduced mod 2.

This work is a continuation of [24] but can be read independently. In [24], a general geometrical approach to the construction of combinatorial formulas of cohomology classes of spaces of knots in $\mathbb{R}^n$, $n \geq 3$, was proposed. Here we show in detail how it works in the most classical and well-studied case of zero-dimensional classes, i.e., of invariants of knots in $\mathbb{R}^3$.

Probably the proof of the Goussarov theorem on the realization of invariants by the Polyak–Viro formulas implies an algorithmic method of computing such formulas. The algorithm described below is by now, from several points of view, worse than the one arising from this approach. Namely,

a) it is realized over $\mathbb{Z}_2$ only, i.e., without accounting for orientations of arising singular chains;
b) the answers are not so uniform, containing some terms other than just the Polyak-Viro diagrams;
c) the main advantage, the possibility of an efficient computerization, is not yet realized.

This list is in fact a program of the further work. An extension to the case of integer coefficients is just a technical problem. We need only to choose the (co)orientations of all basic chains of which our combinatorial formulas consist (these chains are described in §2) and to calculate their incidence indices; cf. §3.3 in [17]. These indices always are equal to 0, 1 or -1; therefore all the results of §3 of the present work (where we describe the differentials of our complexes) and §4 (where the main algorithm is described and justified) will become true over the integers if we put proper signs $\pm$ in their formulas.

The inconvenience b) can be explained by the fact that our approach provides too many ways to span the cycles homologous to zero by semialgebraic varieties in the space of curves; see e.g. §4.2 below. I do not select the most economical ways, and use the one having the simplest formulation but not causing the simplest calculations. For this reason the existing algorithm is called *direct*. For example, in §5 we show how this algorithm calculates a combinatorial formula for the simplest invariant (of degree two). This formula consists of three terms

(1)

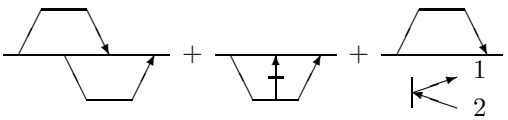

Namely, this formula says that the value of this invariant on an arbitrary generic *long knot* (i.e., embedding $f : \mathbb{R}^1 \hookrightarrow \mathbb{R}^3$ coinciding with a standard one outside some compact) is equal (mod 2) to the sum of three numbers:

a) the number of configurations $(a < b < c < d) \subset \mathbb{R}^1$ such that $f(c)$ is above $f(a)$ in $\mathbb{R}^3$ and $f(d)$ is above $f(b)$;

b) the number of configurations ($a < b < c$) such that $f(c)$ is above $f(a)$ and the projection of $f(b)$ to $\mathbb{R}^2$ lies to the east from the (common) projection of $f(a)$ and $f(c)$;

c) the number of configurations ($a < b$) such that $f(b)$ is above $f(a)$ and the direction "to the east" in $\mathbb{R}^2$ is a linear combination of projections of derivatives $f'(a)$ and $f'(b)$, such that the first of these projections participates in this linear combination with a positive coefficient, and the second with a negative one.

Almost the same algorithm with one nontrivial switch (which is easy for the human eye but is not formalized yet) gives the Polyak-Viro formula consisting of one term; see §2 in [24] and Figure 5. One of the first problems is to make the existing algorithm not so direct, i.e., to teach it to select the most economical choices. On the other hand, the multitude of choices provides many comparison results on the combinatorial formulas such as those in [16]. In §7, I describe one other algorithm referring to both our homological techniques and Goussarov's theorem. It has a slightly simpler formulation and simpler results (exactly the Polyak–Viro formulas); however, the systems of linear equations to be solved in its execution are exponentially greater (over the degree of the invariant). Also, I do not see how it could be extended to the calculation of other cohomology classes of spaces of knots, cf. [24].

I invite the volunteers acquainted with the mathematical programming to solve problem c). I hope that a computer itself will then find some ways to make best choices in problem b), so that it will remain to systematize its experience.

This work is only a step in the general program of realizing arbitrary-dimensional cohomology classes in spaces of knots; cf. [24] (which, in its turn, is just a sample of a wide class of similar problems concerning efficient methods in the topology of spaces of nonsingular objects).

Like in [24], our algorithm is based on the study of the *discriminant subvariety* Σ in the space $\mathcal{K}$ of smooth parametrized curves $f : \mathbb{R}^1 \to \mathbb{R}^3$ with a fixed behavior at infinity (i.e., of the set of maps $f \in \mathcal{K}$ that are not smooth embeddings). The main tool is the *simplicial resolution* of the discriminant, i.e., a certain topological space σ together with a continuous surjective map $\pi : \sigma \to \Sigma$. Homology groups of Σ and σ are closely related to each other and to the cohomology groups of the space of knots $\mathcal{K} \setminus \Sigma$. The resolved discriminant σ admits a natural filtration $\sigma_1 \subset \sigma_2 \subset \dots$ which generates a spectral sequence calculating its homology groups.

As in [24], the algorithm is essentially a direct calculation of this spectral sequence in terms of relative chains.[1] We start from a *weight system* of rank k, i.e., from a relative cycle γ in the term σ_k reduced modulo σ_{k-1} represented as a sum of open cells of maximal dimension in $\sigma_k \setminus \sigma_{k-1}$. (Such cells are in a one-to-one correspondence with *equivalence classes of k-chord diagrams*; see [20], [2], and §1 below.) Then we calculate its first boundary $d^1(\gamma) \subset \sigma_{k-1} \setminus \sigma_{k-2}$ and *span* it there, i.e., we construct a chain $\gamma_1 \subset \sigma_{k-1} \setminus \sigma_{k-2}$ such that $\partial\gamma_1 = -d^1(\gamma)$ in $\sigma_{k-1} \setminus \sigma_{k-2}$. Then we define $d^2(\gamma)$ as the boundary of the chain $\gamma + \gamma_1$ in $\sigma_{k-2} \setminus \sigma_{k-3}$, span it by a chain $\gamma_2 \subset \sigma_{k-2} \setminus \sigma_{k-3}$, etc. If the initial weight system is that of some knot invariant, then the entire sequence of operations can be accomplished, and we get a cycle $\gamma + \gamma_1 + \dots + \gamma_{k-1}$ defining an absolute cycle in the one-point compactification of the resolved discriminant σ. Pushing it down, we get a semialgebraic cycle in the nonresolved discriminant Σ. Finally we span this cycle by a relative cycle (mod Σ) in the whole space of curves $\mathcal{K}$: tautologically,

[1] By the calculation of a homological spectral sequence one usually means the calculation of its isomorphism class, including the existence theorem claiming that any element of the calculated group $E^\infty_{p,q}$ can be extended to a cycle with this principal part. The proof of this theorem usually is implicit and follows from the vanishing of all the homological obstructions to such an extension. By the *direct* calculation I mean an explicit step-by-step construction of such cycles.

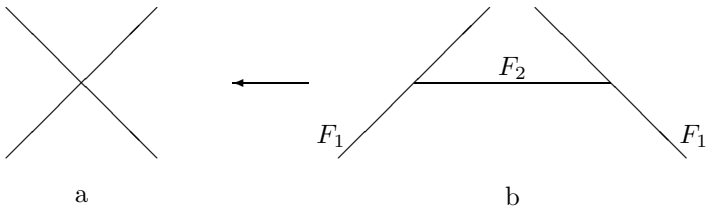

FIGURE 1. Resolution of the cross

this relative cycle is the desired combinatorial formula. In [24] this method was used to realize certain positive-dimensional cohomology classes of spaces of knots.

This theory has a deep analogy with the homological study of affine plane arrangements (i.e., of finite collections of affine planes in Euclidean spaces), especially with the explicit realization of their homology classes proposed in [28]. For more on this analogy see [25], [26]. Let us consider an example.

Similarly to the knot theory, the most convenient way of calculating homology groups of plane arrangements is based on the method of simplicial resolutions. This method is a continuous analog of the combinatorial formula of inclusions and exclusions.

Our main example is the line arrangement $\mathbf{X} \subset \mathbb{R}^2$ consisting of two crossing lines; see Figure 1a. Suppose that we need to calculate its *Borel–Moore homology group* $\bar{H}_*(\mathbf{X})$, i.e., the homology group of its one-point compactification $\bar{\mathbf{X}}$ reduced modulo the added point (or, which is here the same, the homology group of the complex of locally finite chains of $\mathbf{X}$). This group is related by Alexander duality to the usual (reduced modulo a point) cohomology group of the complementary space:

$$\bar{H}_i(\mathbf{X}) \sim \tilde{H}^{N-i-1}(\mathbb{R}^N \setminus \mathbf{X})$$

(in our case $N = 2$). The simplicial resolution of $\mathbf{X}$ is shown in Figure 1b. Namely, we first take two lines forming $\mathbf{X}$ separately, and then join by a segment their points arising from the intersection point. The resulting space $\mathbf{X}!$ admits a natural proper projection to $\mathbf{X}$ defining an isomorphism of Borel–Moore homology groups of these spaces (and moreover extending to a homotopy equivalence of their one-point compactifications). This space $\mathbf{X}!$ admits a natural increasing filtration: its term F_1 consists of two divorced lines, and F_2 coincides with all of $\mathbf{X}!$.

In the case of an arbitrary arrangement Ψ in $\mathbb{R}^N$ we also take first all planes forming it separately, and then insert simplices spanning their common points in such a way that the resulting space $\Psi!$ admits a proper projection to Ψ with contractible (although maybe different) fibers. There are several different constructions of this simplicial resolution; see e.g. [28], [19], [26]. We use the one defined in terms of the *order complex* of our arrangement. For its definition; see §1.2. The resulting resolved space $\Psi!$ always admits a natural increasing filtration of length $\leq N - 1$: its ith term is the union of all *proper preimages* under the projection $\Psi! \to \Psi$ of all intersection planes of our arrangement having codimension $\leq i$ in $\mathbb{R}^N$.

In the case of the arrangement $\mathbf{X}$ shown in Figure 1, the corresponding spectral sequence calculating the Borel–Moore homology group is as follows: its unique two nonzero terms

$$E^1_{p,q} \simeq \bar{H}_{p+q}(F_p \setminus F_{p-1})$$

are $E^1_{1,0} \sim \bar{H}_1(F_1) \cong \mathbb{Z}^2$ and $E^1_{2,-1} \sim \bar{H}_1(F_2 \setminus F_1) \cong \mathbb{Z}$. The reduced cohomology classes of $\mathbb{R}^2 \setminus \mathbf{X}$ of degree (= filtration) one are exactly the linear combinations of linking numbers with either of two lines forming $\mathbf{X}$.

In particular we see that the homological spectral sequence calculating the group $\bar{H}_*(\mathbf{X})$ stabilizes at the first term, and we have

$$\bar{H}_i(\mathbf{X}) \equiv \bar{H}_i(\mathbf{X}!) \cong E^1_{1,i-1} \oplus E^1_{2,i-2}. \tag{2}$$

The similar stabilization in the first term is a general fact taking place for arbitrary affine plane arrangements. Moreover, there is the *homotopy splitting* formula [28], [19]: the one-point compactification of any finite collection of affine planes in $\mathbb{R}^N$ is homotopy equivalent to the wedge of one-point compactifications of spaces $F_k \setminus F_{k-1}$ of the natural filtration of the simplicial resolution of this plane arrangement. The homological version of this splitting coincides with the Goresky-MacPherson formula [7] for the cohomology of the complement of a plane arrangement.

Denote by A the relative cycle in the resolved cross $\mathbf{X}!$ generating the group $E^1_{2,-1} \equiv \bar{H}_1(F_2 \setminus F_1)$, i.e., just the fundamental class of the horizontal interval in Figure 1b. Although we have the splitting (2) for the group

$$\bar{H}_1(\mathbf{X}) \cong \tilde{H}^0(\mathbb{R}^2 \setminus \mathbf{X}),$$

this cycle A itself does not define any cohomology class and cannot take values on the 0-cycles in $\mathbb{R}^2 \setminus \mathbf{X}$. The formula (2) says only that this relative cycle *can be* extended to a Borel–Moore cycle in all of $\mathbf{X}$, which will then define such a cohomology class. However, in order to define well such a cohomology class, we need to construct such an extension explicitly.

To do this, we first consider the boundary of this relative cycle in F_1; it consists of two points. Formula (2) tells us that this boundary can be *spanned* in F_1, i.e., represented as the boundary of a locally finite chain in F_1. We need to choose such a chain A_1,. Then the difference $A - A_1$ will be a cycle in all of $\mathbf{X}!$. Further, we take the direct image of this cycle in $\mathbf{X}$ and choose a relative cycle in the pair $(\mathbb{R}^2, \mathbf{X})$ spanning this cycle in $\mathbb{R}^2$. This relative cycle already can take values on particular points of the space $\mathbb{R}^2 \setminus \mathbf{X}$, defining thus a "combinatorial formula". In the case of an arbitrary plane arrangement in $\mathbb{R}^N$ we need to do the same, but with more steps. Given an element of the group $E^1_{p,q}$, we first choose a locally finite cycle A in F_p mod F_{p-1} realizing it, then consider its boundary $d^1(A)$ in $F_{p-1} \setminus F_{p-2}$, span it there by a chain A_1, consider the boundary $d^2(A)$ of the cycle $A + A_1$ in $F_{p-2} \setminus F_{p-3}$, etc.

In the case of plane arrangements in $\mathbb{R}^N$, there is an obvious way to make all these choices. Indeed, let us choose an arbitrary constant vector field in $\mathbb{R}^N$ generic with respect to our arrangement. It is convenient to imagine it as the gradient of a generic linear function ℓ. Any term $F_i \setminus F_{i-1}$ of the standard filtration of the resolution splits into the disjoint union of direct products of certain planes $L_I \subset \mathbb{R}^N$ of dimension $N - i$ and appropriate simplicial complexes arising in the construction of the resolution. We always can span any cycle $d^k(A)$ in these components of $F_i \setminus F_{i-1}$ by the union of rays issuing from the points of this cycle, and such that their projections to corresponding planes L_I coincide with trajectories of gradients of restrictions of the function ℓ to these planes, while projections to simplicial objects are constant. The genericity condition implies that these rays are always transversal to these spanned cycles.

In particular, for the arrangement $\mathbf{X}$ this procedure is shown in Figure 2. We assume that the vector field is directed down. In the left-hand top picture we distinguish by a thick line only the initial relative cycle $A \subset F_2 \setminus F_1$; in the right-hand top picture we distinguish additionally the segments in F_1 spanning the boundary of this cycle; in the right-hand bottom picture we see the projection of the resulting cycle to $\mathbf{X}$, and in the left-hand bottom picture we shadow the chain spanning this cycle in $\mathbb{R}^2$ and swept out by the trajectories of our vector field issuing from the points of this cycle.

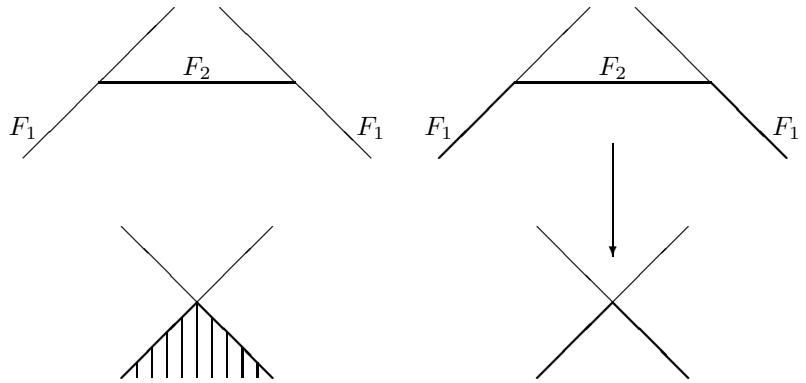

FIGURE 2. "Combinatorial formula" for the degree 2 cohomology class

Of course, another choice of the direction in $\mathbb{R}^N$ will give a different relative cycle ("combinatorial formula"); however, the difference of these cycles will have a strictly lower filtration. For illustration, it is useful to make a similar construction in Figure 2 based on some other direction in $\mathbb{R}^2$, say on the direction to the left or up, and to compare the obtained combinatorial formula with the previous one.

In fact, in the case of plane arrangements it is not necessary to accomplish all steps of this calculation, because its result can be guessed from the very beginning: it is the realization of the Goresky–MacPherson formula given in [28]. Our algorithm is an analog of this calculation in the more complicated case of knot spaces, when such a prediction is probably impossible.

The simplicial resolution of the discriminant set Σ in the space $\mathcal{K}$ of parametric curves $f : \mathbb{R}^1 \to \mathbb{R}^n$ (with fixed behavior at infinity) can be constructed in precisely the same way. First we take the *tautological normalization* of Σ, i.e., the total space of the affine bundle, whose base is the configuration space $\overline{B(\mathbb{R}^1, 2)}$ of all unordered pairs of points $a, b \in \mathbb{R}^1$, and the fiber over such a point (a, b) is the affine subspace $L(a, b) \subset \mathcal{K}$ consisting of all maps $f : \mathbb{R}^1 \to \mathbb{R}^n$ such that $f(a) = f(b)$ if $a \neq b$ or $f'(a) = 0$ if $a = b$. This space is supplied with the obvious projection onto Σ and is the natural analog of the "union of lines taken separately", i.e., the set F_1 in Figure 1b. However such spaces $L(a, b)$ with different pairs (a, b) intersect in $\mathcal{K}$; therefore we need to span their corresponding points by segments, triangles, etc. in such a way that the resulting space σ admits a natural projection onto Σ, all of whose fibers are contractible.

The exact construction of this space σ can be formulated in terms of the (naturally topologized) order complex of the space of all affine subspaces in $\mathcal{K}$ equal to intersections of several spaces of type $L(a, b)$. It also admits a natural increasing filtration $\sigma_1 \subset \sigma_2 \subset \cdots$, whose first term coincides with the tautological normalization and the common term σ_i is the union of proper preimages of all planes $L(a_1, b_1) \cap L(a_2, b_2) \cap \cdots$ of codimensions $\leq ni$.

The resulting space σ is very similar to Σ. If $n > 3$, then their Borel–Moore homology groups of finite codimension are well-defined and isomorphic to each other (and are Alexander dual to the cohomology group of the space of knots). If $n = 3$, then the situation is more complicated. A priori only a part of Borel–Moore homology classes of finite codimension of Σ (= cohomology classes of the space of knots in $\mathbb{R}^3$) can be represented by images of cycles from σ. These are exactly the *finite degree* cohomology classes; their *degrees* (or *orders*) are defined by our filtration in σ. However this subgroup

is quite ample: at this time, no free homology class of the space of knots in $\mathbb{R}^3$ is known on which all the finite degree cohomology classes vanish.

The first term of the filtration, σ_1, is homologically trivial: it is the total space of an affine bundle over the half-plane $\mathbb{R}^2/\{(a,b)=(b,a)\}$, whose fiber is an affine subspace of codimension n in $\mathcal{K}$. Therefore $\bar{H}_*(\sigma_1)\equiv 0$, and the first column $E^r_{1,q}$ of the related spectral sequence identically vanishes. It is convenient to split the space σ_1 into two cells: one is the affine bundle over the open half-plane $\{(a<b)\}$, and the second is equal to its boundary and is fibered over the diagonal line $\{(a,a)\}$. Similar natural decompositions into open cells exist for all terms $\sigma_i\setminus\sigma_{i-1}$ of our spectral sequence.

Furthermore, easy calculations show that the second column $E^1_{2,q}\equiv\bar{H}_{2+q}(\sigma_2\setminus\sigma_1)$ contains a unique nontrivial term which is isomorphic to $\mathbb{Z}$ and is generated by the space of a fiber bundle over a 4-dimensional open cell with fiber equal to the product of an open interval and an affine subspace of codimension $2n$ in $\mathcal{K}$. For dimensional reasons, this column survives up to E^∞; moreover, the corresponding cycles survive the projection $\sigma\to\Sigma$ and form a subgroup isomorphic to $\mathbb{Z}$ in the Borel–Moore homology group of codimension $2n-5$ of Σ. By the Alexander duality this means that the unique nontrivial group of cohomology classes of degree 2 of the space of long knots lies in dimension $2n-6$ and is isomorphic to $\mathbb{Z}$; for $n=3$ it is generated by the Casson knot invariant v_2.

We shall discuss a combinatorial formula for this basic class v_2 in analogy with the above-considered class A generating the group of degree 2 Borel–Moore homology classes of the line arrangement from Figure 1 reduced modulo the group of classes of degree 1. For simplicity, we give all calculations mod 2 only, i.e., without accounting for orientations of chains.

The principal part of the class v_2 is the cycle generating the group $\bar{H}_*(\sigma_2\setminus\sigma_1)$. This cycle in $\sigma_2\setminus\sigma_1$ is swept out by the triples of the form

$$\big((a_1<a_2<b_1<b_2)\subset\mathbb{R}^1, f, t\big)\,, \tag{3}$$

where $f\in\mathcal{K}$ is a map $\mathbb{R}^1\to\mathbb{R}^n$ such that $f(a_1)=f(b_1)$, $f(a_2)=f(b_2)$, and $t\in(-1,1)$ is the parameter along an inserted interval arising in the construction of the simplicial resolution and analogous to the horizontal interval in Figure 1b. The endpoints of any such interval lie in the bigger cell $\breve{\sigma}_1$ of the term σ_1, i.e., in the space of pairs

$$\big((a<b)\subset\mathbb{R}^1, f\big) \tag{4}$$

such that $f(a)=f(b)$. Namely, these endpoints sweep out the subset in this cell $\breve{\sigma}_1$, consisting of all points (4) such that additionally $f(a')=f(b')$ for some pair of points $a'<b'\in\mathbb{R}^1$ where

$$\text{either}\quad a'<a<b'<b \tag{5}$$

$$\text{or}\quad a<a'<b<b'. \tag{6}$$

Our basic cycle (3) in $\sigma_2\setminus\sigma_1$ is naturally depicted by the "chord diagram"

(7) 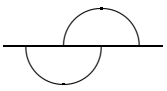

which indicates the mutual disposition of possible pairs of points (a_i,b_i) glued together by the maps f participating in its definition.

Two summands of its boundary in σ_1 corresponding to two possible dispositions (5) and (6) will be denoted respectively by two parts of the expression

(8) 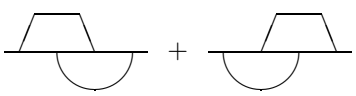

These two summands are analogues of the two endpoints of the horizontal segment in Figure 1b.

Let us span this boundary by a chain in the cell $\breve{\sigma}_1$. Recall that the first summand in (8) is the union of all points $((a,b),f) \in \sigma_1$ such that additionally there exist two points a', b' with $a' < a < b' < b$ such that $f(a') = f(b')$.

It is natural to try to span this chain in $\breve{\sigma}_1$ by (i.e., to represent it as a piece of the boundary of) the set of points $((a,b),f)$ satisfying all the same conditions, but with the equality $f(a') = f(b')$ replaced by the condition that the projections of $f(a')$ and $f(b')$ to the "blackboard plane" $\mathbb{R}^2$ coincide, and the projection of $f(a')$ to its orthogonal line lies below the projection of $f(b')$.

The latter condition is depicted by the "broken arrow" as in the left-hand side of (9).

In a similar way, we try to span the second summand in (8) by the variety depicted in the left-hand side of (10).

Unfortunately, these two varieties have additional pieces of boundary, so that their sum does not span the entire chain (8). These pieces correspond to possible degenerations of the configurations of four points a, b, a' and b' participating in the definition of these varieties.

Namely, the full boundaries of these two varieties are described by the right-hand sides of (9) and (10). Let us analyze for instance the first of them:

(9)

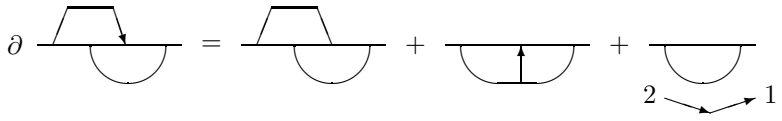

(10)

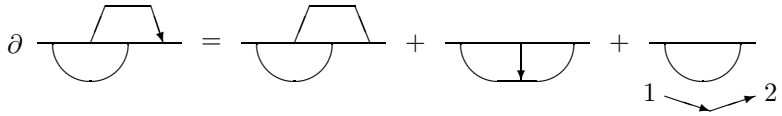

The second summand in its right-hand side appears when the first point a' and the second point a participating in the definition of our variety coincide. It consists of all points $((a,b),f) \in \sigma_1$ such that there is a point $c \in (a,b)$ such that $f(c)$ lies above $f(a) = f(b)$ in $\mathbb{R}^3$.

In fact, this formula should have two summands more, arising when the third point b' tends to either a or b. However, these two summands coincide since $f(a) = f(b)$ and cancel each other. (This cancellation happens also in the similar integral homology calculation: these two summands appear in the integral boundary of our variety with opposite orientations.)

Finally, the last summand arises when a' tends to a and simultaneously b' tends to b. The spatial picture of the corresponding degeneration is shown in Figure 3a. The labeled arrows in the notation of this summand express the following condition: the projections to the blackboard plane $\mathbb{R}^2$ of derivatives of the knot at the points $a < b$ are co-directed there, but the direction of $f'(a)$ in $\mathbb{R}^3$ goes "above" that of $f'(b)$. The second formula (10) can be analyzed in exactly the same way.

We obtain that the cycle (8) is homologous in $\breve{\sigma}_1$ to the sum of the second and third summands of the right-hand sides of formulas (9) and (10). The sum of these second (respectively, third) summands can be depicted by the first (respectively, the second) summand in the next formula:

(11)

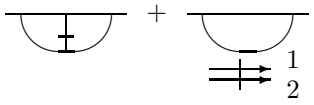

By definition, the first summand in (11) consists of points $((a,b),f) \in \breve{\sigma}_1$ which, in addition to the usual condition $f(a) = f(b)$, satisfy the following one: there is a point

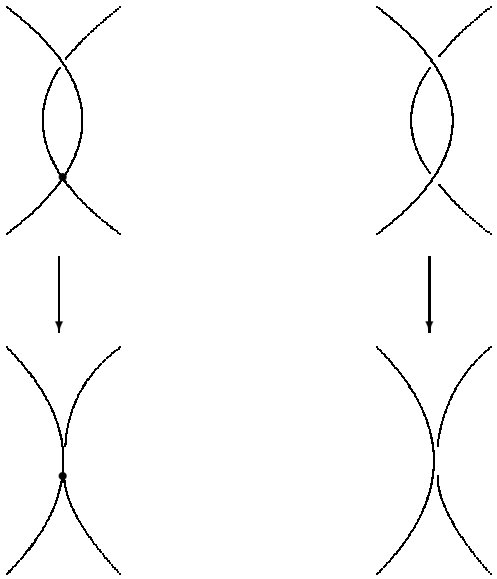

FIGURE 3. Some standard degenerations of singular knot diagrams

$c \in (a, b)$ such that the projection of $f(c)$ to the blackboard plane coincides with that of the point $f(a) \equiv f(b)$. The additional condition expressed by two crossed arrows under the second summand in (11) says that projections to the blackboard plane of the derivatives $f'(a)$ and $f'(b)$ should be co-directed.

So, the sum of varieties in the left-hand sides of formulas (9) and (10) provides the homology between the cycles (8) and (11), and we need to find a zero-homology of the latter cycle. This cycle is simpler than the initial one: it consists of two varieties, each of which is defined by certain conditions on the behavior of the map f at 3 or 2 points of $\mathbb{R}^1$, while for both summands of the initial cycle (8) the number of such "active" points was equal to 4. This situation occurs systematically. At any step of the algorithm we need to span a cycle consisting of several varieties, any of which is defined by certain conditions on the behavior of f at several points. At least one of these conditions should be an equality-type condition distinguishing a subset of codimension one (e.g., a self-intersection of $f(\mathbb{R}^1)$ in $\mathbb{R}^3$, self-tangency or triple self-intersection of the projection of $f(\mathbb{R}^1)$ to $\mathbb{R}^2$, etc.). Then we try to span such a variety by a similar variety in whose definition this equality is replaced by the inequality relating the same quantities. The latter variety usually has additional pieces of boundary, but these pieces appear at degenerations of the configurations of active points, hence are simpler than the initial cycle. By induction on the number of active points, the algorithm necessarily terminates.

The algorithm inventory thus includes a list of varieties (*subalgebraic chains*) of full dimension in the space of curves and in the resolution of its discriminant, of which all our spanning chains can consist, plus the list of all irreducible varieties of codimension 1, of which the boundaries of the previous chains consist. These varieties are listed in §2 below. All the same holds for the similar (not written yet) algorithm over the integers, which will differ from the existing mod 2 one by defining coorientations of all

these varieties and calculating their incidence coefficients. The similar inventory for the algorithmic calculation of combinatorial formulas for r-dimensional cohomology classes should include similar lists of varieties of codimensions r and $r+1$; thus these algorithms will be more complicated.

Let us apply this process to the cycle (11). We replace the equality-type condition distinguishing its first summand, i.e., the condition "there is a point $c \in (a,b)$ such that the projections of $f(c)$ and $f(a) \equiv f(b)$ to $\mathbb{R}^2$ coincide" by the inequality-type condition: "there is a point $c \in (a,b)$ such that the projection of $f(c)$ to $\mathbb{R}^2$ lies *to the east* of the projection of $f(a) = f(b)$". This condition is depicted by the once crossed arrow as in the left-hand side of (12).

Also we replace the equality-type condition distinguishing the second summand of (11), i.e., the condition "projections of vectors $f'(a)$ and $f'(b)$ to $\mathbb{R}^2$ are co-directed" by the inequality type condition: "the chosen direction "to the east" in $\mathbb{R}^2$ lies in the angle between the projections of the two vectors $f'(a)$ and $-f'(b)$". The latter condition is expressed by the subscript under the left-hand side of (13):

(12)

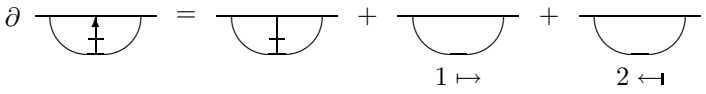

(13)

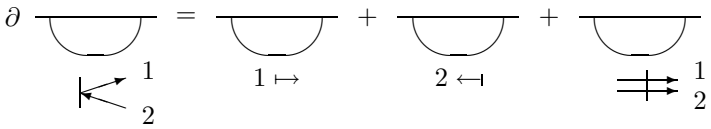

Again, the chains shown in the left-hand sides of equalities (12), (13) have some additional pieces of boundary described in the right-hand sides of these equalities. For instance, the condition $1 \mapsto$ means that the projection to $\mathbb{R}^2$ of the derivative f' at the first active point is directed to the east. The complexities of these additional terms are lower than those of terms which we try to span. For instance, the homology given by the formula (13) does not reduce the number of all active points of its very right-hand picture (i.e., the second picture in (11)), but it replaces a condition involving two such points (expressed by the subscript under this picture) by conditions involving only one point each; thus the complexity of the chain again decreases.

These additional summands in the right-hand sides of equalities (12), (13) cancel each other; therefore the sum of all their summands is equal to the cycle (11). The same will necessarily hold also in the similar calculation over the integers (with proper signs before all participating terms) because of the homological conditions: all right-hand sides of our equations and also the cycle which we are going to kill have no boundaries.

We obtain that the desired chain spanning the cycle (8) in $\breve{\sigma}_1$ is equal to the sum of four varieties indicated in the left-hand sides of equations (9), (10), (12), and (13). This sum establishes a homology between the cycle (8) and some cycle in the smaller cell of σ_1. By dimensional reasons, the latter cycle can be equal only to the fundamental cycle of the latter cell taken with some coefficient. Also, it is easy to see that the boundary positions of our four varieties form subvarieties of positive codimension in this cell. Therefore this coefficient is equal to zero, and the sum of our four varieties forms a zero-homology of the cycle (8) in all of σ_1; this sum together with the initial relative cycle (7) forms the cycle in σ_2 generating its group $\bar{H}_*(\sigma_2)$.

Remark 1. In the previous paragraph we have avoided successfully the unique dangerous instant in the integration of weight systems, i.e., the instant when the integration procedure can fail and prove that there is no knot invariant corresponding to our initial weight system γ. Namely, if the degree of γ is equal to k, then the (successful) algorithm

consists of k steps. Its initial data is the Borel–Moore cycle of maximal dimension in $\sigma_k \setminus \sigma_{k-1}$ encoded by γ. At the rth step, the algorithm considers (a geometric realization of) the rth differential $d^r(\gamma)$, which is a Borel–Moore cycle of codimension 1 in $\sigma_{k-r} \setminus \sigma_{k-r-1}$, and tries to span it there, i.e., to represent it as the boundary of a subalgebraic chain of maximal dimension. If this works, then the boundary of this spanning chain in $\sigma_{k-r-1} \setminus \sigma_{k-r-2}$ is the initial data $d^{r+1}(\gamma)$ for the next step.

At any such step, our algorithm has no problem establishing a homology between $d^r(\gamma)$ and a cycle in the union of vice-maximal cells; the latter cycle can be only a linear combination of these cells. If the homology class of this cycle is equal to zero, i.e., the cycle is equal to the boundary of a linear combination of maximal cells, then we subtract this linear combination from the above homology and obtain the desired zero-homology of $d^r(\gamma)$. However, if this homology class is not equal to zero, then we obtain an obstruction to the integration. (By the Kontsevich theorem, this is impossible over the rational numbers, but the obstruction can be a torsion element and thus prevent the integration over the integers.) In principle, it can happen that this obstruction is not fatal: if exactly the same nontrivial homology class arose previously as an obstruction to the integration of a weight system γ' of a lower degree, then the difference of chains obtained in these calculations for γ and γ' is a relative cycle in $(\sigma_k, \sigma_{k-r-1})$ which can be integrated at least one step further; however, the system γ' will remain an example of a nonintegrable system.

Fortunately, in all known examples all these obstructions are trivial; thus it remains to formulate the corresponding general conjecture. In fact, in all these examples the triviality of the obstruction follows from the fact that the boundary positions of our homologies (spanning the cycles $d^r(\gamma)$ in maximal cells of $\sigma_{k-r} \setminus \sigma_{k-r-1}$) form subvarieties of positive codimensions in the vice-maximal cells; thus the homological boundaries of these homologies in the union of the latter cells are not only homologous but even equal to zero. A stronger conjecture says that this also is a general situation.

Now we go to the last step of the algorithm and consider the projection of the obtained cycle from σ to Σ. The projection of its part (7) is of codimension 2 and does not participate in cycles of codimension 1 responsible for knot invariants. On the other hand, the projections to Σ of four chains in σ_1 found previously (i.e., the left-hand sides of (9), (10), (12) and (13)) are depicted by four summands of the following formula:

(14)

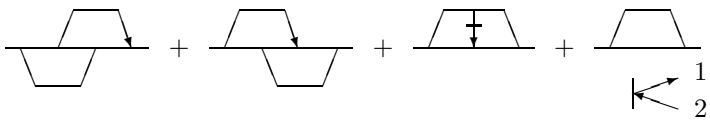

The passage from a chain in σ_1 to the chain in Σ (expressed by replacing round arcs by broken arcs without arrows) consists in posing the quantifier $\exists$: we replace the set of points $((a, b), f)$ satisfying the condition $f(a) = f(b)$ plus some other conditions by the set of maps f such that there exist points a, b such that $f(a) = f(b)$ plus all the same conditions are satisfied; if f satisfies these conditions several times, then we take it with the corresponding multiplicity.

Again, it is natural to try to span the obtained chain by another one, in whose definition the condition $f(a) = f(b)$ is replaced by the condition that $f(a)$ is below $f(b)$ in $\mathbb{R}^3$. In the language of pictures, this variety is obtained from the initial one by putting an arrow at an endpoint of the broken arc. Then we obtain three pictures indicated in the left-hand sides of equalities (15)–(17); note that both the first and the second summands

in (14) appear in the right-hand side of (15):

(15)

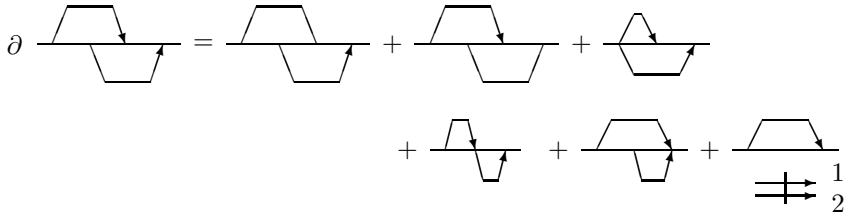

(16)

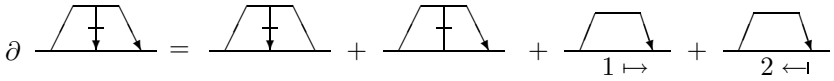

(17)

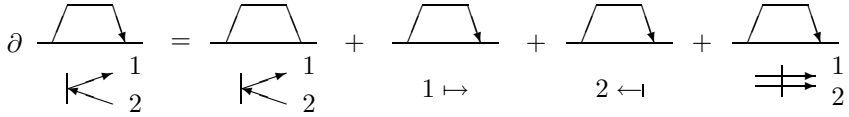

All the other summands in the right-hand sides of these equalities are obvious, except maybe for the last summand in (15), which is analogous to the last summands in (9), (10), and reflects the second Reidemeister degeneration shown in Figure 3b.

The sum of the third, fourth, and fifth terms in the right-hand side of (15) equals the second summand in (16). Therefore the sum of the right-hand sides of (15)–(17) is equal to the cycle (14), and the sum of chains indicated in the left-hand sides of (15)–(17) is the desired combinatorial formula, i.e., the relative cycle of the space of curves modulo Σ, whose boundary coincides with the cycle generating the degree two Borel–Moore homology group of Σ. This sum coincides with formula (1).

Remark 2. We could try to kill two summands of (8) not by the left parts of the equalities (9) and (10) but by similar pictures with reversed orientations of broken arcs. If we make such a switch for exactly one of these summands, then the additional summands in the right-hand sides of the resulting versions of (9) and (10) cancel each other, so that the sum of their left-hand sides spans the cycle (8). Continuing our algorithm, we obtain in this case exactly the Polyak–Viro formula shown in Figure 5 and consisting of a single term, and not of the three terms given in Theorem 1 in §5. Unfortunately at this stage we have not found a way to make the process both algorithmic and sensitive to such optimal choices.

In §2, we describe some standard subvarieties and chains in the space of curves and in terms $\sigma_i \setminus \sigma_{i-1}$ of the resolved discriminant of this space: all spanning chains γ_j and their boundaries will be built of these chains. In §3 we study the incidence relations between these chains, which is necessary for checking the homological conditions. In §4 the main algorithm is described. In §5 we comment in these terms on the previous calculation of the combinatorial formula for the unique invariant v_2 of filtration 2. In §6 we show how the same algorithm calculates a formula for the next complicated invariant v_3 of filtration 3.

I thank A. B. Merkov very much, whose help and critical attention were very essential. Presumably the idea of this work arose from our previous conversations; also he has found many bugs in the first version of the algorithm.

I acknowledge the hospitality of the Isaac Newton Institute, Cambridge, where a main part of the work was accomplished.

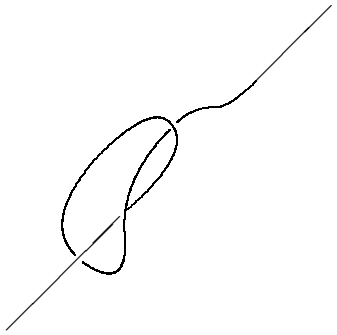

FIGURE 4. A long knot

FIGURE 5. Polyak–Viro formula for the Casson invariant

1. Preliminary remarks

1.1. **Chains in the space of knots.** We consider *long knots* (see [17], [24]), i.e., smooth embeddings $\mathbb{R}^1 \to \mathbb{R}^3$ coinciding with a standard linear embedding outside some compact subset in $\mathbb{R}^1$; see Figure 4. We denote by $\mathcal{K}$ the space of all maps $\mathbb{R}^1 \to \mathbb{R}^3$ with these boundary conditions and define the *discriminant* $\Sigma \subset \mathcal{K}$ as the set of such maps having either self-intersections or singular points. Long knots are exactly the points of the difference $\mathcal{K} \setminus \Sigma$. The points of Σ are called *singular knots*.

We work with the space $\mathcal{K}$ as with a real affine space of a very large but finite dimension. A justification for this, based on the techniques of finite-dimensional approximations, is described in [17]–[21]. The quotes ‘ , ’ below indicate formally nonstrict statements and terms which refer to this justification. In particular, we use the ‘Alexander duality’ in $\mathcal{K}$,

$$\tilde{H}^i(\mathcal{K} \setminus \Sigma) \simeq \bar{H}_{3\omega-i-1}(\Sigma), \tag{18}$$

where $\tilde{H}^i$ is the cohomology group reduced modulo a point, 3ω is the notation for the ‘dimension’ of $\mathcal{K}$ (so that ω symbolizes the ‘dimension’ of the space of functions $\mathbb{R}^1 \to \mathbb{R}^1$ with a fixed behavior at infinity), and $\bar{H}_{3\omega-j}$ is the ‘*Borel–Moore* homology group of codimension j’. We realize the homology classes in the right-hand side of (18) by ‘semialgebraic chains’ of infinite dimension but finite codimension.

In this subsection we discuss the following statement.

Remark–Definition. Given a cohomology class of the space of knots in $\mathbb{R}^n$ (e.g. a knot invariant if $n = 3$), a *combinatorial formula* for it is a *subalgebraic relative Borel–Moore cycle* in the space of curves $\mathcal{K}$ modulo the discriminant space Σ, such that our cohomology class is equal to the intersection number with this relative cycle (or, equivalently, to the linking number with the boundary of this cycle).

The *subalgebraic chains* will be defined shortly. First let us consider an example.

The *Polyak–Viro formulas* [15] are the pictures like Figure 5 (“arrow diagrams”) or linear combinations of similar pictures. The Polyak–Viro formula shown in Figure 5 corresponds to the simplest knot invariant (or degree 2). It should be read as follows.

Consider a generic long knot $f : \mathbb{R}^1 \to \mathbb{R}^3$, e.g. the knot shown in Figure 4. A *representation* of the arrow diagram of Figure 5 in the knot f is any collection of points $\{a < b < c < d\} \subset \mathbb{R}^1$ such that $f(a)$ lies below $f(c)$ and $f(d)$ lies below $f(b)$ (with respect to a chosen direction in $\mathbb{R}^3$). The value of this diagram on our knot is equal to the number of its representations (counted with appropriate signs described explicitly in [15]). An immediate calculation shows that this number is a knot invariant of order 2. General arrow diagrams consist of several oriented arcs connecting different points of $\mathbb{R}^1$.

Let us understand in which sense the above diagram defines a subalgebraic chain.

Consider the Cartesian product $\mathcal{K} \times \mathbb{R}^4$ of the space of curves $f : \mathbb{R}^1 \to \mathbb{R}^3$ and the space of quadruples of points $a, b, c, d \in \mathbb{R}^1$. Then all the above conditions obviously define a very easy collection of linear restrictions in this enlarged space: 5 restrictions of inequality type and $2(n-1) = 4$ restrictions of equality type. The relative cycle in $\mathcal{K}(\mathrm{mod}\ \Sigma)$, expressed by the Polyak–Viro formula of Figure 5, is just the direct image under the projection to $\mathcal{K}$ of the fundamental cycle of the set distinguished by these linear conditions.

In the finite-dimensional algebraic geometry, projections of semialgebraic sets or chains remain in the same class of objects by the Tarski–Zeidenberg lemma. We do not have a similar lemma in the functional space; therefore we use the word "*subalgebraic*" for images of projections of semialgebraic objects from slightly greater spaces.

All chains in the space of curves $\mathcal{K}$, occurring in our algorithm, are subalgebraic in exactly the same sense. Namely, they are linear combinations of projections of certain semialgebraic chains.

Let us give the exact definitions.

Denote by W^m the configuration space of collections of m points $a_1 < \cdots < a_m \in \mathbb{R}^1$; this is an open subset in the space $\mathbb{R}^m$. Let r be a nonnegative integer, and $\tilde{A}$ a semialgebraic chain of codimension c in $\mathbb{R}^{3m(r+1)}$, i.e., a semialgebraic stratified set, the minimal codimension of whose smooth strata is equal to c, and any such stratum of codimension c is supplied with a coefficient from the fixed coefficient group and (unless the coefficient group is of second order) a coorientation (= orientation of the normal bundle) in $\mathbb{R}^{3m(r+1)}$. The union of closures of strata of codimension c, whose coefficients are not equal to 0, is called the *support* of the semialgebraic chain.

The *formally semialgebraic chain* $A \subset \mathcal{K} \times W^m$ associated with the chain $\tilde{A}$ is defined as the preimage of $\tilde{A}$ under the *multijet map* j^r_m sending a map f and a point configuration $(a_1, \dots, a_m) \subset \mathbb{R}^1$ to the collection of r-jets of the map f at these points. In other words, A is the union of points $(f, (a_1, \dots, a_m)) \in \mathcal{K} \times W^m$ such that the point

$$\Big(f(a_1), f'(a_1), \dots, f^{(r)}(a_1), \dots, f(a_m), \dots, f^{(r)}(a_m)\Big) \tag{19}$$

of the space $\mathbb{R}^{3m(r+1)}$ belongs to the support of the chain $\tilde{A}$; such a point $(f, (a_1, \dots, a_m))$ becomes supplied with the same coefficient as the point (19) in the chain $\tilde{A}$, and a neighborhood of the point $(f, (a_1, \dots, a_m))$ in A has the coorientation in $\mathcal{K} \times W^m$ induced from the coorientation of $\tilde{A}$ by the multijet map j^r_m (which, by the Thom transversality theorem, is transversal to the chain $\tilde{A}$ at its nonsingular strata).

Remark 3. When (in future) we shall consider cohomology classes of the space of *compact* knots $S^1 \hookrightarrow \mathbb{R}^n$, we shall need to define the formally semialgebraic chains by means of pairs of chains $\tilde{A} \subset \mathbb{R}^{nm(r+1)}$ and $\tilde{B} \subset (S^1)^m$. Considering the spaces of knots in some M^n instead of $\mathbb{R}^n$, we need additionally to replace $\mathbb{R}^{nm(r+1)}$ by the m-th Cartesian power of the space $J^r_0(\mathbb{R}^1, M^n)$ of r-jets of maps $\mathbb{R}^1 \to M^n$ at the origin of $\mathbb{R}^1$.

By the Thom transversality theorem, the codimension of the chain A in $\mathcal{K} \times W^m$ is equal to the codimension of $\tilde{A}$ in $\mathbb{R}^{3m(r+1)}$.

The *subalgebraic chains* in $\mathcal{K}$ will be defined by the projections of formally semialgebraic chains from spaces $\mathcal{K} \times W^m$. We shall always assume that the codimension $\operatorname{codim}(A)$ of the chain $A \subset \mathcal{K} \times W^m$ to be projected is at least m.

Definition 1. A point of the formally semialgebraic chain $A \subset \mathcal{K} \times W^m$ is *nonsingular* if the corresponding point (19) is a regular point of the set $\tilde{A}$ (i.e., it belongs to a stratum of minimal codimension $\operatorname{codim}(\tilde{A})$ of the chain $\tilde{A}$). A point of the projection $p(A) \subset \mathcal{K}$ of the support of such a chain is called *regular* if all its preimages in A are nonsingular and all points of some its neighborhood in $p(A)$ have equally many preimages. A *nonsingular piece* of $p(A)$ is an arbitrary path-connected component of the set of regular points of $p(A)$.

Proposition 1. *Suppose that the formally semialgebraic chain $A \subset \mathcal{K} \times W^m$ is defined by the semialgebraic chain $\tilde{A}$ of codimension $\geq m$ in $\mathbb{R}^{3m(r+1)}$. Then*

1. the set $p(A)$ looks like a smooth regular submanifold of codimension $\operatorname{codim}(A) - m$ in $\mathcal{K}$ close to any of its regular points (i.e., its section by almost any finite-dimensional affine plane in $\mathcal{K}$, whose dimension is greater than $\operatorname{codim}(A) - m$, is locally (close to any regular point) a submanifold of this codimension in this plane);

2. the codimension of the set of nonregular points of $p(A)$ in $\mathcal{K}$ is strictly greater than $\operatorname{codim}(A) - m$, i.e., the intersection of this set with almost any such plane has codimension greater than $\operatorname{codim}(A) - m$ in this plane.

All this follows immediately from the multijet Thom transversality theorem; see e.g. [6]. □

By definition, the *subalgebraic chain* $p_!(A)$ corresponding to the chain A is equal to the sum of the nonsingular pieces of the set $p(A)$ taken with appropriate multiplicities. Namely, if we study the $\mathbb{Z}_2$-cohomology of the space of knots (e.g. invariants mod 2), then such a piece should be taken with multiplicity 0 or 1 depending on the parity of the sum of the coefficients at all preimages of this piece. If we consider cohomology with integer coefficients, then we need to consider the coorientations (i.e., orientations of normal bundles) in the following way. The contraction with the standard orientation in W^m takes the coorientation of any nonsingular piece of the chain A to a coorientation of the regular part of the image of this piece in $p(A)$. The chain $p_!(A)$ is equal to the sum of regular pieces of the set $p(A)$, any of which should be taken with an arbitrary coorientation and with a coefficient equal to the sum of certain indices over all preimages of this piece in A: the index corresponding to some preimage is equal to the product of the coefficient at this preimage in the chain A and the number equal to 1 (respectively, -1) if the chosen coorientation of our piece in $p(A)$ coincides with (respectively, differs from) the coorientation induced from the coorientation of this preimage. Of course, if we choose another coorientation of a smooth piece in $p(A)$, then the corresponding coefficient in $p_!(A)$ will be multiplied by -1.

In concrete examples, this accounting for coorientations has an easy geometrical interpretation, like the local writhe used in the Polyak–Viro formulas.

Definition 2. An *elementary subalgebraic chain* of codimension $c \geq 0$ in $\mathcal{K}$ with integer coefficients is the projection of an arbitrary formally semialgebraic chain $A \subset \mathcal{K} \times W^m$ ($\operatorname{codim}(A) = c + m$), whose smooth pieces are accounted for with the above-defined multiplicities and coorientations. The *support* of an elementary subalgebraic chain of codimension c in $\mathcal{K}$ is the union of the closures of all its nonsingular pieces, whose multiplicities are not equal to 0. *Subalgebraic chains* of codimension c in $\mathcal{K}$ are finite formal sums of elementary subalgebraic chains $p_!(A_i)$ of this codimension, considered up to the following relation: a sum $\sum p_!(A_i)$ of elementary subalgebraic chains of codimension c is *equal* to another such chain $\sum p_!(B_j)$ if for any regular piece of the union of supports of

all these elementary chains in $\mathcal{K}$ we have $\sum m_i = \sum n_j$, where m_i (respectively, n_j) is the multiplicity of this piece in the smooth piece of $p_!(A_i)$ (respectively, $p_!(B_j)$) containing it.

The definitions for the case of $\mathbb{Z}_2$-coefficients are almost the same, but we do not need to consider coorientations.

For these chains the boundary operator is well defined (this means that the boundary of any subalgebraic chain also can be represented by a subalgebraic chain), and hence also the 'Borel–Moore homology groups of finite codimension' of the complex of all such chains. A chain of codimension c is a *relative Borel–Moore cycle* (mod Σ) in $\mathcal{K}$ if its homological boundary can be represented by a subalgebraic chain, whose support is contained in Σ. If this condition is satisfied, then the intersection indices of the initial chain with c-dimensional cycles in the knot space $\mathcal{K} \setminus \Sigma$ are well defined; moreover, these indices depend only on the homology classes of these cycles.

1.2. **Simplicial resolution of the discriminant.** As in [17]–[21] and [24], we use a *simplicial resolution* of Σ, i.e., another 'semialgebraic' space σ together with a 'proper' map $\pi : \sigma \to \Sigma$ that induces a homomorphism of 'Borel–Moore homology groups of finite codimension'. The *finite type cohomology classes* in $\mathcal{K} \setminus \Sigma$ are defined as cohomology classes Alexander dual (18) to the images of elements of $\bar{H}_*(\sigma)$ in $\bar{H}_*(\Sigma)$ under this homomorphism. These classes form an important subgroup $H^*_f \subset H^*(\mathcal{K}\setminus\Sigma)$. The space σ admits a natural filtration $\sigma_1 \subset \sigma_2 \subset \dots$, generating a spectral sequence $E^r_{p,q}$ calculating the 'Borel–Moore homology group of finite codimension' of σ, i.e., $E^r_{p,q} \to \bar{H}_{p+q}(\sigma)$, $E^1_{p,q} \simeq \bar{H}_{p+q}(\sigma_p \setminus \sigma_{p-1})$; here q takes values 'almost equal to' the dimension of the space $\mathcal{K}$. The resulting filtration in the Borel–Moore homology group of σ induces a filtration in the 'Alexander dual' group H^*_f. E.g. the 0-dimensional cohomology classes (i.e., knot invariants) of finite filtration are known as finite-type knot invariants, and the filtration of an invariant often is called its *order* or *degree*.

In the case of knots in $\mathbb{R}^n$, $n > 3$, the *entire* (very nontrivial) cohomology group of the space of knots can be calculated by a similar construction: $H^*_f = H^*(\mathcal{K} \setminus \Sigma)$. For $n = 3$ this construction gives us a priori only a subgroup of $H^*(\mathcal{K} \setminus \Sigma)$ (however no example is known of a free homology class in $\mathcal{K} \setminus \Sigma$ taking zero values on all cohomology classes from this subgroup). In the rest of this paper we consider the case of knot invariants in $\mathbb{R}^3$ only.

Any term $\sigma_i \setminus \sigma_{i-1}$, $i \geq 1$, of the standard filtration of the space σ is the total space of a $(3\omega - 3i)$-dimensional affine bundle over a finite-dimensional semialgebraic variety canonically separated into finitely many nonclosed cells. Therefore also the space $\sigma_i \setminus \sigma_{i-1}$ consists of finitely many such cells (so that its one-point compactification $\bar{\sigma}_i/\bar{\sigma}_{i-1}$ is a 'cell complex').

The homology group of the cell complex defined by these cells and their incidence coefficients is exactly the desired term $E^1_{i,*}$ of our spectral sequence (up to a shift of dimensions). In the next subsubsections 1.2.1–1.2.5 we describe the construction of the simplicial resolution and enumerate those cells of interest for us (i.e., participating in the calculation and realization of knot invariants). Here we use the construction of the resolution σ introduced in [18]. It is slightly more economical than (although homotopy equivalent to) the one from [17]–[21].

1.2.1. *Simplicial resolutions of plane arrangements.* Following our analogy with the theory of finite plane arrangements in $\mathbb{R}^N$, we first construct simplicial resolutions of such collections.

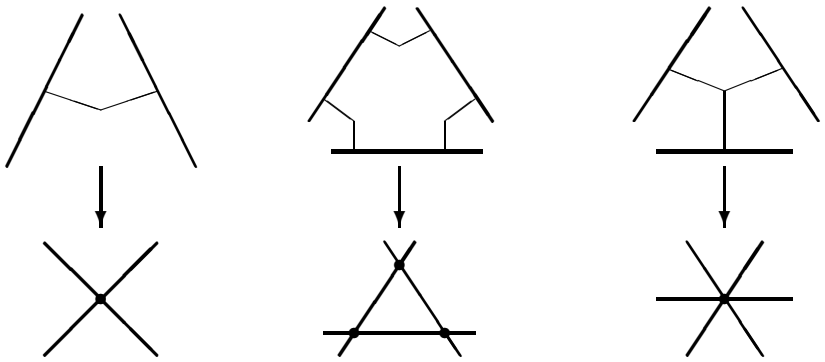

FIGURE 6. Simplicial resolutions of line arrangements

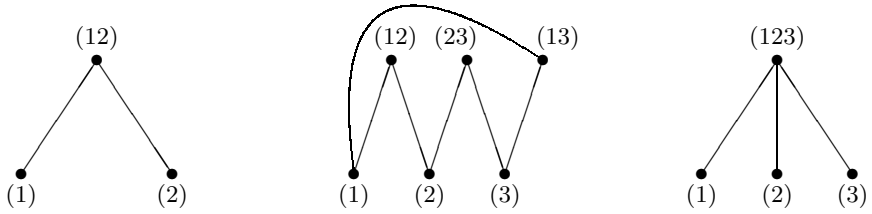

FIGURE 7. Order complexes for line arrangements of Figure 6

Consider a finite collection $\mathcal{L} = \{L_1, \dots, L_m\}$ of affine planes of arbitrary dimensions in $\mathbb{R}^N$. Denote by L their union $\bigcup L_j$; for any set of indices $I \subset \{1, \dots, m\}$ denote by L_I the plane $\bigcap_{j \in I} L_j$.

The best method of computing homology groups of L is based on the simplicial resolutions of $\mathcal{L}$. There are several constructions of such resolutions. We use here the one from [28] which is based on the notion of the order complex of a partially ordered set.

Definition 3. Given a poset $(A, <)$, the corresponding *order complex* $\Upsilon(A)$ is the simplicial complex, whose vertices are the points of the set A, and the simplices span all the sequences of such points monotone with respect to the partial order.

Every plane arrangement $\mathcal{L} = \{L_1, \dots, L_m\}$ defines the poset whose points correspond to nonempty sets L_I, $I \subset \{1, \dots, m\}$, and the partial order, to their incidences; hence also the corresponding order complex $\Upsilon(\mathcal{L})$ is defined.

For instance, for three line arrangements shown in the lower row of Figure 6, the corresponding order complexes are given in Figure 7.

To any collection I with $L_I \neq \varnothing$ the order subcomplex $\Upsilon(I) \subset \Upsilon(\mathcal{L})$ is associated: this is the union of all simplices in $\Upsilon(\mathcal{L})$ all of whose vertices correspond to planes L_J containing L_I. Any such subcomplex $\Upsilon(I)$ is contractible: indeed, all its maximal simplices have the common vertex corresponding to the plane L_I itself. Denote by $\partial\Upsilon(I)$ the *link* of this subcomplex, i.e., the union of all its simplices not containing its extremal vertex $\{L_I\}$.

The simplicial resolution $\mathcal{L}'$ of $\mathcal{L}$ is defined as a subset of the Cartesian product $\Upsilon(\mathcal{L}) \times \mathbb{R}^N$, namely,

$$\mathcal{L}' \equiv \bigcup \Upsilon(I) \times L_I, \tag{20}$$

where the union is taken over all geometrically distinct nonempty planes L_I.

The obvious projection $\Upsilon(\mathcal{L})\times\mathbb{R}^N \to \mathbb{R}^N$ defines a proper continuous map $\pi : \mathcal{L}' \to \mathcal{L}$. All fibers of this map coincide with appropriate complexes $\Upsilon(I)$ and thus are compact and contractible. This easily implies that the projection π defines a homotopy equivalence $\mathcal{L}' \sim \mathcal{L}$ and a homotopy equivalence of the one-point compactifications of these spaces, $\bar{\mathcal{L}}' \sim \bar{\mathcal{L}}$; in particular it defines isomorphisms of both ordinary and Borel–Moore homology groups of $\mathcal{L}'$ to similar homology groups of $\mathcal{L}$.

It turns out that the calculation of homology groups of $\mathcal{L}'$ is much easier than that of (isomorphic to them) homology groups of $\mathcal{L}$. Indeed, the space $\mathcal{L}'$ admits a convenient increasing filtration $F_1 \subset F_2 \subset \cdots \subset F_{N-1} = \mathcal{L}'$: its term F_i is a union similar to (20) but is taken only over spaces L_I of codimension $\le i$.

For instance, for three line arrangements of the lower row of Figure 6, terms F_1 of their resolutions are shown by thick lines in the top row and consist of the corresponding lines taken separately; terms F_2 coincide with entire resolutions and are obtained by adding broken lines, whose breakpoints symbolize intersection points of our lines in $\mathbb{R}^2$.

Proposition 2 (see [28])**.** *The induced filtration of the one-point compactification $\bar{\mathcal{L}}'$ of the space $\mathcal{L}'$,*

$$\bar{F}_1 \subset \bar{F}_2 \subset \cdots \subset \bar{F}_{N-1} = \bar{\mathcal{L}}',$$

homotopically splits into the wedge of consecutive factors, i.e., there is a homotopy equivalence

$$\bar{\mathcal{L}}' \sim \bar{F}_1 \vee (\bar{F}_2/\bar{F}_1) \vee \cdots \vee (\bar{F}_{N-1}/\bar{F}_{N-2}).$$

In particular,

$$\bar{H}_* \simeq \bigoplus_{j=1}^{N-1} \bar{H}_*(F_j \setminus F_{j-1}).$$

But any term $F_j \setminus F_{j-1}$ splits into the disjoint union of spaces $(\Upsilon(I) \setminus \partial\Upsilon(I)) \times L_I$ over all planes L_I of codimension exactly j; this gives immediately the Goresky–MacPherson formula (see Chapter III in [7]) reducing the Borel–Moore homology group of $\mathcal{L}$ to information on the dimensions of different spaces L_I only.

1.2.2. *Simplicial resolution of the discriminant of singular curves.* Let $\mathcal{K}$ be the space of smooth maps $f : \mathbb{R}^1 \to \mathbb{R}^3$ coinciding with a standard linear embedding outside some compact in $\mathbb{R}^1$. The discriminant Σ in it is the set of maps f such that there exists a pair of points $(a, b) \subset \mathbb{R}^1$ such that

$$f(a) = f(b) \text{ if } a \ne b \quad \text{or} \quad f'(a) = 0 \text{ if } a = b. \tag{21}$$

The study of the space Σ is very similar to that of plane arrangements because this space is swept out by a very easy family of planes of codimension 3 in $\mathcal{K}$: these planes $L(a, b)$ are parametrized by the points of the configuration space of unordered pairs $(a, b) \subset \mathbb{R}^1$ and, for any a and b, consist of all maps f satisfying the condition (21).

Following the previous subsection, we can construct the simplicial resolution σ of Σ as follows: we consider the (appropriately topologized and augmented) order complex $\Delta(\mathcal{K})$ of all planes obtained as intersections of several planes of the form $L(a, b)$, and define σ as a subset in the Cartesian product $\Delta(\mathcal{K}) \times \mathcal{K}$ just as previously.

Namely, for any natural i we consider the set of all affine subspaces of codimension $3i$ in $\mathcal{K}$, obtained as intersections of i planes $L(a, b)$ with all different a and b. Denote by $\rho(i)$ the closure of this set in the Grassmannian space of all subspaces of this codimension; this is a $2i$-dimensional semialgebraic set. It is naturally stratified in correspondence with combinatorial types of degenerations of collections of $2i$ points defining these i planes. Let us describe these strata.

For any multi-index $A = (a_1, a_2, \dots, a_k; m_1, \dots, m_l)$, where $a_1 \geq a_2 \geq \dots \geq a_k$, the a_i are natural numbers greater than 1, and the m_j are arbitrary naturals, a *multiconfiguration* of type A is an arbitrary collection of $a_1 + \dots + a_k$ distinct points in $\mathbb{R}^1$ divided into groups of cardinalities $a_1, \dots, a_k$ and completed by some l pairwise distinct points (some of which can coincide with some of the previous $a_1 + \dots + a_k$ points), supplied with indices ("multiplicities") $m_1, \dots, m_k$. It is convenient to consider any such configuration as a subspace in the space of maps $\mathcal{K}$: namely, as the space of all maps taking equal values at the points of any group of cardinality $a_1, \dots, a_k$, and satisfying the condition $f' = f'' = \dots = f^{(m_j)}$ at the point labeled by m_j. The codimension of this subspace in $\mathcal{K}$ is equal to $3(\sum_{i=1}^{k}(a_i - 1) + \sum_{i=1}^{l} m_i)$. Therefore the number $\sum_{i=1}^{k}(a_i - 1) + \sum_{i=1}^{l} m_i$ is called the *complexity* of the multi-index A and of any multiconfiguration of type A.

Denote by $W(A)$ the space of all A-configurations in $\mathbb{R}^1$. The space $\rho(i)$ splits into varieties $W(A)$ corresponding to all possible multi-indices A of complexity i. This is still not the complete topological classification of its points, because it does not take into account possible coincidences of points of a- and m-groups. Dividing all subspaces $W(A)$ in the correspondence with topological types of these coincidences, we obtain the desired stratification.

Example 1. $W(2; \varnothing)$ is the space of pairs $\{a < b\}$ in $\mathbb{R}^1$, i.e., an open half-plane. Its closure $\overline{W(2; \varnothing)}$ is the closed half-plane consisting of pairs $\{a \leq b\}$; it coincides with the entire $\rho(1)$. Their difference $\overline{W(2; \varnothing)} \setminus W(2; \varnothing)$ is the line $W(\varnothing; 1)$. The space $W(2; 1)$ consists of three maximal strata (see formula (26) separated by two degenerate strata.

The disjoint union of spaces $\rho(i)$ over all $i \leq d$ is a poset by a natural subordination of multiconfigurations (this subordination can be interpreted as the inverse inclusion of corresponding functional subspaces). Denote by $\Delta(d)$ the corresponding *continuous order complex*. Namely, for any d we consider the join of all spaces $\rho(i)$, $i \leq d$, i.e., a naturally topologized union of all simplices whose vertices are points of different spaces $\rho(i)$, and select only those such simplices all of whose vertices correspond to a chain of incident subspaces in $\mathcal{K}$. Such simplices will be called *coherent*, and the union of them is the desired space $\Delta(d)$. For any point $L \in \rho(i)$ define $\Delta(L)$ as the union of coherent simplices in $\Delta(d)$, all of whose vertices correspond to subspaces containing the subspace of codimension $3i$ corresponding to L.

Furthermore, we define the d-th term σ_d of the resolution of Σ as a subset in $\Delta(d) \times \mathcal{K}$, namely, as the union of spaces $\Delta(L) \times L$ over all points L of all spaces $\rho(i)$, $i \leq d$. By construction, $\sigma_d \subset \sigma_{d+1}$, and we define σ as the union of all these spaces with the topology of direct limit.

For instance, the space σ_1 is the *tautological resolution* of Σ, i.e., the space of a fiber bundle over the half-plane $\rho(1)$ with fibers equal to affine subspaces of codimension 3 in $\mathcal{K}$.

In general, any space $\sigma_d \setminus \sigma_{d-1}$ is the space of a fiber bundle whose fibers are subspaces of codimension $3d$ in $\mathcal{K}$, and whose base is the naturally topologized union of spaces $\Delta(L) \setminus \partial\Delta(L)$ over all $L \in \rho(d)$. The latter union is a finite-dimensional semialgebraic variety. Thus by the Thom isomorphism the Borel–Moore homology groups of finite codimension of this space $\sigma_d \setminus \sigma_{d-1}$ reduce to ordinary (finite-dimensional) Borel–Moore homology groups of a certain finite-dimensional object.

1.2.3. *Primary cell structure of consecutive terms of the simplicial resolution.* As we have seen above, any space $\rho(i)$ has a natural stratification in correspondence with the combinatorial types of multi-configurations A of complexity i. All strata of this stratification are nonclosed cells. For any such configuration $L \in \rho(i)$ the corresponding order complex $\Delta(L)$ is an $(i-1)$-dimensional polyhedron, in particular a compact cell complex; thus

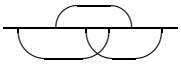

FIGURE 8. A chord diagram

also the space $\Delta(L) \setminus \partial\Delta(L)$ is canonically divided into cells. These divisions of all such spaces L with L from one and the same cell of $\rho(i)$ are canonically homeomorphic to one another and form a trivial bundle over the cell. Thus also the space $\Delta(i) \setminus \Delta(i-1)$ becomes canonically divided into finitely many cells: these cells are numbered by a) our cells in $\rho(i)$ and b) for any such cell, the cells of our decomposition of the complex $\Delta(L) \setminus \partial\Delta(L)$ for an arbitrary L from this cell. Correspondingly, the space $\sigma_i \setminus \sigma_{i-1}$ of our affine bundle $\sigma_i \setminus \sigma_{i-1} \to \Delta(i) \setminus \Delta(i-1)$ splits into equally many cells (of infinite dimensions), namely, into preimages of all previous cells.

The dimension of such a cell cannot exceed the number $3(\omega - i) + i - 1 + |A|$, where $|A| = a_1 + \cdots + a_m + l$. We deal further with invariants of knots in $\mathbb{R}^3$, i.e., (by the isomorphism (18)) with homology classes of full dimension in the discriminant. Therefore we are interested only in such cells of maximal $(3\omega - 1)$ and vice-maximal $(3\omega - 2)$ dimensions.

All cells of dimension $3\omega - 1$ are related with the space $W(A)$, where $A = (2, \dots, 2; \varnothing)$ (i twos). This space $W(A)$ is $2i$-dimensional, and its connected components are in the canonical one-to-one correspondence with equivalence classes of (long) chord diagrams. Such a diagram consists of a horizontal line ("Wilson line") and $2i$ distinct points in it matched somehow into pairs (see [17]), since such Gauss pairs of points are depicted by arcs ("chords") with ends at these points; see Figure 8. The Wilson line symbolizes the source line $\mathbb{R}^1$ of our long knots and singular knots $f : \mathbb{R}^1 \to \mathbb{R}^3$. We shall consider also some other lines $\mathbb{R}^1$; therefore we denote the Wilson line by $\mathbb{R}^1_w$. (In the parallel theory of *compact knots* $S^1 \hookrightarrow \mathbb{R}^3$ we have not the Wilson line but the Wilson loop S^1, the matched pairs of points of which are connected by segments; this explains the terms "chord" and "chord diagram"; see [3], [2].) Two chord diagrams are *equivalent* if they can be transformed one into the other by an orientation-preserving homeomorphism of the Wilson line.

For any configuration $L \in W(2, \dots, 2; \varnothing)$ the order complex $\Delta(L)$ is the barycentric subdivision of the $(i-1)$-dimensional simplex, whose vertices correspond to the chords of the corresponding chord diagram. So, we have $i!$ cells of maximal dimension for any equivalence class of chord diagrams.

The cells of vice-maximal dimension, defining the homology conditions for the linear combinations of maximal cells, are of the following three types.

B. With any connected component of the same space $W(2, \dots, 2; \varnothing)$, i.e., with an equivalence class of i-chord diagrams, there are related vice-maximal cells, corresponding to vice-maximal simplices of the barycentric subdivision of the complex $\Delta(L)$ (L being any chord diagram in this equivalence class) not in its link $\partial\Delta(L)$.

Two other classes of vice-maximal cells of $\Delta(i) \setminus \Delta(i-1)$ are related with different vice-maximal strata of the space $\rho(i)$.

1T. The strata of the first class are open subsets in $W(2, \dots, 2; 1)$ ($i-1$ twos) and consist of configurations of $2i-1$ distinct points in $\mathbb{R}^1_w$ separated into $i-1$ pairs (depicted by chords) and one "singular" point $*$. For any such configuration L, the corresponding order complex $\Delta(L)$ again is the barycentric subdivision of the $(i-1)$-dimensional simplex, whose vertices correspond to these pairs and the singular point. For any equivalence class of such configurations, there are $i!$ vice-maximal cells of our decomposition

of $\Delta(i) \setminus \Delta(i-1)$ related with all *maximal* simplices of the barycentric subdivision of this simplex for an arbitrary L of this class.

4T. The vice-maximal strata of the second class in $\rho(i)$ consists of configurations of type $(3, 2, \dots, 2; \varnothing)$, i.e., configurations of $2i-1$ points separated into $i-2$ pairs (depicted by chords) and one triple (depicted by a tripod) like 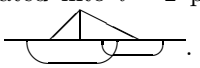 . For any such configuration L, the order complex $\Delta(L)$ contains $3i!/2$ maximal simplices: they correspond to all ordered sequences of i elements, $i-2$ of which correspond to chords of the configuration L, one more to some pair of points inside its triple, and one to the triple itself; the ordering of these elements in a sequence can be arbitrary unless the pair inside the triple should precede the triple itself. If $i = 2$, then the support of such a complex $\Delta(L)$ is shown in the right-hand picture of Figure 7, and for an arbitrary $i \geq 2$ it is homeomorphic to the $i-2$ times iterated cone over this complex (i.e., to the join of this complex and an $(i-2)$-dimensional simplex).

1.2.4. *Reduced cell decomposition.* The above described decomposition of complexes $\Delta(i) \setminus \Delta(i-1)$ (and hence also of complexes $\sigma_i \setminus \sigma_{i-1}$) into nonclosed cells is highly noneconomic. For our purposes, we can ignore many of its cells and combine the other ones into larger cells.

Indeed, we are seeking linear combinations of maximal cells forming cycles. All $i!$ maximal cells, corresponding to one and the same equivalence class of $(2, \dots, 2; \varnothing)$-configurations L should have one and the same coefficient in such a cycle, because the vice-maximal cells of type **B** separating them should appear in the boundary of a cycle with zero coefficient. Therefore we can combine all these $i!$ cells into one large cell, corresponding to the entire interior of the complex $\Delta(L)$, and not think any more about the vice-maximal cells of type **B**.

The obtained cell of $\sigma_i \setminus \sigma_{i-1}$ consists of all triples of type

$$(C, f, t), \tag{22}$$

where C is any chord diagram of our equivalence class, f is a smooth map $\mathbb{R}^1_w \to \mathbb{R}^3$ gluing together the endpoints of any chord of C, and t is an interior point of an $(i-1)$-dimensional simplex arising in the construction of the resolution similar to the horizontal interval in Figure 1b: the vertices of this simplex are in the natural one-to-one correspondence with the chords of the diagram C. If $i = 0$, then by definition the unique such cell (corresponding to the chord diagram with no chords) coincides with the entire space $\mathcal{K}$ of long curves $f : \mathbb{R}^1_w \to \mathbb{R}^3$.

So, we have $(2i)!/(i!2^i)$ maximal cells in $\sigma_i \setminus \sigma_{i-1}$, in correspondence with all possible matchings of $2i$ given points. The dimension of any such cell is equal to $2i + (3\omega - 3i) + (i-1) = 3\omega - 1$, i.e., to the dimension of the hypersurfaces in $\mathcal{K}$.

Furthermore, all vice-maximal cells of type **1T** related with one and the same equivalence class of generic $(2, \dots, 2; 1)$-configurations appear in the boundary of any linear combination of such enlarged maximal cells with one and the same coefficient; therefore we also can combine them into a single cell.

Any point of such a cell also has the form (22), where C is an arbitrary configuration from our equivalence class, f is a map respecting it (i.e., gluing together the points of any pair and satisfying the condition $f'(*) = 0$), and t is a point of the nonclosed $(i-1)$-dimensional simplex, whose $i-1$ vertices correspond to the pairs from this configuration, and the last vertex corresponds to the point $*$. The homological condition on a linear combination of maximal cells (i.e., chord diagrams), following from the consideration of cells of **1T** type, requires that any chord diagram such that the endpoints of some of its

chords are not separated by endpoints of other chords participates in any cycle with zero multiplicity; this condition is called the *one-term relation* or **1T**-*relation*.

Finally, the above-described vice-maximal cells of type **4T** related with some $(3, 2, \dots, 2; \varnothing)$-configuration are characterized by the choice of a pair inside the triple. All cells for which this pair is the same appear in any boundary with one and the same coefficient and can without difficulty be combined into a single cell. So we obtain three vice-maximal cells related with any equivalence class of $(3, 2, \dots, 2; \varnothing)$-configurations.

Such a cell is depicted by a chord diagram with one tripod like 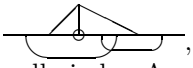 , where the point of the triple *not in the chosen pair* is marked by a small circle. Any point of such a cell also has the form (22), where C is a configuration in our equivalence class, f is a map $\mathbb{R}^1_w \to \mathbb{R}^3$ gluing together all points inside any pair or triple of C, and t is a point of a certain $(i-1)$-dimensional simplex arising in the construction of the resolution: its first $i-2$ vertices correspond formally to the chords of C, one vertex more to the triple in C, and the last vertex to the distinguished pair inside this triple.

1.2.5. *Boundaries of maximal cells.* The boundary of a maximal cell in $\sigma_i \setminus \sigma_{i-1}$ corresponding to the i-chord diagram C consists of $2i-1$ summands. These summands correspond to all segments in $\mathbb{R}^1_w$ bounded by neighboring points of the configuration C. Namely, let us contract any such segment. If the endpoints of such an interval belong to one pair, then it will be contracted into a singular point $*$ and we obtain one vice-maximal cell of **1T** type. If these bounding points belong to different pairs, then this couple of pairs degenerates to a triple. The corresponding summand in the boundary of our maximal cell is the sum of some two vice-maximal cells of **4T** type related with the arising configuration, namely, the two cells in whose notation the point arising from the contracted segment is *not* encircled. Moreover, these boundary chains should be taken with appropriate signs; see [17]. We shall not consider these signs here, because all our calculations are mod 2 only.

Example 2. The term σ_1 of the filtration consists of exactly two cells, one of maximal dimension, and the second equal to its boundary:

(23) ∂ 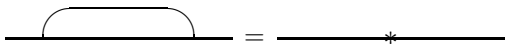 =

Therefore there are no cohomology classes of filtration 1 of the space of long knots, in particular no knot invariants of degree 1.

Example 3. The term $\sigma_2 \setminus \sigma_1$ contains three cells of maximal dimension,

(24) 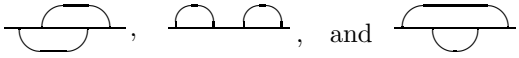

three vice-maximal cells of **4T** type

(25) 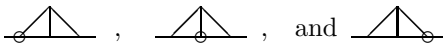

and three vice-maximal cells of **1T** type

(26) 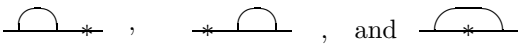

The boundary operator (mod 2) acting from the linear combinations of maximal cells to the vice-maximal ones is described in three equations (27)–(29):

(27) ∂ 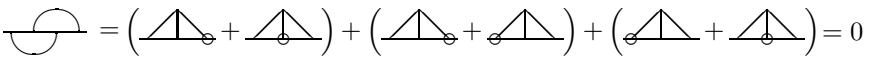 $= 0$

where the sum in the first pair of brackets (respectively, in the second, respectively, in the third) arises from the contraction of the segment between the first and the second (re-

spectively, second and third, respectively, third and fourth) points of the chord diagram;

(28) 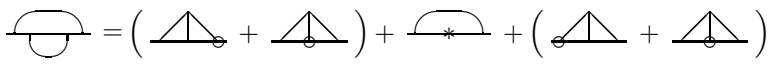

(29) 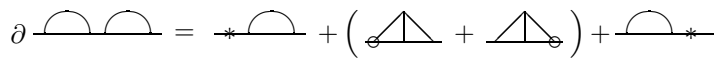

Therefore the kernel of this operator is generated by the first chord diagram in (24).

This chord diagram generates the kernel also in the case of integer homology calculations, and it defines the unique (up to scalings) invariant of degree 2.

The boundary of any maximal cell (considered as a subset in the entire resolved discriminant) is contained not only in the same term $\sigma_i \setminus \sigma_{i-1}$ of the filtration, but also in its lower term σ_{i-1}. The codimension of the intersection of this boundary with any term σ_{i-j} is equal to j; therefore for homological calculations only the part of this additional boundary lying in $\sigma_{i-1} \setminus \sigma_{i-2}$ is interesting. This part of the boundary of a maximal cell consists of i summands corresponding to all chords of the chord diagram indexing this cell or, which is the same, to all $(i-2)$-dimensional faces of an arbitrary $(i-1)$-dimensional simplex among ones sweeping out our cell; see the letter t in (22). These summands are neither the cells nor linear combinations of cells of the similar cell decomposition of the term $\sigma_{i-1} \setminus \sigma_{i-2}$: their supports are some singular hypersurfaces in the maximal cells of this decomposition. Namely, let us choose any chord of the initial i-chord diagram C_0. Erasing it we obtain an $(i-1)$-chord diagram C_0', i.e., the code of some maximal cell $V(C_0')$ in $\sigma_{i-1} \setminus \sigma_{i-2}$. The corresponding summand of the boundary of the cell $V(C_0)$ encoded by the i-chord diagram C_0 is a singular hypersurface in this cell of $\sigma_{i-1} \setminus \sigma_{i-2}$. This hypersurface consists of all triples (C', f, t') of this cell (cf. (22)) such that C' is equivalent to C_0', and the map f additionally glues together some two points of $\mathbb{R}^1_w$ placed among the $2i-2$ points of the $(i-1)$-chord diagram C' in the same way as the endpoints of the erased chord. In the notation of §2.4 this hypersurface will be depicted by a drawing obtained from the initial i-chord diagram by replacing the chosen chord by a broken line with the same endpoints.

1.3. **Subalgebraic chains in cells of the simplicial resolution.** The pieces of boundaries just described are an important example of subalgebraic chains in the cells of the space of resolution. (In §1.1 subalgebraic chains were defined in the functional space $\mathcal{K}$ only.)

Namely, let us consider some maximal cell $V(C_0)$ of the set $\sigma_i \setminus \sigma_{i-1}$, consisting of all points of the form (22) where C is equivalent to a fixed chord diagram C_0. Suppose that $m \geq 2i$, and some $2i$ of m indices $1, \dots, m$ are fixed and divided into i pairs $(j_1, j_1'), \dots, (j_i, j_i')$. Consider the space $\mathbb{R}^{3m(r+1)}$ with 3-dimensional coordinates $\phi_1, \phi_1', \dots, \phi_1^{(r)}, \dots, \phi_m, \phi_m', \dots, \phi_m^{(r)}$. Then any semialgebraic chain $\tilde{A}$ of codimension $c > m$ in $\mathbb{R}^{3m(r+1)}$, contained in the plane distinguished by $3i$ conditions $\phi_{j_1} = \phi_{j_1'}, \dots, \phi_{j_i} = \phi_{j_i'}$, defines an *elementary subalgebraic chain* $p_!(A)$ in our cell. A point (C, f, t) of this cell (see (22)) belongs to this chain if there exists a subset C_1 of cardinality $m - 2i$ in $\mathbb{R}^1_w \setminus C$ such that the pair $(f, C \cup C_1)$ belongs to the formally semialgebraic chain $A \subset \mathcal{K} \times W^m$ defined by $\tilde{A}$, and the orders of points of the set C among all points of the set $C \cup C_1$ (ordered from the left to the right in $\mathbb{R}^1_w$) run over the fixed set of indices. As above, nonsingular pieces of the set of such points in our cell should be counted with appropriate multiplicities and orientations, and the space of subalgebraic chains in our cell is defined as the space of linear combinations of elementary subalgebraic chains (with various m and r), factored by the natural equivalence relation; cf. Definition 2.

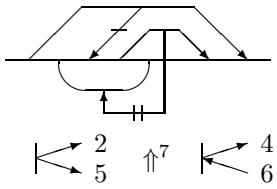

FIGURE 9. Notation of a chain in the resolved discriminant

The spaces of subalgebraic chains in vice-maximal (and other) cells of the term $\sigma_i \setminus \sigma_{i-1}$ are defined analogously.

Our algorithm uses only subalgebraic chains defined by semialgebraic chains $\tilde{A}$ of several special types, which will be described in the next section.

2. Zoo of chains in the space of curves and in the resolved discriminant

2.1. **General conventions.** In our algorithm, only the subvarieties and chains in maximal and vice-maximal cells of terms $\sigma_i \setminus \sigma_{i-1}$ are considered.

Any picture, describing such a chain, consists of a chord diagram (maybe with one tripod or asterisk) indicating the cell in which the support of the chain lies, and some additional furniture (including broken lines and some subscripts) indicating further conditions distinguishing the chain. For examples; see Figure 9 and the rest of the paper.

These pictures are similar to the *arrow-segment diagrams* introduced by A. Merkov [14] in connection with the study of invariants of generic plane curves, but have many additional elements arising from the three-dimensionality of our problem, and also from the fact that we consider chains in the resolved discriminant, and not in the function space $\mathcal{K}$ only.

Additional conditions defining our subalgebraic chains will be described in §§2.2 and 2.4; now we give some preliminary explanations.

All endpoints of chords and broken lines in the picture will be called its *active points*; cf. [13], [14]. They will be ordered from the left to the right in $\mathbb{R}^1_w$. The numbers in subscripts mean the orders of active points participating in the corresponding conditions.

Let us fix a complete flag of directions in $\mathbb{R}^3$. The first direction will be called "up". The "table" plane $\mathbb{R}^2$ in which the knot diagrams are drawn will be considered as the quotient space of $\mathbb{R}^3$ by this direction. Saying that some point in $\mathbb{R}^3$ is *above* or *below* another one, we refer to exactly this direction; in particular two such points have one and the same projection to $\mathbb{R}^2$ along this direction.

Further, we choose the direction "*to the east*" in this quotient space $\mathbb{R}^2$ and say that some point $x \in \mathbb{R}^3$ is to the east from y if the projection to $\mathbb{R}^2$ of the vector $y\vec{x}$ has this direction (in particular two such points lie in one and the same affine 2-plane spanned by the directions "up" and "to the east"). In our drawings this direction coincides with the direction from the left to the right. The opposite direction is called "*to the west*", of course.

A single bar crossing a broken line or participating in a subscript (see e.g. the first and the last subscripts under Figure 9 and the arrow of this picture oriented as $\swarrow$) indicates that the corresponding condition deals with the projections of some objects (points or tangent vectors) to $\mathbb{R}^2$.

Similarly, we consider the quotient space $\mathbb{R}^1$ of $\mathbb{R}^2$ by the direction "to the east", fix the direction "*to the north*" in it, and mark with the double bar $\|$ all conditions referring to the projections to this space along the sum of two directions considered above; see

e.g. the second subscript $\Uparrow^7$ and some broken line in Figure 9. In our drawings this is the direction to the top of the page; the opposite direction is called "*to the south*".

The projection $\mathbb{R}^3 \to \mathbb{R}^2$ along the direction "up" is denoted by ρ_1, the projection $\mathbb{R}^3 \to \mathbb{R}^1$ along both directions "up" and "to the east" is denoted by ρ_2. For any map $f : \mathbb{R}^1_w \to \mathbb{R}^3$ we denote by f_1 (respectively, by f_2) the composition $\rho_1 \circ f : \mathbb{R}^1_w \to \mathbb{R}^2$ (respectively, $\rho_2 \circ f : \mathbb{R}^1_w \to \mathbb{R}^1$). The latter line $\mathbb{R}^1$ will sometimes be called the *meridian* of our chart, and the images of points of $\mathbb{R}^3$ under the projection ρ_2 to this line will be called their *latitudes*.

We assume that the fixed direction of all long knots "at infinity" is generic with respect to this flag of directions, namely, for any long knot f the projection $f_2 : \mathbb{R}^1_w \to \mathbb{R}^1$ has a constant *positive* derivative outside some compact subset in $\mathbb{R}^1_w$; see Figure 4.

2.2. **Chains of full dimension.** Here we describe all additional conditions of the "inequality" type, distinguishing necessary for us subalgebraic chains of full dimension in our maximal cells of $\sigma_i \setminus \sigma_{i-1}$. Such chains serve as blocks for constructing the spanning chains γ_r, $r = k - i$. In particular, such chains with no arcs are the blocks in $\mathcal{K}$, of which the desired combinatorial formulas are built. E.g.; see Figure 9 for the notation of such a chain in the maximal cell of σ_1: it could occur as an intermediate step in the calculation of a combinatorial formula of a knot invariant of degree 8 or more.

There are five types of such additional conditions. They are described in paragraphs **1**, ..., **5** of this subsection. In parentheses after the numbers **1, ..., 5** of these paragraphs we indicate mnemonic symbols denoting the corresponding conditions.

1 (⊓↾). The oriented noncrossed broken line 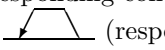 (respectively, 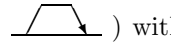) with endpoints $a < b$ in the Wilson line denotes the condition "$f(a)$ is above $f(b)$" (respectively, "$f(a)$ is below $f(b)$"), where f is our map $\mathbb{R}^1_w \to \mathbb{R}^3$. *In the picture of a chain of full dimension in $\sigma_i \setminus \sigma_{i-1}$, endpoints of different broken lines of this type cannot coincide with one another and with endpoints of chords.*

Remark 4. The condition 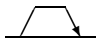 is thus very close to that expressed by the arrow 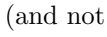 (sic!) by Polyak–Viro and coincides with it in the case of chains in the space $\mathcal{K}$ (and not in the resolved discriminant).

Remark 5. In fact, in our algorithm only such conditions of type 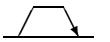 occur, while the conditions 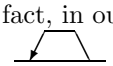 are reserved for less direct algorithms.

Definition 4. Endpoints of chords or oriented noncrossed broken lines are called the *×-points* of our picture (in contrast with φ-points, which will be defined in the following paragraph **2**). The ×-points of a picture describing a chain of full dimension are obviously matched into pairs. Such a pair of points together with the chord or broken line joining them is called a *×-pair*.

For instance, in Figure 9 we have three ×-pairs. By definition, the images of ×-points of any ×-pair under the map f_1 coincide in $\mathbb{R}^2$.

2 (↘). An oriented broken line (which can occasionally have only one segment, i.e., to be a vector) crossed by a single bar and connecting the center of a chord or a noncrossed broken line ⊓↾ with a point of the Wilson line (e.g. as in the pictures of Figure 10) tells us that the image under the map f_1 of the point (or ×-pair) corresponding to its tail lies in $\mathbb{R}^2$ to the west of the image of the point (respectively, ×-pair) corresponding to the endpoint with arrow. The endpoint of such a crossed broken line lying on the Wilson line is called a φ-point. *In the picture of a chain of full dimension in $\sigma_i \setminus \sigma_{i-1}$, a point of the Wilson line can be a φ-point of at most one such broken line.*

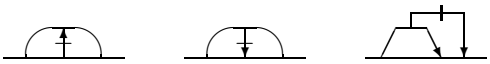

FIGURE 10. Conditions of type **2**

Remark 6. In our algorithm, only conditions of type **2** satisfying the following two restrictions occur:

a) the crossed broken line defining such a condition is directed from the center of the $\times$-pair to the φ-point;
b) the φ-point of this broken line lies between the $\times$-points of the corresponding $\times$-pair.

So, among the three pictures of Figure 10 we can get only the middle one.

Property a) follows immediately from the construction of our algorithm, and property b) follows from statement 2a of Corollary 1.

Definition 5. The tree formed by a $\times$-pair together with all once crossed oriented broken lines connecting its center with some φ-points is called a *bridge*; the crossed broken lines described in paragraph **2** its *piers*, and φ-points of such broken lines its *footholds*.

By definition, if a map $f : \mathbb{R}^1_w \to \mathbb{R}^3$ satisfies the conditions expressed by a picture with a bridge, then all the images of its footholds are "equally northern" as the image of its basic $\times$-pair, i.e., their images under the map f_2 coincide.

3 ($\mathbb{k}$). The subscript of type

(30) 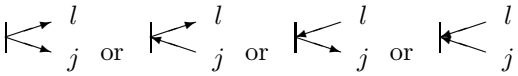

(where j and l are the numbers of $\times$-points a_j, a_l of some $\times$-pair among all active points of the picture) means that the direction "to the east" in $\mathbb{R}^2$ is a linear combination of projections to $\mathbb{R}^2$ of derivatives of f at these endpoints, and both coefficients in this combination are positive (respectively, the coefficient at the projection of $f'(a_l)$ is positive and that of $f'(a_j)$ is negative, respectively, the coefficient at $f'_1(a_j)$ is positive and that at $f'_1(a_l)$ is negative, respectively, both are negative).

These pictures say nothing on the orientations of frames formed by these projections in $\mathbb{R}^2$. In particular, the picture  (respectively, ) denotes the same condition as the same picture with numbers l and j permuted, while  denotes the same condition as 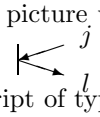

4 ($\Uparrow$ / $\Downarrow$). A subscript of type $\Uparrow^j$ (respectively, $\Downarrow^j$) means that the projection $f'_2(a_j)$ of the derivative $f'(a_j)$ of f at the jth active point to (the tangent bundle of) $\mathbb{R}^1$ is directed "to the north" (respectively, "to the south").

4a ($\|$ / $\nparallel$). A subscript $\|^j_l$ (respectively, $\nparallel^j_l$), where j and l are numbers of two active points a_j, a_l of one and the same bridge, means that the vectors $f'_2(a_j)$ and $f'_2(a_l)$ are co-directed (respectively, opposite directed) in $\mathbb{R}^1$. These conditions can be reduced to the previous ones by the *identities*

$$\|^j_l \equiv \left(\Uparrow^j \,\&\, \Uparrow^l\right) + \left(\Downarrow^j \,\&\, \Downarrow^l\right), \qquad \nparallel^j_l \equiv \left(\Uparrow^j \,\&\, \Downarrow^l\right) + \left(\Downarrow^j \,\&\, \Uparrow^l\right). \tag{31}$$

For instance, the first of these identities means that any subalgebraic chain of codimension 1 in our maximal cell, defined by some collection of our standard conditions, including the condition $\|^j_l$, is equal to the sum of two chains, all of whose other defining

FIGURE 11. Conditions of type **5**

conditions are the same, but in the first of them the condition $\|_l^j$ is replaced by the pair of conditions $\Uparrow^j$ and $\Uparrow^l$, and in the second one by $\Downarrow^j$ and $\Downarrow^l$.

5 ($\not\swarrow$). For some two $\times$-pairs (and their bridges) we can fix the information that the image of $\times$-points of one of these pairs in $\mathbb{R}^2$ is "more northern" than that of the other (i.e., its latitude is higher). We express this condition by a twice crossed (and maybe broken) arrow directed from the center of the more southern $\times$-pair to the center of the more northern one, as e.g. in Figure 11.

Remark 7. In our algorithm, this condition always has the following feature: $\times$-points of either of these two $\times$-pairs are separated in $\mathbb{R}^1_w$ by a $\times$-point of the other one.

This follows from Proposition 18b below.

Definition 6. Any chord diagram together with finitely many conditions of types **1**–**5** drawn at or under it is called an *$\mathcal{F}$-picture*. Such a picture consists of the *main part*, i.e., the chord diagram and broken lines drawn at it as in conditions of types **1, 2** or **5**, and the *subscript*, i.e., the notation of conditions of types **3** and/or **4** drawn under it. The *degree* of such a picture is the number of chords in it.

Any such picture Θ of degree i defines in the following way a subalgebraic chain $V(\Theta)$ in the cell of $\sigma_i \setminus \sigma_{i-1}$ corresponding to the chord diagram consisting of all chords of this picture.

Definition 7. A map $f : \mathbb{R}^1_w \to \mathbb{R}^3$, $f \in \mathcal{K}$, *respects* our $\mathcal{F}$-picture if it glues together the endpoints of any chord and satisfies all other conditions encoded in the picture.

Similarly to [15], a *representation* of an $\mathcal{F}$-picture in the singular knot $f \in \mathcal{K}$ is any orientation-preserving diffeomorphism $h : \mathbb{R}^1_w \to \mathbb{R}^1$ such that the map $f \circ h$ respects this $\mathcal{F}$-picture.

The subalgebraic chain $V(\Theta)$ defined by an $\mathcal{F}$-picture Θ of degree i is the subvariety of the corresponding maximal cell in $\sigma_i \setminus \sigma_{i-1}$, in which any point of this cell (i.e., a triple (C, f, t) as in (22)) participates with multiplicity equal to the algebraic number of representations of our picture in the singular knot f.

In the present paper we consider only $\mathbb{Z}_2$-homology; therefore the "algebraic number" means just the parity of the number of representations. In a future work the orientations of these varieties will be specified, and the "algebraic numbers" will take any integer values.

In nondegenerate cases (if we have no contradictory conditions, like e.g. the pictures $\overset{l}{\underset{j}{\lessdot}}$, $\Uparrow^l$ and $\Uparrow^j$ simultaneously) the chain $V(\Theta)$ defined by an $\mathcal{F}$-picture Θ has full dimension in the corresponding maximal cell.

Example 4. The arrow diagrams of [15] can be considered as $\mathcal{F}$-pictures of degree 0 (i.e., with empty chord diagrams), having only conditions of type **1** ($\uparrow$). In [15] a natural accounting of signs of corresponding representations was specified. In our terms, this allows one to relate with any such diagram an integral subalgebraic chain in the space $\mathcal{K}$. Goussarov's theorem [8] says that any knot invariant of finite degree can be realized as a rational linear combination of such chains.

Definition 8. An $\mathcal{F}$-*block* is an arbitrary subalgebraic chain $V(\Theta)$ *of full dimension* in a maximal cell of $\sigma_i \setminus \sigma_{i-1}$, defined by an $\mathcal{F}$-picture Θ. By the *sum* of several $\mathcal{F}$-pictures we mean the homological sum of corresponding $\mathcal{F}$-blocks.

Remark 8. We could consider only normalized pictures in which signs $\Uparrow^j$ or $\Downarrow^j$ are put at *any* active point. Indeed, any $\mathcal{F}$-picture, some r active points of which are free of such signs, can be decomposed into the sum of 2^r similar pictures with all possible combinations of such arrows. Also, we could consider only the pictures with *linear* orderings of bridges from the south to the north (indicated by twice-crossed oriented broken lines $\not\swarrow$ as in paragraph **5**), decomposing any picture with only a partial order into the sum of pictures corresponding to all its extensions to linear orders.

However, all this would increase the number of summands exponentially, which we do not want to have. Any planar picture like a (singular) knot diagram carries all this garbage information (and much more), which makes the algorithms solving our problem and exploiting actively the graphical calculus not very efficient for real computerization.

Remark 9. The *virtual knots* of [10], [8] (and equivalence classes of virtual knots) can also be realized as domains (and, hence, chains of full dimension) in the space of maps $\mathbb{R}^1 \to \mathbb{R}^3$. Indeed, any virtual knot diagram defines a subset in $\mathcal{K}$, consisting of all maps $f : \mathbb{R}^1 \to \mathbb{R}^3$ having the given projection $f_1 : \mathbb{R}^1 \to \mathbb{R}^2$, satisfying certain inequalities over the classical crossing points, and behaving arbitrarily (maybe having intersections) over the virtual ones. The union of such subsets corresponding to a class of isotopic diagrams (up to the usual isotopies of $\mathbb{R}^2$ fixed at infinity) is obviously an open domain in $\mathcal{K}$. Finally, to any virtual knot (i.e., according to [10], [8], to an equivalence class of such isotopy classes) we associate the union of all such domains corresponding to these isotopy classes, augmented by the "walls" between them, i.e., by all maps f close to which this union is dense.

Similarly, the singular virtual knots of [8] can be thought of as certain domains in appropriate terms of the simplicial resolution of the discriminant.

Remark 10. Conditions **1**–**5** satisfy many relations. Here are several examples.

(1) Besides (31), conditions $\|^j_l$ and $\nparallel^j_l$ satisfy also identities

(32) $\|^j_l = \overset{l}{\underset{j}{\swarrow\!\!\swarrow}} + \overset{l}{\underset{j}{\swarrow\!\!\searrow}}$ and $\nparallel^j_l = \overset{l}{\underset{j}{\swarrow\!\!\swarrow}} + \overset{l}{\underset{j}{\leftarrow\!\!\swarrow}}$

relating them to conditions of type **3**; see (30).

(2) Any condition of type **3** on a $\times$-pair, together with a condition of type **4** on some point of this pair, implies a condition of type **4** on its second point.

(3) We also have trivial relations of the following type. The sum of four almost coinciding pictures, whose different unique fragments are subscripts of four types (30) with the same numbers j and l is equal to the single picture with these subscripts removed. Similarly, the sum of two almost coinciding pictures with subscripts $\Uparrow^j$ and $\Downarrow^j$ is equal to a single picture with this subscript removed.

2.3. **Standard degenerations.** We are going to study some subalgebraic chains of codimension one in our maximal cells, namely, the chains constituting the boundaries of all $\mathcal{F}$-blocks considered in the previous subsection. They can be achieved by the following standard degenerations of singular knots from these full-dimensional blocks.

X. One additional self-intersection can occur at some pair of points distant from the endpoints of chords and also from φ-points; see Figure 12.

R1, R2, R3: Degenerations occurring at the standard Reidemeister moves; see Figure 13. In the left-hand bottom picture it is assumed that the derivative of f at the

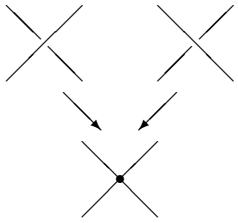

FIGURE 12. **X**-degenerations

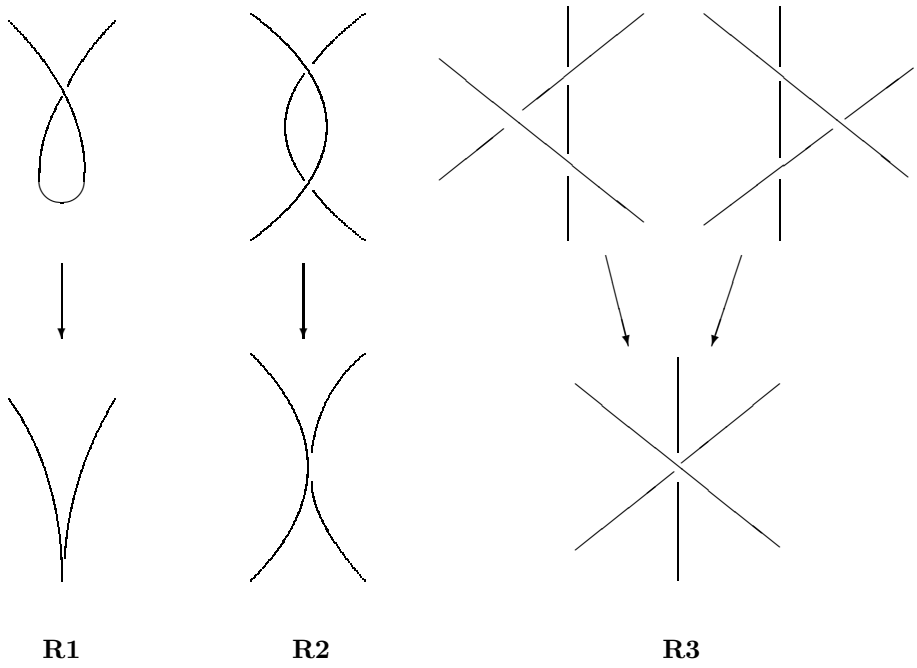

FIGURE 13. Standard Reidemeister degenerations

"cusp" point is not equal to zero and is directed "up" (respectively, "down") if the parameter in $\mathbb{R}^1_w$ grows "from the right to the left" (respectively, "from the left to the right") in this picture.

$\tilde{\mathbf{R}}$2, $\tilde{\mathbf{R}}$3: Reidemeister moves of singular knots; cf. [3]. In the left-hand bottom picture of Figure 14 it is assumed that the projections to $\mathbb{R}^2$ of two branches at the intersection point are tangent, but the tangent vectors of these branches themselves form a nonzero angle in the vertical plane containing them.

Since we have fixed a flag of directions in $\mathbb{R}^2$, there are many classes of nonisotopic degenerate curves of these types (via isotopies preserving the foliations of $\mathbb{R}^3$ into fibers of projections ρ_1 and ρ_2 along these directions, but not the particular fibers): in total 4 classes of type **R1**, 2 of type **R2**, 6 of type **R3**, 2 of type $\tilde{\mathbf{R}}$**2** and 6 of type $\tilde{\mathbf{R}}$**3**. If we distinguish orientations of branches of our curve participating in the degeneration, then the number of possibilities will be even more: it should be multiplied additionally by the corresponding power of 2.

M2, M3, M4 (cf. [14]): essential changes of the Morse structure of the function $f_2 \equiv \rho_2 \circ f : \mathbb{R}^1_w \to \mathbb{R}^1$; see Figure 15. (The numbers 2, 3 and 4 in their notation are the

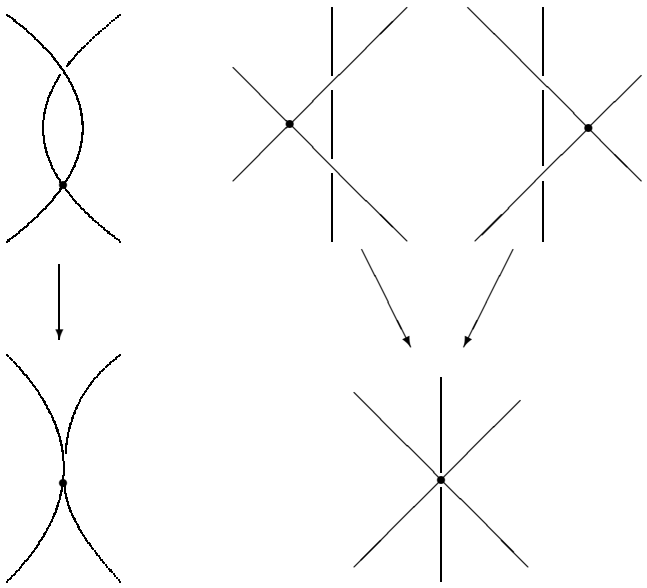

FIGURE 14. Reidemeister degenerations of singular knots

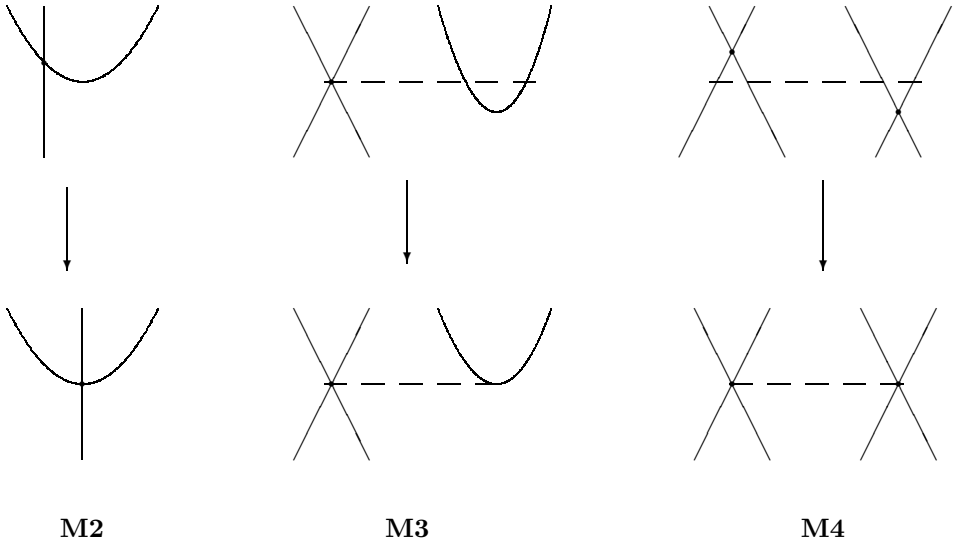

FIGURE 15. Essential Morse degenerations

numbers of involved branches of the curve.) The crossing points of solid lines in these pictures denote any possible $\times$-pairs, i.e., over/under crossings corresponding to oriented noncrossed broken lines, or intersection points corresponding to chords.

Remark 11. The explicit formulas for the homological boundaries of $\mathcal{F}$-blocks (which we shall study in §3 below) are formalizations of these degenerations applied to points (22) of these $\mathcal{F}$-blocks. From this point of view, each of the degenerations **R3** and $\tilde{\mathbf{R}}\mathbf{3}$ should be

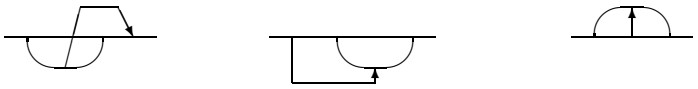

FIGURE 16. Conditions of type $\bar{\mathbf{2}}$

separated into two essentially different types. Namely, in any of these degenerations three double points of the knot diagram meet. The algebraic expression of the corresponding component of the boundary of our $\mathcal{F}$-block depends essentially on whether all three points or only some two of them correspond to $\times$-pairs of the initial $\mathcal{F}$-picture. (If only one or none, then the corresponding degeneration causes no contribution to the boundary.)

2.4. **Chains of codimension one.** In this subsection we specify a class of subalgebraic chains of codimension one in the maximal cells of $\sigma_i \setminus \sigma_{i-1}$. The boundaries of all $\mathcal{F}$-blocks described in §2.2 and participating in our algorithm can be represented as sums of chains of this class (plus something in vice-maximal cells and in σ_{i-1}). Any such chain of codimension 1 can be distinguished by a collection of the same conditions as in §2.2 plus one condition of "equality" type or a nongeneric coincidence of some active points participating in the description of $\mathcal{F}$-blocks; the latter condition may be supplied by a new "satellite" condition of inequality type. These standard chains of codimension one will be called $\mathcal{B}$-*blocks*, and the pictures distinguishing them the $\mathcal{B}$-*pictures*.

These pictures and the corresponding equality-type conditions are described in the following items $\bar{\mathbf{1}}$–$\bar{\mathbf{6}}$. In round brackets after the numbers of items we indicate their mnemonic symbols, and in square brackets we indicate the types of degenerations at which a singular knot satisfying the corresponding condition can occur.

In paragraphs $\bar{\mathbf{2}}$**!**, $\bar{\mathbf{4}}$**!**, $\bar{\mathbf{5}}$**!**, and $\bar{\mathbf{6}}$**!** we describe important linear combinations of subalgebraic chains distinguished by the conditions from paragraphs $\bar{\mathbf{2}}$, $\bar{\mathbf{4}}$, $\bar{\mathbf{5}}$, and $\bar{\mathbf{6}}$ respectively, and in paragraphs $\bar{\mathbf{2}}$**a**, $\bar{\mathbf{2}}$**b**, $\bar{\mathbf{3}}$**a**/$\bar{\mathbf{3}}$**b**, $\bar{\mathbf{4}}$**!!**, $\bar{\mathbf{5}}$**a**, and $\bar{\mathbf{5}}$**b** we describe corresponding satellite inequality-type conditions.

$\bar{\mathbf{1}}$ **(** $\sqcap$ **) [X].** One nonoriented broken line  denotes the condition $f(a) = f(b)$ on its endpoints a, b. *These points cannot coincide with endpoints of chords of our picture.* A chain, whose notation contains such a condition, appears as a piece of the boundary of the $\mathcal{F}$-block $V(\Theta)$ of full dimension, described by the same picture, but with this nonoriented broken line replaced by the oriented (to either side) one; see Figure 12 and formula (38). Moreover, such nonoriented broken lines appear from the chords when we take boundary operators $\bar{H}_*(\sigma_{i+1} \setminus \sigma_i) \to \bar{H}_*(\sigma_i \setminus \sigma_{i-1})$ of our spectral sequence; see §3.7 and formulas (8), (14), (51), and (92)–(100).

The pair of points connected by such a broken line also is considered as a $\times$-*pair*. It carries all the possibilities specified in §2.2 for such pairs. In particular, such a broken line forms a *bridge*, and conditions (30) ($\vdash$) can be imposed on the endpoints of such a nonoriented broken line. Also, the conditions of type $\Uparrow^j$ or $\Downarrow^j$ can be attached at these endpoints.

$\bar{\mathbf{2}}$ **(** $\cap$ **) [$\tilde{\mathbf{R}}$3].** It can happen that a self-intersection point of a singular knot, described by a chord, lies in $\mathbb{R}^3$ above or below some nonsingular point of the knot. This condition is described by a noncrossed broken line (maybe consisting of only one link!) connecting the corresponding point of the Wilson line and the center of the chord and oriented to the point (or the chord) whose image in $\mathbb{R}^3$ is higher; see e.g. Figure 16.

In the description of our chains of codimension 1, any condition of type (30) can be imposed at any two of three active points of the Wilson line participating in the figure consisting of such a broken line and chord.

Remark 12. All conditions of type $\bar{\mathbf{2}}$, occurring in our algorithm, satisfy the following additional condition. If an endpoint of the noncrossed oriented broken line, participating in the notation of this condition, lies on the Wilson line to one and the same side from both endpoints of this chord, then this broken line is oriented to the right in $\mathbb{R}^1_w$. Indeed, only such $\mathcal{B}$-blocks can occur as boundary components of $\mathcal{F}$-blocks satisfying the restriction from Remark 5.

$\bar{\mathbf{2}}$a ($\Lsh$). The additional condition of type 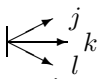 (where j, k, l are the numbers of active points a_j, a_k, a_l participating in a configuration of type $\bar{\mathbf{2}}$) means that the vector $f_1'(a_k)$ (i.e., the projection of the derivative $f'(a_k)$ to $\mathbb{R}^2$) is a linear combination of vectors $f_1'(a_j)$ and $f_1'(a_l)$ with positive coefficients.

$\bar{\mathbf{2}}$b ($\prec$). Conversely, the condition 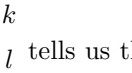 tells us that none of these three vectors in $\mathbb{R}^2$ lies in the angle between the other two.

These conditions **$\bar{\mathbf{2}}$a** or **$\bar{\mathbf{2}}$b** can arise at degenerations of type **$\tilde{\mathbf{R}}$3** if all three double points of the singular knot diagram colliding at this degeneration correspond to $\times$-pairs of the original $\mathcal{F}$-picture; see Remark 11.

These two conditions can be expressed also through more standard conditions $\Lsh$ described in item **3** of §2.2. Indeed, the vectors $f_1'(a_j)$ and $f_1'(a_l)$ should satisfy exactly one of four conditions of type **3**. Correspondingly, the condition **$\bar{\mathbf{2}}$a** splits into the sum of four chains:

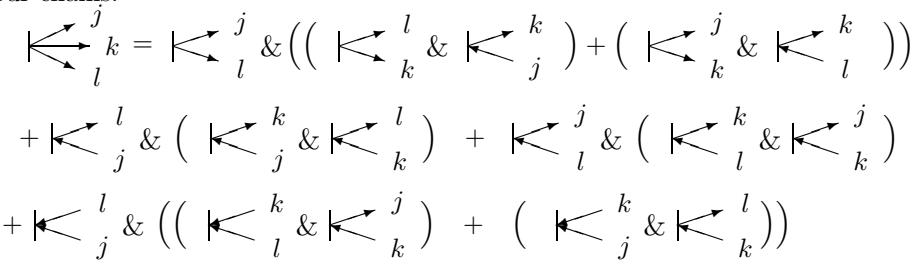

$\bar{\mathbf{2}}$! (). Suppose that some two chains of codimension 1 ("$\mathcal{B}$-blocks") in M are defined by sets of conditions coinciding up to the orientation of the noncrossed arrow participating in the degeneration $\bar{\mathbf{2}}$. Then the sum of these two chains will be expressed by a single picture with all the same furniture, but with these opposite arrows replaced by the once crossed nonoriented broken line, e.g. as follows:

In general, a nonoriented broken line crossed by one bar means that the projections to $\mathbb{R}^2$ of the points or $\times$-pairs corresponding to the endpoints of this broken line coincide. The variety defined by this condition is the union of two similar varieties with this crossed nonoriented broken line replaced by two differently oriented noncrossed broken lines. However in our algorithm this condition can appear only in combination with a chord (as in paragraph $\bar{\mathbf{2}}$ above) or with a noncrossed arrow (as in paragraph $\bar{\mathbf{3}}$ below). The endpoint of such a nonoriented crossed broken line lying on the Wilson line also qualifies as a $\times$-*point*.

$\bar{\mathbf{3}}$ ( ) **[R3].** Exactly one endpoint of some noncrossed oriented broken line can coincide with that of exactly one other such broken line. The corresponding conditions

satisfy obvious relations like

(33) 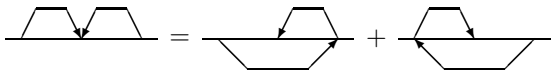

and

(34) 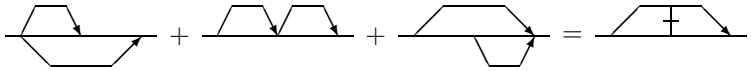

$\bar{3}$a/$\bar{3}$b. Again, the conditions of type 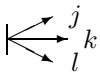 or 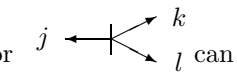 can be imposed on the derivatives of maps f_1 at three points participating in such a configuration; see items **$\bar{2}$a, $\bar{2}$b** above. This happens if our chain occurs at the degeneration of type **R3**, and all three double points of the planar knot diagram colliding at this degeneration define $\times$-pairs of the initial $\mathcal{F}$-picture.

$\bar{4}$ ($\vee$) [$\tilde{\mathbf{R}}$2]. A subscript of type

(35) 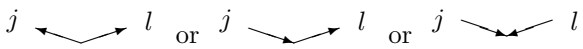

(where j and l are numbers of endpoints a_j, a_l of one and the same chord) means that the direction "up" in $\mathbb{R}^3$ is a linear combination of derivatives $f'(a_l)$ and $f'(a_j)$, both with positive coefficients (respectively, $f'(a_l)$ with a positive coefficient and $f'(a_j)$ with a negative one, respectively, both with negative coefficients).

$\bar{4}$! ($\rightrightarrows$, $\not\rightrightarrows$) [R2]. a) The condition  (where l and j are numbers of points a_l, a_j of one and the same $\times$-pair) means that the projections of $f'(a_l)$ and $f'(a_j)$ to $\mathbb{R}^2$ are co-directed. If our $\times$-pair is a chord, then the corresponding condition can occur also as the sum of two conditions defined in the previous paragraph:

(36) 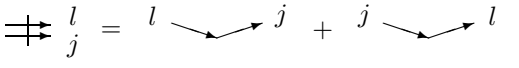

b) The condition  means that the projections of $f'(a_l)$ and $f'(a_j)$ to $\mathbb{R}^2$ are of opposite directions. If a_l and a_j are endpoints of a chord, then the corresponding condition can occur also as the sum

(37) 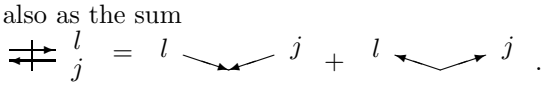

Any of these conditions **a), b)** is symmetric over the letters l and j.

$\bar{4}$!! ($\emptyset$). The conditions $\bar{4}$, **$\bar{4}$!a** and **$\bar{4}$!b** can be escorted by an inequality-type condition, indicating which of the local branches of the plane curve $f_1(\mathbb{R}^1_w)$ lies further to the west in $\mathbb{R}^2$. This condition is denoted as follows: 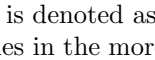 , where l is the number of the active point whose image lies in the more western branch. An obvious relation: the sum of two $\mathcal{B}$-blocks each containing such a condition and obtained one from the other only by the permutation of j and l in this condition is equal to the single block without this condition.

$\bar{5}$ ($\mapsto$). [M2, M3]. The condition $j \mapsto$ or $j \longmapsto$, where j is the number of an active point a_j, means that the projection of the vector $f'(a_j)$ to $\mathbb{R}^2$ is directed to the east (respectively, to the west).

$\bar{5}$! ($\leftrightarrow$). The sum of these two conditions is denoted by ; it means simply that $f'_2(a_j) = 0$.

$\bar{5}$a ($\twoheadrightarrow$). If the projection f'_2 of the first derivative to the "meridian" line $\mathbb{R}^1$ is equal to zero, as follows from the conditions of type $\bar{5}$ or **$\bar{5}$!**, then the projection of the second derivative can be positive or negative; the latter conditions are expressed respectively by

a b

FIGURE 17. Clinching bridges

the notation $\Uparrow^j$ or $\Downarrow^j$. By definition, these conditions can occur only in combination with conditions of type $\bar{\mathbf{5}}$ or $\bar{\mathbf{5}}$**!**.

$\bar{\mathbf{5}}$b ( ). An important linear combination of the above-described conditions is expressed by the subscript of type $\overset{j}{l}$ (which also can appear only in combination with a condition of type $\bar{\mathbf{5}}$ or $\bar{\mathbf{5}}$**!**). It is equal to $\left(\Downarrow^j \& \Downarrow^l\right) + \left(\Uparrow^j \& \Uparrow^l\right)$ and tells us that the vectors $f_2''(a_j)$ and $f_2'(a_l)$, i.e., projections to the meridian $\mathbb{R}^1$ of the second derivative $f''(a_j)$ and the first derivative $f'(a_l)$, are directed into one and the same side. A similar picture with opposite directions

$$\overset{j}{l} \equiv \left(\Downarrow^j \& \Uparrow^l\right) + \left(\Uparrow^j \& \Downarrow^l\right)$$

can also appear.

$\bar{\mathbf{6}}$a, $\bar{\mathbf{6}}$b [M4]. (Clinching bridges.) For some two different bridges, some footholds of one of them can coincide with $\times$-points or footholds of the second, and maybe simultaneously some footholds of the second bridge coincide with one or both of the $\times$-points of the first one; however the $\times$-points of these bridges do not meet. This degeneration is of type $\bar{\mathbf{6}}$**a** if only footholds of different bridges meet at it, and of type $\bar{\mathbf{6}}$**b** if at least one of them meets a $\times$-point of the other bridge. For examples; see Figures 17a and 17b respectively. In both pictures the segment of the Wilson line of the nondegenerate map, contracted at this collision, is marked by thickening.

As in Figure 17b, the limit condition arising at the degeneration of type $\bar{\mathbf{6}}$**b** shown there from the condition expressed by the pier (and consisting in the fact that the image of $\times$-points of one $\times$-pair in $\mathbb{R}^2$ lies to the east from that of the other one) is encoded by a once crossed broken line connecting the centers of these $\times$-pairs.

Remark 13. In our algorithm there cannot occur clinching bridges such that both $\times$-points of one $\times$-pair lie to the left from both $\times$-points of the other one in $\mathbb{R}^1_w$. More precisely, if our clinching bridges have a common foothold, then this foothold is placed between the $\times$-points of either $\times$-pair; if the bridges are connected by a crossed arrow directed from one $\times$-pair to the other one (as in Figure 17b), then at least one of the $\times$-points of the $\times$-pair *to which* the crossed arrow is directed should lie between the $\times$-points of the other $\times$-pair.

This follows from the fact that before the clinch the bridges satisfy condition b) of Remark 6.

$\bar{\mathbf{6}}$! ( ). The *normal* pair of clinching bridges is a sum of two conditions as in the right-hand part of Figure 18 (i.e., of conditions expressed by once crossed broken lines with opposite orientations, connecting one and the same $\times$-pairs; this sum is equal to the single condition that the images of these two $\times$-pairs in $\mathbb{R}^2$ have equal latitudes) satisfying the following conditions:

a) the $\times$-points of either of these two $\times$-pairs are separated in $\mathbb{R}^1_w$ by a $\times$-point of the other $\times$-pair;

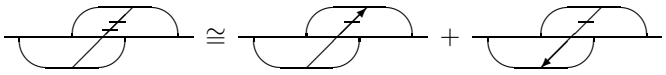

FIGURE 18. Normal couple of bridges of type $\bar{\mathbf{6}}$**!**

b) both these $\times$-pairs have no piers;
c) both these $\times$-pairs are the chords (and not the broken lines).

Such a sum of two conditions is denoted by the single picture, in which these two once crossed oriented broken lines are replaced by the nonoriented twice crossed broken line; see the left-hand side of Figure 18.

In general, a nonoriented twice crossed broken line means that the projections to $\mathbb{R}^1$ of points or $\times$-pairs, corresponding to its endpoints, coincide. The variety distinguished by this condition is the union of two varieties defined by conditions expressed by once crossed broken lines having the same endpoints but oriented to different sides. However, in our algorithm this condition occurs only in combination with two $\times$-pairs connected by such a broken line, as in condition $\bar{\mathbf{6}}$**!**.

Remark 14. In the algorithms calculating the higher cohomology classes we shall need many other singularity classes; the most important of them are as follows (see [24]).

$\bar{\mathbf{7}}$. The subscript $\uparrow^j$ (respectively, $\downarrow^j$) means that the derivative $f'(a_j)$ is directed up (respectively, down) in $\mathbb{R}^3$.

$\bar{\mathbf{7}}$**!**. The subscript $\updownarrow^j$ means that $f'_1(a_j) = 0$. Of course $\updownarrow^j = \uparrow^j + \downarrow^j$.

However these conditions cannot occur in our calculations related with knot invariants; see Proposition 6.

Definition 9. A $\mathcal{B}$-*picture* is an arbitrary chord diagram supplied with finitely many additional conditions of types **1**–**5** of §2.2 and exactly one condition of type $\bar{\mathbf{1}}$, $\bar{\mathbf{2}}$, $\bar{\mathbf{2}}$**!**, $\bar{\mathbf{3}}$, $\bar{\mathbf{4}}$, $\bar{\mathbf{4}}$**!a**, $\bar{\mathbf{4}}$**!b**, $\bar{\mathbf{5}}$, $\bar{\mathbf{5}}$**!**, $\bar{\mathbf{6}}$**a**, $\bar{\mathbf{6}}$**b**, or $\bar{\mathbf{6}}$**!** from §2.4, drawn at or under it; moreover, a condition $\bar{\mathbf{2}}$ or $\bar{\mathbf{2}}$**!** can be supplied with a condition of type $\bar{\mathbf{2}}$**a** or $\bar{\mathbf{2}}$**b**; a condition of type $\bar{\mathbf{3}}$ can be supplied with a condition of type $\bar{\mathbf{3}}$**a** or $\bar{\mathbf{3}}$**b**; a condition $\bar{\mathbf{4}}$ or $\bar{\mathbf{4}}$**!a** or $\bar{\mathbf{4}}$**!b** can be completed by a condition of type $\bar{\mathbf{4}}$**!!**; a condition $\bar{\mathbf{5}}$ or $\bar{\mathbf{5}}$**!** can be completed by a condition $\bar{\mathbf{5}}$**a** or $\bar{\mathbf{5}}$**b**.

Conditions of types **1, 2, 3, 4, 4a, 5,** $\bar{\mathbf{2}}$**a,** $\bar{\mathbf{2}}$**b,** $\bar{\mathbf{3}}$**a,** $\bar{\mathbf{3}}$**b,** $\bar{\mathbf{4}}$**!!,** $\bar{\mathbf{5}}$**a** or $\bar{\mathbf{5}}$**b** are called *inequality-type conditions*, while conditions $\bar{\mathbf{1}}$**,** $\bar{\mathbf{2}}$**,** $\bar{\mathbf{2}}$**!,** $\bar{\mathbf{3}}$**,** $\bar{\mathbf{4}}$**,** $\bar{\mathbf{4}}$**!a,** $\bar{\mathbf{4}}$**!b,** $\bar{\mathbf{5}}$**,** $\bar{\mathbf{5}}$**!,** $\bar{\mathbf{6}}$**a,** $\bar{\mathbf{6}}$**b,** and $\bar{\mathbf{6}}$**!** are called *equality-type conditions* or *degenerations*.

Any $\mathcal{B}$-picture defines a subalgebraic chain in the cell encoded by its chord diagram. This chain is covered by the set of all points (C, f, t) as in (22) such that the picture has representations in f: these points should be taken with multiplicities equal to the parities of numbers of these representations.

In interesting cases such a subvariety has codimension one in the cell of $\sigma_i \setminus \sigma_{i-1}$ corresponding to its chord diagram. However; see §3.2.1 for some situations when its codimension is greater.

Definition 10. Any subalgebraic chain *of codimension one* defined by a $\mathcal{B}$-picture in the cell corresponding to the chord diagram of this picture is called a $\mathcal{B}$-*block*.

Remark 15. Conditions **1**–**5** and $\bar{\mathbf{1}}$–$\bar{\mathbf{6}}$**!** (or, more precisely, the chains distinguished by these conditions) satisfy many relations. For a few of them; see Lemmas 6 and 9.

3. The boundary operator

The homological boundary of any $\mathcal{F}$-block is naturally divided into three parts contained respectively

a) in the same maximal cell of the term $\sigma_i \setminus \sigma_{i-1}$,

b) in vice-maximal cells of $\sigma_i \setminus \sigma_{i-1}$, and

c) in the lower term $\sigma_{i-1} \setminus \sigma_{i-2}$ of the main filtration of σ. In §§3.1–3.5 of this section we describe part a), in §3.6 part b), and in §3.7 part c).

Let us recall that for any $i \geq 1$ the maximal cells of the canonical cell decomposition of the term $\sigma_i \setminus \sigma_{i-1}$ of the resolved discriminant are in one-to-one correspondence with equivalence classes of i-chord diagrams.

Proposition 3. *For any maximal cell of the canonical cell decomposition of $\sigma_i \setminus \sigma_{i-1}$, $i \geq 0$, and any $\mathcal{F}$-block $V(\Theta)$ in it (see Definition 8), the boundary of this $\mathcal{F}$-block in this maximal cell is equal to a finite sum of $\mathcal{B}$-blocks, defined by $\mathcal{B}$-pictures, any of which has no more active points and no more standard conditions* **1–5** *and* **$\bar{1}$–$\bar{6}$!** *than the initial $\mathcal{F}$-picture Θ specifying the $\mathcal{F}$-block $V(\Theta)$.*

The proof of this proposition follows from the list of degenerations given in §2.3. In §§3.1–3.5 below we describe these boundary components explicitly. Although we deal here with $\mathbb{Z}_2$-chains only, a similar statement is true in the case of any coefficient group and follows from the same considerations.

3.1. **Degenerations preserving the number of active points.** The most important for us are the degenerations of $\mathcal{F}$-blocks that do not decrease the number of active points. They can be formulated as degenerations of the conditions themselves, and not of the configurations of active points. They are listed in the following eight equations:

(38) 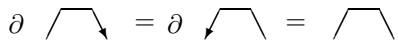

(39) 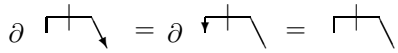

(40) 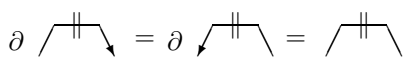

(41) 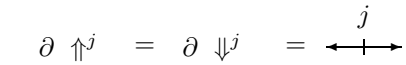

(42) 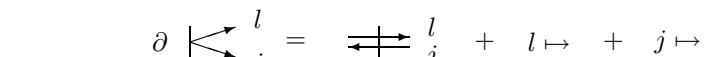

(43) 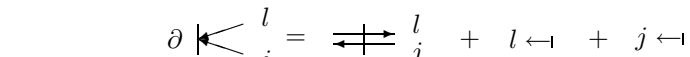

(44) 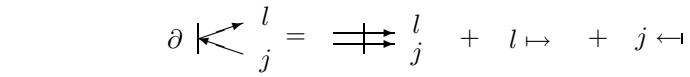

(45) 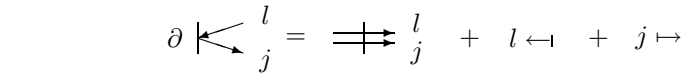

Namely, if the $\mathcal{F}$-picture of our $\mathcal{F}$-block contains some fragment indicated in the left-hand side of some of these equations under the ∂ sign, then the boundary of this block contains the $\mathcal{B}$-block in whose picture this fragment is replaced by an arbitrary summand of the right-hand side of the same equation (i.e., of the part not containing the sign ∂). Of course, the broken lines in formulas (38)–(40) can have other shapes than the ones drawn here.

3.2. **Collisions of active points: main notions.** The other part of the boundary operator, formulated in terms of degenerations of active point configurations, is more difficult to describe because of the multitude of possibilities. Such a description occupies Subsections 3.2–3.5. Roughly speaking, for each collection of segments bounded by active points of the $\mathcal{F}$-picture, we have to

a) contract all these segments into points,

b) consider the limit set to whose points the points (22) of our $\mathcal{F}$-block tend when the active points of corresponding maps $\mathbb{R}^1_w \to \mathbb{R}^3$ undergo such a collision,

c) check whether the codimension of this limit set is equal to 1, and

d) describe the intersection of the homological boundary of our $\mathcal{F}$-block with this set in terms of our standard conditions **1**–**5** and $\bar{\mathbf{1}}$–$\bar{\mathbf{6}}$**!**.

Let us give exact definitions.

Definition 11. Let us have an $\mathcal{F}$-block $V(\Theta)$ in a maximal cell of $\sigma_i \setminus \sigma_{i-1}$, specified by an $\mathcal{F}$-picture Θ of degree i (i.e., with i chords), and a marked collection of disjoint segments in the Wilson line of this picture, any of which is bounded by some (not necessarily neighboring) active points of this picture. The *geometric contraction* of $V(\Theta)$ along this collection of segments is a subset in the same maximal cell, contained in the closure of the support of the chain $V(\Theta)$, and defined by the following condition: the point $X = (C, f, t)$ belongs to this subset if and only if there exists a continuous curve $\lambda : [0, \varepsilon] \to \sigma_i \setminus \sigma_{i-1}$ (i.e., a family of triples (C_τ, f_τ, t_τ) as in (22) depending continuously on the parameter $\tau \in [0, \varepsilon]$) and continuous family of homeomorphisms $h_\tau : \mathbb{R}^1_w \to \mathbb{R}^1$, $\tau \in (0, \varepsilon]$, such that

(1) $\lambda(0) = X$ (i.e., $C_0 = C, f_0 = f, t_0 = t$);
(2) for any $\tau \in (0, \varepsilon]$, $\lambda(\tau)$ lies in the support of $V(\Theta)$, and h_τ transforms the chord diagram of the picture Θ into C_τ and is a representation of the $\mathcal{F}$-picture Θ in f_τ;
(3) for τ tending to $+0$, the images of all marked segments under the corresponding maps h_τ become arbitrarily small.

The geometric contraction along a collection of segments is *contradictory*, if the codimension of this limit set in the corresponding maximal cell of $\sigma_i \setminus \sigma_{i-1}$ is greater than one.

Proposition 4. *For any $\mathcal{F}$-block $V(\Theta)$ and any collection of disjoint segments in $\mathbb{R}^1_w$, bounded by the active points of its $\mathcal{F}$-picture Θ, either the geometric contraction of $V(\Theta)$ along this collection is contradictory or the intersection of the homological boundary of the chain $V(\Theta)$ with this geometric contraction is a $\mathcal{B}$-block.*

A proof of this proposition follows from the explicit description of these contractions, which occupies Subsections 3.2.2–3.5.

Definition 12. The *homological contraction* of the $\mathcal{F}$-block $V(\Theta)$ along our collection of segments is the subalgebraic chain of codimension 1 in our cell, equal to 0 if the geometric contraction along this collection is contradictory, and otherwise represented by the intersection of the homological boundary of the chain $V(\Theta)$ with this geometric contraction.

Proposition 5. *For any $\mathcal{F}$-block $V(\Theta)$, contained in some maximal cell of the term $\sigma_i \setminus \sigma_{i-1}$, the intersection of its homological boundary $\partial V(\Theta)$ with the same maximal cell is equal to the sum of*

a) homological contractions of the chain $V(\Theta)$ along all collections of segments bounded by active points of the picture Θ, and of

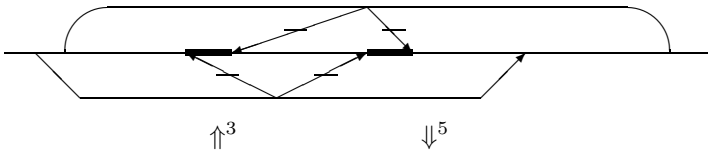

FIGURE 19. A contradictory pair of segments

b) all $\mathcal{B}$-blocks, whose pictures are obtained from Θ by replacing some fragment of Θ, shown in the left-hand side of any of formulas (38)–(45) *by an arbitrary summand of the right-hand side of the same formula.*

This proposition follows immediately from the definitions. □

3.2.1. *Several important examples of contradictory contractions.* Contradictory geometric contractions occur, in particular, in the following situations.

(1) At least two marked segments are "independent", i.e., their endpoints are not joined by any chain of chords and broken lines of the original $\mathcal{F}$-picture.
(2) A marked segment contains more than three active points.
(3) Some marked segment contains two endpoints of (not necessarily different) chords. In this case the resulting limit variety lies in the union of other (non-maximal) cells of $\sigma_i \setminus \sigma_{i-1}$.
(4) A marked segment contains two active points of two different bridges with conditions $\Uparrow^j$ and $\Downarrow^l$ imposed at these two points. In this case for any point f of the limit variety the corresponding plane curve $f_1(\mathbb{R}^1_w)$ has on one horizontal line a point with $f_2' = 0$ and either two $\times$-pairs or a triple point.
(5) A marked segment contains two points of two different bridges, at least one of these points is supplied with the subscript $\Uparrow^j$, and these two bridges are connected by a twice crossed arrow directed from the bridge containing the right-hand point of the segment to the bridge containing the left-hand point. In this case the point obtained from the shrinked segment will satisfy both conditions $\Uparrow$ and $\Downarrow$. Replacing in our assumptions $\Uparrow^j$ by $\Downarrow^j$ and simultaneously changing the orientation of the broken line, we also obtain an obstruction to the contraction.
(6) Two segments are marked. The left-hand endpoints of these segments are active points of one bridge, and the right-hand endpoints belong to the other bridge. One of the endpoints of the first segment is supplied with the subscript $\Uparrow^l$, and one of the endpoints of the second with the subscript $\Downarrow^j$. Then the simultaneous shrinking of these two segments is contradictory. (For an example, see Figure 19 where two marked segments are thickened, namely the segments bounded by the third and the fourth (respectively, by the fifth and the sixth) active points of the picture.) Indeed, the sign $\Uparrow^3$ in this picture shows that immediately before the contraction the bridge containing the points 1, 3, 5 and 7 was more southern than the other bridge, while the sign $\Downarrow^5$ says that it was more northern than it. Another version: we have the condition $\Uparrow$ (or $\Downarrow$) at some point of one segment, and the same condition at some point of the second one, but one of these segments is bounded by a point of the first bridge from the left and by a point of the second from the right, and vice versa for the second segment.
(7) A marked segment contains two points of one and the same bridge, and we have conditions $\Uparrow^j$ and $\Uparrow^l$ associated with these endpoints. In this case any limit curve will satisfy two conditions $f_2' = 0$ and $f_2'' = 0$ at some active point. In a similar

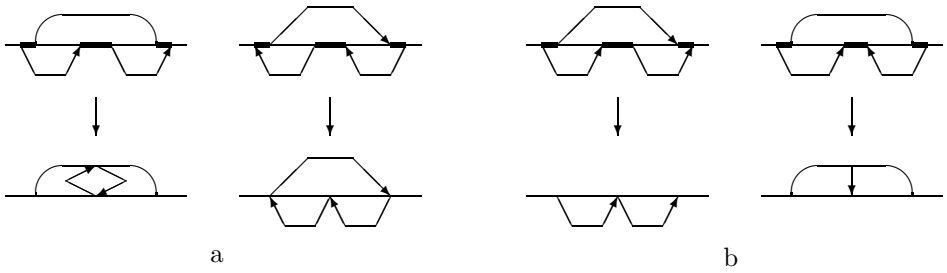

FIGURE 20. Contradictory and reduced contractions of pictures

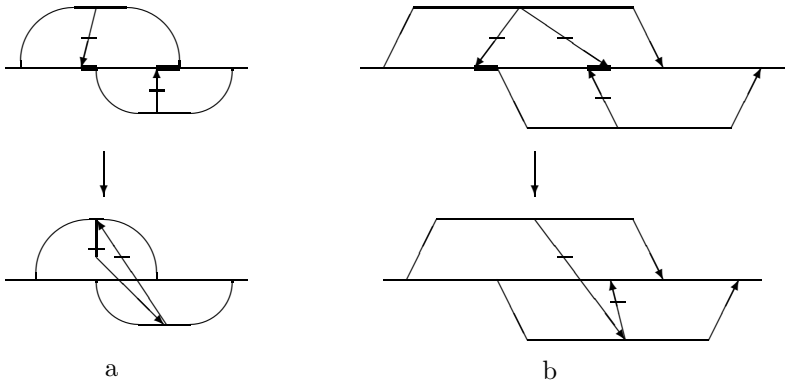

FIGURE 21. Some other contradictory and reduced contractions

way, the pair of conditions $\Downarrow^j$ and $\Downarrow^l$ on such two points does not allow us to contract such a segment.

(8) After the contraction we obtain a *closed* chain of inequalities on the heights of images of several points which came to one and the same vertical line in $\mathbb{R}^3$; see Figure 20a. To formalize this condition, consider the graph, whose vertices are active points of the initial $\mathcal{F}$-picture Θ, while the edges are its chords, oriented noncrossed broken lines, and also our marked segments of the Wilson line (or parts of such segments containing more than two active points). An *admissible path* along this graph can go along the chords and marked segments in any direction, but going along the broken lines it should follow their orientation. If this graph has a nontrivial admissible *cycle*, then the contraction along these marked segments is contradictory. For instance, the contraction of three thickened segments in any of two $\mathcal{F}$-pictures in the top row of Figure 20a is contradictory.

(9) One more example of contradictory contractions is shown in Figure 21a: after the contraction we can obtain a closed chain of inequalities on the longitudes of images of some points.

Besides all these prohibited contractions, we exclude from consideration the cases when a marked segment contains both endpoints of some noncrossed oriented broken line $\sqcap\!\!\uparrow$. Although such a contraction itself is not contradictory, it cannot occur in our algorithm; see Remark 16.

In §3.3 we shall study how the segments connecting active points of one and the same bridge can be contracted (this happens at degenerations of types **M2** and **M3**). In

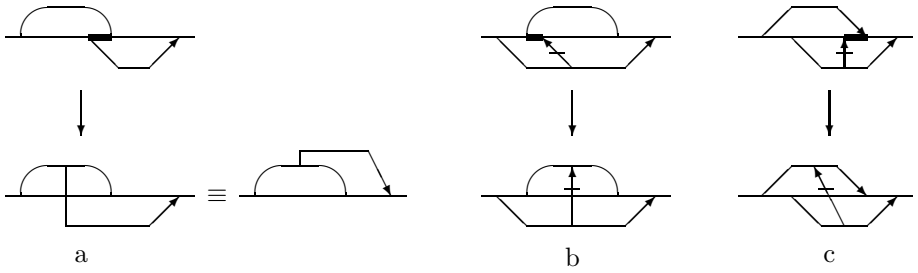

FIGURE 22. How the broken lines are inherited

§3.4 we study collisions of points of different bridges not related with collisions of their ×-pairs: this happens in degenerations of type **M4**.

In §§3.5.1–3.5.4 we describe the way in which different ×-pairs can coalesce (this can happen in degenerations of types **R2, R3, $\tilde{\mathbf{R}}$2,** and **$\tilde{\mathbf{R}}$3**). In §3.5.5 we study what can then happen with the piers of these bridges.

Let us introduce several auxiliary notions.

3.2.2. *Easy and reduced contraction.* The homological contraction of any $\mathcal{F}$-block along an arbitrary collection of segments is defined by a $\mathcal{B}$-picture, whose basic part is the *easy contraction* described in the following definition or *reduced contraction* described a bit later.

Definition 13. Suppose that we have an $\mathcal{F}$-picture Θ of degree i (i.e., with i chords) and a marked collection of disjoint segments of its Wilson line, any of which is bounded by some (not necessarily neighboring) active points of the picture, such that none of these segments contains both endpoints of a chord or a noncrossed oriented broken line of the picture.

The *easy contraction* of the picture Θ along our collection of segments is the new picture, in which

(1) each marked segment is shrunk into a single point;
(2) if some marked segment contains a ×-point and a φ-point of one and the same bridge, then the pier ↘ ending at the latter point should be removed;
(3) if a marked segment contains active points of two bridges connected by a twice crossed oriented broken line ⇉, then the latter broken line should be removed;
(4) all
   – chords,
   – noncrossed oriented broken lines,
   – once crossed oriented broken lines not considered in item 2 above,
   – twice crossed oriented broken lines not considered in item 3 above, and
   – any fragments related with the active points not in the marked segments

   are inherited by the resulting picture. In some cases an endpoint of the inherited broken line moves from the Wilson line to the center of the chord or broken line denoting a more strong condition; see Figures 22 and 17b. Namely, if the marked segment contains an endpoint of a chord and an endpoint of either an oriented noncrossed broken line ⊓ (see Figure 22a) or a once crossed broken line ↘ (see Figure 22b) of a different bridge, then the inherited broken line will be of the same type, but its corresponding endpoint will no longer lie on the Wilson line but in the center of the chord; in a similar way, if a marked segment contains an endpoint of an oriented noncrossed broken line ⊓ and an endpoint (φ-point) of an oriented crossed broken line ↘ (see Figure 22c), then the latter broken line

will turn to one of the same type but its endpoint will be moved into the center of the former broken line.

(5) any point obtained as a contraction of any marked segment, all of whose active points belong to different bridges, inherits all conditions of types **3** and **4** imposed previously on active points in this segment; similar conditions on the points of a marked segment containing the points of one and the same bridge should be removed.

Already this picture can be contradictory (i.e., specify a subset of codimension ≥ 2 in the discriminant). Then a fortiori the homological contraction of the chain $V(\Theta)$ along this system of segments will be contradictory.

On the other hand, if the easy contraction is not contradictory, then some of the conditions expressed by the broken lines of the contracted picture can be corollaries of some other broken lines and chords. Say, if we contract the thickened segments in the left-hand (respectively, right-hand) picture of the top row in Figure 20b, then we obtain a picture with three broken lines (respectively, with two broken lines and one chord) where one of the broken lines is a corollary of two others (respectively, coincides with the other one) and can be removed. The *reduced contraction* of an $\mathcal{F}$-picture along a collection of segments is the composition of the easy contraction and the subsequent elimination of such superfluous broken lines; see the bottom row of Figure 20b. For some other examples of a reduced contraction, see Figure 21b.

If the homological contraction of an $\mathcal{F}$-block along a collection of segments is not contradictory, then it is defined by the picture of the reduced contraction, and may be augmented by some more refined conditions, which we shall describe in the next Subsections 3.3–3.5.

3.3. **Collisions of points inside bridges.**

3.3.1. *Collisions of φ-points of one and the same bridge.* This is a formalization of the degeneration **M3**. For its illustration; see the last summands in (135) and (150).

Suppose that two footholds of one and the same bridge of our $\mathcal{F}$-picture are neighbors (i.e., are not separated by other active points), and the corresponding piers are oriented towards these footholds (we shall not assume the converse because of Remark 6. If moreover none of these footholds is supplied with the condition $\Uparrow$ or $\Downarrow$, then the boundary of the corresponding $\mathcal{F}$-block contains the $\mathcal{B}$-block whose picture is the reduced contraction along this segment (i.e., the easy contraction with these two piers replaced by one pier) and the condition $\overset{j}{\dashv\!\!+\!\!\vdash}$ of type $\bar{\mathbf{5}}$**!** imposed at its foothold a_j obtained at the contraction.

If however the condition $\Uparrow$ or $\Downarrow$ was imposed at one of these two footholds, then the contraction of this segment gives us the $\mathcal{B}$-block defined by the $\mathcal{B}$-picture consisting of this reduced contraction supplied with this condition of type $\bar{\mathbf{5}}$**!** and an additional condition of type $\Downarrow$ or $\Uparrow$ at the point obtained by this contraction. Namely, the condition $\Uparrow$ would appear if we had the condition $\Downarrow$ at the left-hand endpoint of the contracted segment or the condition $\Uparrow$ at the right-hand one; in the remaining two cases we obtain the condition $\Downarrow$. Finally, if equal conditions of type **4** were imposed on both endpoints of this segment, then the contraction of this segment would be contradictory; see item 7 of §3.2.1.

3.3.2. *Collision of a φ-point and a $\times$-point of one and the same bridge.* This is a formalization of the degeneration **M2**. See e.g., the two last summands in (12).

Suppose that a φ-point of some bridge is a neighbor in $\mathbb{R}^1_w$ of a $\times$-point of the same bridge, the corresponding pier is directed to this φ-point, and neither a condition of

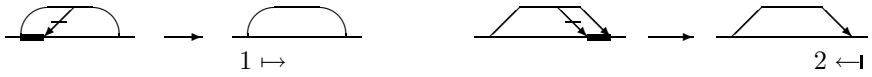

FIGURE 23. Some contractions

type **4** at either of these two active points is imposed nor a condition of type **3** on both $\times$-points of the bridge. Then the boundary of our $\mathcal{F}$-block contains the $\mathcal{B}$-block whose picture is the easy contraction of the segment bounded by these φ- and $\times$-points (i.e., a similar picture with this φ-point and the corresponding pier eliminated) supplied with one of two conditions $\mapsto$, $\quad\longmapsto|$ of item $\bar{\mathbf{5}}$ (depending on the orientation of this pier) imposed at the $\times$-point. Namely, we add the condition $j\mapsto$ (respectively, $\quad j\longmapsto|$) if this φ-point lies to the right (respectively, to the left) in $\mathbb{R}^1_w$ from this $\times$-point; see Figure 23, where the marked segments are thickened.[2] For an explanation of this rule see Figure 15, column **M2**.

On the other hand, if one of conditions of type **3** ($|\!<$) is imposed at the $\times$-pair of this bridge, then depending on this condition either the contraction of the segment is contradictory or after the contraction we additionally obtain a condition of type $\overset{j'}{\underset{l'}{\rightrightarrows}}$ or $\overset{j'}{\underset{l'}{\leftrightarrows}}$, where j' is the order of the active point obtained in the new picture from the contracted segment and l' is the new order of the other $\times$-point of the same bridge; see paragraph $\bar{\mathbf{5}}\mathbf{b}$ of §2.4 and also the last summands in (136) and (151). Namely, let us suppose that the corresponding pier of the bridge is directed to its foothold (as only can happen in our algorithm), and j is the number of the $\times$-point participating in the contraction. Then the contraction of our segment will be contradictory in the following cases:

– we had the first or the third condition of type **3** (see (30)), and $j > l$;
– we had the second or the fourth condition of type **3**, and $j < l$.

Furthermore, we obtain the condition $\rightrightarrows$ if we have the first condition (30) and $j < l$, or we have the second condition (30) and $j > l$. We obtain the condition $\leftrightarrows$ in the remaining two cases, i.e., for the third condition (30) and $j < l$ or the fourth condition (30) and $j > l$.

If the condition $\Uparrow$ or $\Downarrow$ of type **4** were imposed on the $\times$-point participating in our contraction, then the point obtained after it would be supplied with the condition $\Downarrow$ or $\Uparrow$; see item $\bar{\mathbf{5}}\mathbf{a}$. The choice of one of these two conditions is the same as in the end of the previous subsubsection 3.3.1. An illustration of this rule is encoded in the last summands of equalities (137) and (152): to see it explicitly we need to decode the condition $\|^2_3$ in the last parts of these equalities in correspondence with identity (31).

Here the initial conditions of types **3** and **4** are independent; i.e., if we had the conditions of both of these types before the contraction, then after it we would obtain the picture with the union of the conditions described in the previous two paragraphs. Note only that if we had a condition of type **3** on the $\times$-pair and a condition of type **4** on the point of this pair *not participating in the contraction*, then they would imply also a condition of type **4** on the $\times$-point participating in it, and this condition should be included into the list of initial conditions.

[2]If the pier is oriented from the φ-point, then the arrow in this subscript should be oriented in the opposite way; however we do not need to consider this possibility because of Remark 6.

Remark 16. A priori there is one possibility more, when both endpoints of the contracted segment belong to the $\times$-pair of the bridge, i.e., are connected by an oriented noncrossed broken line, and the corresponding degeneration is of type **R1**. However, this situation cannot occur in the real calculations related with the knot invariants, because the initial data of our algorithm should satisfy the *one-term relations*; see Proposition 6 and the paragraph following its proof. On the other hand, this situation can occur in an essential way in the calculation of combinatorial formulas for higher-dimensional cohomology classes; see e.g. [24].

3.4. **Clinching bridges.** This is the formalization of the degeneration **M4**, after which two bridges become one and the same latitude, but their $\times$-points do not meet. If their φ-points also do not meet each other or $\times$-points of the other bridge, then depending on whether these two bridges are related by the condition of type **5** or not, either the corresponding part of the boundary is completely described by the formula (40) or no degeneration happens. Therefore let us study the remaining cases.

Consider all active points of some two bridges and suppose that there is a nonempty set of nonintersecting pairs of points $(a_{j_\alpha}, a_{l_\alpha}) \subset \mathbb{R}^1_w$, $\alpha = 1, \dots, r$, such that for any α

a) the point a_{j_α} is an active point of the first bridge, and the point a_{l_α} is an active point of the second one;
b) $|j_\alpha - l_\alpha| = 1$, i.e., the points a_{j_α} and a_{l_α} are neighbors in $\mathbb{R}^1_w$;
c) a_{j_α} and a_{l_α} are not $\times$-points simultaneously;
d) the simultaneous contraction of all segments $[a_{j_\alpha}, a_{l_\alpha}]$ is not contradictory in the sense of §3.2 (all reasons why it can be contradictory are listed in items 4–6 of Subsection 3.2.1 modulo relation (2) from Remark 10 on page 28).

Then the boundary of the initial $\mathcal{F}$-block contains the $\mathcal{B}$-block whose picture is the *reduced* contraction of all segments $[a_{j_\alpha}, a_{l_\alpha}]$; see e.g. Figure 21b; if $r > 1$, then additionally for any pair of indices α, β satisfying $1 \le \alpha < \beta \le r$ the pair of points obtained by the contraction of segments $[a_{j_\alpha}, a_{l_\alpha}]$, $[a_{j_\beta}, a_{l_\beta}]$ becomes supplied with a condition $\|$ or $\nparallel$ of type **4a** depending on the sign of the number $(a_{l_\alpha} - a_{j_\alpha})(a_{l_\beta} - a_{j_\beta})$ (of course, only $r - 1$ of these $\binom{r}{2}$ conditions will be independent, and it is convenient to remove the rest). Moreover, if these two bridges were related by a condition of type **5**, then all points, obtained as contractions of these segments, would be supplied with conditions $\Uparrow$ or $\Downarrow$. Namely, if a marked segment contains two points of different bridges connected by a twice crossed oriented broken line, then the point a_j obtained by its contraction should be supplied with the sign $\Uparrow^j$ (respectively, $\Downarrow^j$) if this broken line is oriented towards the bridge containing the right-hand (respectively, left-hand) one of these two points.

3.5. **Collision of different $\times$-pairs.** In this subsection we consider the components of boundaries of $\mathcal{F}$-blocks, occurring in the contraction of segments, at least one of which contains $\times$-points of different $\times$-pairs.

We describe first only a restricted part of such possible collisions. Namely, in §§3.5.1–3.5.3 we suppose that no conditions of types **3** and **4** are imposed at the points of $\times$-pairs participating in our collisions, and these pairs are not related by conditions of type **5**.

There are the following three principal cases.

3.5.1. *Collision of three $\times$-pairs.* This collision is a formalization (in terms of $\mathcal{F}$- and $\mathcal{B}$-pictures) of degenerations **R3** and $\tilde{\mathbf{R}}$**3** in the case when all three double points of the knot diagram participating in this degeneration (see upper right-hand pictures of Figures 13 and 14) are $\times$-pairs of the initial $\mathcal{F}$-picture; see Remark 11 on page 30.

It is illustrated by the last summands of formulas (102)–(105), (108), (109), and (138)–(140). Let us describe it.

Suppose that our $\mathcal{F}$-picture contains three $\times$-pairs with endpoints (a_{i_1}, a_{i_2}), (a_{i_3}, a_{i_4}), and (a_{i_5}, a_{i_6}), at most one of which is a chord and at least two are noncrossed oriented broken lines, such that $|i_1 - i_3| = 1$, $|i_2 - i_5| = 1$, $|i_4 - i_6| = 1$. (We do not require that $i_1 < i_2$ or $i_3 < i_4$ or $i_5 < i_6$.)

The easy contraction of all three segments $[a_{i_1}, a_{i_3}]$, $[a_{i_2}, a_{i_5}]$ and $[a_{i_4}, a_{i_6}]$ turns this triple of $\times$-pairs to a triangle whose vertices are these segments shrunk into points, and the sides are formed by three broken lines (or two broken lines and one chord) inherited from these $\times$-pairs. Suppose that this contraction is not contradictory, i.e., this (maybe partially) oriented triangle has no admissible cycles (see item (8) on pagee 39). Then the boundary of the initial $\mathcal{F}$-block contains the $\mathcal{B}$-block whose picture is the *reduced contraction* of our three segments, with an additional condition of type $\bar{\mathbf{2}}\mathbf{a}$ or $\bar{\mathbf{2}}\mathbf{b}$ (or, which is the same, $\bar{\mathbf{3}}\mathbf{a}$ or $\bar{\mathbf{3}}\mathbf{b}$), imposed at the three newborn active points; see e.g. the last summands in formulas (102) and (138). Namely, if all three vectors $[a_{i_1}, a_{i_3}]$, $[a_{i_4}, a_{i_6}]$ and $[a_{i_5}, a_{i_2}]$ are equally oriented in $\mathbb{R}^1_w$, then we have the condition 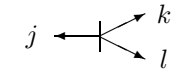

; otherwise we have the condition 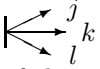

where the middle arrow corresponds to the point obtained by the contraction of the segment for which this orientation is different from those for the other two segments.

3.5.2. *Complete collision of two $\times$-pairs.* This is a formalization of degenerations **R2** and $\tilde{\mathbf{R}}\mathbf{2}$**.** It is illustrated by the last summands in (9), (10) and (15).

Suppose that our $\mathcal{F}$-picture contains two $\times$-pairs with endpoints $(a_{i_1} < a_{i_2})$ and $(a_{i_3} < a_{i_4})$, at most one of which is a chord and at least one is a noncrossed oriented broken line, and $|i_1 - i_3| = 1$, $|i_2 - i_4| = 1$.

Again, we contract the segments $[a_{i_1}, a_{i_3}]$ and $[a_{i_2}, a_{i_4}]$ into points. This contraction can be contradictory only if both $\times$-pairs are broken lines, and the resulting two broken lines have opposite orientations in $\mathbb{R}^1_w$ (in our algorithm, this cannot happen). If the contraction is not contradictory, then the corresponding reduced contraction gives us one chord or one broken line. In this case, the boundary of our $\mathcal{F}$-block contains the $\mathcal{B}$-block, whose picture is this reduced contraction with one additional condition of type $\bar{\mathbf{4}}$ or $\bar{\mathbf{4}}\mathbf{!a}$ or $\bar{\mathbf{4}}\mathbf{!b}$ (see formulas (35), (36), and (37), respectively, where l and j are the numbers of points of the newborn $\times$-pair in the list of all active points of the new $\mathcal{B}$-picture). Namely, if we had two (noncontradictory) broken lines, so that the reduced contraction gives us one broken line, then we obtain an additional condition of type $\bar{\mathbf{4}}\mathbf{!a}$ or $\bar{\mathbf{4}}\mathbf{!b}$ depending on the sign of the product $(a_{i_4} - a_{i_2})(a_{i_3} - a_{i_1})$. If we had a chord and a broken line, so that the reduced contraction is one chord, then we get a condition of type $\bar{\mathbf{4}}$.

3.5.3. *Partial collision of two $\times$-pairs.* This is a formalization of degenerations **R3** and $\tilde{\mathbf{R}}\mathbf{3}$ in the case when only two of three double points of the (singular) knot diagram correspond to $\times$-pairs of the initial $\mathcal{F}$-picture.

Suppose that our $\mathcal{F}$-picture contains two $\times$-pairs (a_{i_1}, a_{i_2}) and (a_{i_3}, a_{i_4}), such that $|i_1 - i_3| = 1$ (again, we do not assume that $a_{i_1} < a_{i_2}$ or $a_{i_3} < a_{i_4}$).

Then the boundary of the initial $\mathcal{F}$-block contains the $\mathcal{B}$-block obtained from it by the easy contraction of the segment $[a_{i_1}, a_{i_3}]$.

Remark 17. The last statement is true even if a more strong condition considered in §3.5.1 (i.e., the existence of an additional $\times$-pair (a_{i_5}, a_{i_6}), such that $|i_2 - i_5| = |i_4 - i_6| = 1$) or in §3.5.2 (i.e., $|i_2 - i_4| = 1$) is satisfied. For instance, formula (138) shows that the boundary of the $\mathcal{F}$-block 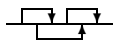 contains not only the subalgebraic chain shown at

the end of (138) (described in §3.5.1) but also some five varieties obtained by partial collisions of different pairs of $\times$-pairs of our picture (see summands 4 through 8 in the right-hand side of (138)); some three of these five partial collisions can be extended to the complete collision. Similarly, formula (15) contains not only its last term (indicated in §3.5.2) but also three terms obtained by partial collisions, two of which can be extended to the complete one.

3.5.4. *Impact of other conditions.* Now, suppose that some conditions of types **3**, **4**, or/and **5** were imposed at the $\times$-points of the initial $\mathcal{F}$-block $V(\Theta)$ participating in a degeneration of one of three kinds mentioned in §§3.5.1–3.5.3 above. Then, generally speaking, the part of the boundary $\partial V(\Theta)$ defined by all possible degenerations of configurations of $\times$-points of Θ will be "smaller" than the sum of $\mathcal{B}$-blocks described in the previous three subsubsections 3.5.1–3.5.3 for the similar $\mathcal{F}$-block without these conditions: some of these $\mathcal{B}$-blocks will be reduced completely or partially. But anyway the homological boundary of our $\mathcal{F}$-block $V(\Theta)$ will be a linear combination of some $\mathcal{B}$-blocks, in correspondence with Proposition 3.

Namely, in the collision of three $\times$-pairs or the *partial* collision of two $\times$-pairs (described in subsubsections 3.5.1 and 3.5.3 respectively) the conditions of type **3** ($\lessdot$) or **4** ($\Uparrow$ / $\Downarrow$) satisfied by the active points before the collision give us exactly the same conditions on the points obtained from them after it. A condition of type **5** ($\not\leqslant$), imposed on two $\times$-pairs, gives us a condition of type **4** at the point obtained by the contraction of a segment containing some points of both of these pairs.

In the complete collision of two $\times$-pairs (as in §3.5.2) a condition of type **4** or a condition of type **5** relating these two pairs produces a condition of type **4**, and the condition of type **3** on any of these two $\times$-pairs gives us a condition of type $\overline{\mathbf{4}}$**!!** ($\lozenge$).

3.5.5. *What can happen with piers of $\times$-pairs when these pairs meet.* If $\times$-points of several different $\times$-pairs of an $\mathcal{F}$-picture tend to one another, then some footholds of corresponding bridges also can coalesce.

The components of the boundary of the $\mathcal{F}$-block $V(\Theta)$ described in Subsections 3.5.1–3.5.4 correspond to the case when it is not so; i.e., all the footholds of different bridges tend to different points of the source line $\mathbb{R}^1_w$ and, moreover, they do not tend to $\times$-points of these (or other) bridges. In the present subsubsection we count all the other possibilities corresponding to the same collisions of $\times$-pairs.

First we consider a complete collision of two $\times$-pairs (a_{i_1}, a_{i_2}) and (a_{i_3}, a_{i_4}) as in §3.5.2 or a partial collision of two such pairs as in §3.5.3. Suppose that we can distinguish several footholds $a_{j_1}, \dots, a_{j_r}$ of the first pair, and equally many footholds $a_{l_1}, \dots, a_{l_r}$ of the other $\times$-pair in such a way that $|j_\alpha - l_\alpha| = 1$ for any $\alpha = 1, \dots, r$. We shall also assume that all piers, corresponding to these $2r$ footholds, are oriented towards them.

Then we can contract these $r+2$ segments $[a_{i_1}, a_{i_3}]$, $[a_{i_2}, a_{i_4}]$, $[a_{l_\alpha}, a_{j_\alpha}]$. The result of this contraction is a subalgebraic variety expressed by the $\mathcal{B}$-picture obtained from the initial $\mathcal{F}$-picture Θ as follows: our two $\times$-pairs are changed in correspondence with §§3.5.2, and additionally for any $\alpha = 1, \dots, r$ the segment $[a_{j_\alpha}, a_{l_\alpha}]$ becomes contracted, and the pair of piers with endpoints at a_{j_α} and a_{l_α} is replaced by only one such pier a_{η_α} supplemented by the subscript $\|^{\eta_\alpha}_{\iota'}$ or $\nparallel^{\eta_\alpha}_{\iota'}$, where ι' is the number of the point obtained by the contraction of the segment (a_{i_1}, a_{i_3}), and the symbol $\|$ or $\nparallel$ depends on the sign of the expression $(a_{i_1} - a_{i_3})(a_{j_\alpha} - a_{l_\alpha})$. Of course, after that we need to check whether this condition does not contradict some other conditions of types **3** and **4** inherited from the similar conditions on the initial active points; otherwise this contraction is contradictory. If it is not, then the resulting variety is a $\mathcal{B}$-block participating in the boundary of the initial $\mathcal{F}$-block.

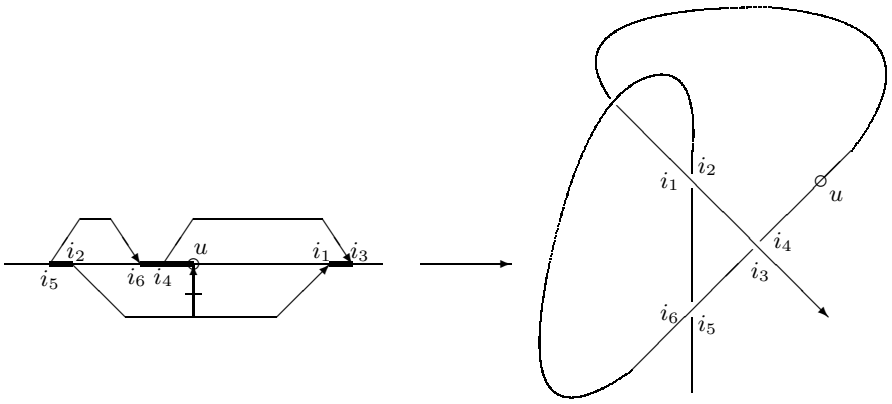

FIGURE 24. A perishing pier

In the case of a partial collision of two ×-pairs as in §3.5.3, we have one additional possibility (see Figure 24 and the last summands in formulas (110)–(119) and (141)–(145)). Namely, suppose that the ×-pair (a_{i_1}, a_{i_2}) has, besides r footholds considered in the previous paragraph, a foothold a_u such that $|i_4 - u| = 1$, $u \notin \{j_1, \dots, j_r, l_1, \dots, l_r\}$. Then the boundary of the $\mathcal{F}$-block $V(\Theta)$ contains also the $\mathcal{B}$-block in whose $\mathcal{B}$-picture

a) these two ×-pairs are changed in correspondence with §§3.5.3 and 3.5.4;

b) for any $\alpha = 1, \dots, r$, the segment $[a_{j_\alpha}, a_{l_\alpha}]$ is contracted, the corresponding pair of piers with endpoints a_{j_α} and a_{l_α} is replaced by one pier with endpoint a_{η_α} obtained by this contraction and supplied with the condition $\|_{\iota'}^{\eta_\alpha}$ or $\nparallel_{\iota'}^{\eta_\alpha}$; and

c) the pier with the foothold a_u disappears, but instead a condition of type **3** ($\mathbb{k}$) (see (30)) becomes imposed on the tangent vectors of f at two points obtained by the contraction of segments $[a_{i_1}, a_{i_3}]$ and $[a_{i_4}, a_u]$.

A geometrical explanation of the last condition can be seen in Figure 24 (ignoring for a while the crossing point with indices i_5, i_6 which will be needed for the illustration of the next difficult case of three colliding ×-pairs described below).

Remark 18. If the initial $\mathcal{F}$-block satisfies the conditions of Remark 6 on page 25, then such a perishing foothold a_u can exist only if the segment $[a_{i_4}, a_u]$ is placed between the segment $[a_{i_1}, a_{i_3}]$ and the point a_{i_2} in $\mathbb{R}^1_w$.

In the general case, one more pier of the ×-pair (a_{i_3}, a_{i_4}) with the foothold a_v, $|v - i_2| = 1$, can perish in the same way. However, if the initial $\mathcal{F}$-block satisfies the conditions of Remark 6, then it is impossible: indeed, in this case by the same reasons the segment $[a_{i_2}, a_v]$ should be placed between the segments $[a_{i_1}, a_{i_3}]$ and $[a_{i_4}, a_u]$. Therefore we shall not consider this possibility in detail.

Finally, let us consider the collisions of three ×-pairs. Suppose that we have three ×-pairs ready for the collision as considered in §3.5.1, and several disjoint subsets of the union of their φ-points are distinguished, such that

a) any subset consists of two or three φ-points, no two of which belong to one and the same bridge;
b) any subset consists of neighboring active points of the picture, i.e., it is not separated by other active points;
c) for all such sets of cardinality three, their middle points belong to one and the same bridge;

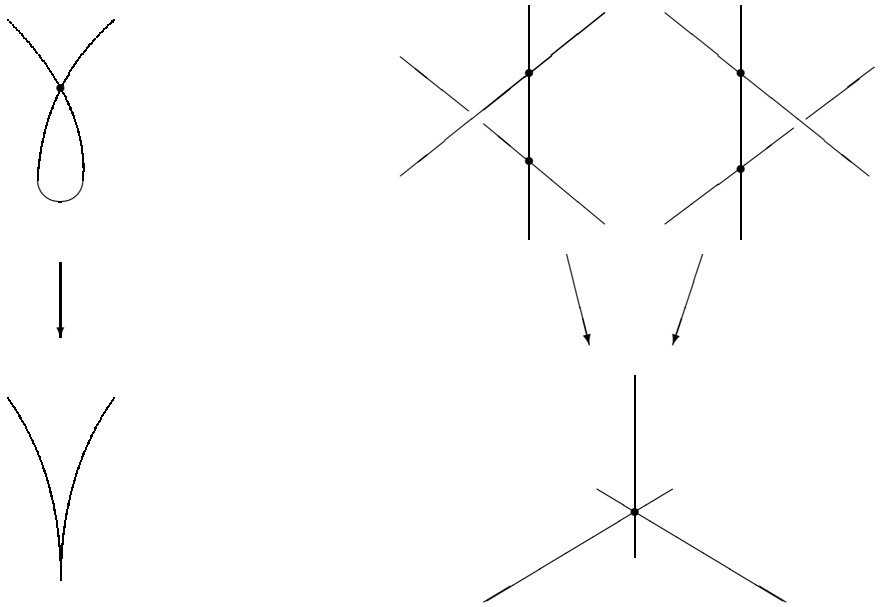

FIGURE 25. Degenerations into smaller cells

d) the simultaneous contraction of three segments $[a_{i_1}, a_{i_3}]$, $[a_{i_2}, a_{i_5}]$, $[a_{i_4}, a_{i_6}]$ (connecting points of our $\times$-pairs) and all segments connecting the footholds inside one and the same distinguished subset is not contradictory.

Then the boundary of our $\mathcal{F}$-block contains a $\mathcal{B}$-block in whose picture our three $\times$-pairs are changed in correspondence with §3.5.1, and additionally any couple or triple of piers with footholds at the points of one subset fixed above is replaced by only one pier; if this pier is obtained by the collision of two piers, then it becomes supplied with one condition of type $\|_{\iota'}^{\eta_\alpha}$ or $\nparallel_{\iota'}^{\eta_\alpha}$; if it is obtained by the collision of three piers, then it should be supplied with three such conditions (two of which it is convenient to reformulate as conditions on the signs of the derivative of the map f_2 at three points obtained in the collision of our $\times$-pairs).

Additionally, in a general situation some pier growing from a $\times$-pair of this triple can disappear imposing instead some condition of type **3** ($\Vdash$) on the derivatives of f_1 at the corresponding three $\times$-points of the arising configuration; see Figure 24. Again, we shall not consider here the possibility of two such perishing piers as it contradicts the conditions of Remark 6. However it can happen that in a less direct algorithm one should not require these conditions, and hence one needs to consider this possibility.

3.6. **The boundary in vice-maximal cells.** In the previous subsections of §3 we have considered the pieces of the boundary of an $\mathcal{F}$-block that are contained in the same maximal cell of the term $\sigma_i \setminus \sigma_{i-1}$ of the standard filtration of the resolved discriminant as the initial $\mathcal{F}$-block. Now we consider some other part of this boundary: the one inside the vice-maximal cells of the same term $\sigma_i \setminus \sigma_{i-1}$. It is related with degenerations of the set of chords of our $\mathcal{F}$-picture; see Figure 25 and Examples 2, 3 (page 22).

In the left-hand bottom picture of Figure 25 it is assumed (unlike the similar picture of Figure 13) that the derivative of the parameter map $f : \mathbb{R}^1_w \to \mathbb{R}^3$ itself is equal to

zero at the "cusp" point, and not only the derivative of its projection f_1. In the right-hand bottom picture it is assumed that the vector "up" in $\mathbb{R}^3$ (directed "to us") belongs to the octant consisting of positive linear combinations of three vectors tangent at the intersection point to three segments drawn there and oriented from the intersection point to the longer parts of these segments. Degenerations of type $\breve{\mathbf{R}}\mathbf{1}$ define the part of the boundary of $\mathcal{F}$-blocks, contained in the vice-maximal cells of **1T** type, and degenerations of type $\breve{\mathbf{R}}\mathbf{3}$ define the part contained in **4T**-cells.

Proposition 6. *The degeneration* $\breve{\mathbf{R}}\mathbf{1}$ *actually cannot occur in our calculation of combinatorial formulas for knot invariants.*

Proof. The proof is by induction over our algorithm (which will be described in the next section); here is its idea. The initial data γ of our algorithm (i.e., the "weight system") satisfies the *one-term* (or **1T**-) *relation*, which means that the endpoints of any chord of any chord diagram constituting γ are separated in $\mathbb{R}^1_w$ by endpoints of some other chords of the same chord diagram; see page 22. In the next steps of the algorithm some of these separating chords can be destroyed, but not tracelessly. It follows from the construction of the algorithm (as it appears in §4 below) that for any chord of any $\mathcal{F}$-picture actually occurring in its execution one of two conditions holds:

a) there is an active point of this picture between the endpoints a, b of this chord,
b) the vectors $f_1'(a)$ and $f_1'(b)$, i.e., the projections to $\mathbb{R}^2$ of tangent vectors of f at these endpoints, are co-directed.

Any of these two conditions prevents the degeneration of type $\breve{\mathbf{R}}\mathbf{1}$ colliding these endpoints, i.e., the corresponding piece of the boundary has too large a codimension to participate in homological calculations related with the knot invariants. □

For illustrations of this proposition, see Lemma 5 and Proposition 26. A similar consideration allows us to not consider the degeneration **R1**; see Remark 16 in §3.3.

The study of degeneration $\breve{\mathbf{R}}\mathbf{3}$ is very similar to that of degenerations **R3** and $\tilde{\mathbf{R}}\mathbf{3}$ above. Again, from the point of view of formal calculations it should be subdivided into two subcases depending on whether the unique overcrossing point of the singular diagram participating in this degeneration (see the upper picture of Figure 25, column $\breve{\mathbf{R}}\mathbf{3}$) is counted in the initial $\mathcal{F}$-picture by an oriented broken line or not. The first (respectively, the second) possibility is illustrated by the last two (respectively, by all but the last two) summands in the right-hand side of any of equations (71)–(79). As in §3.5.5, some piers can coincide or vanish in such a collision. If we follow the direct algorithm then there will be no more than one vanishing pier; see e.g. last two summands in any of equations (80)–(83) or the last four summands in equation (84).

The notation of a piece of the boundary obtained by such a degeneration is very similar to what we had previously: it consists of the notation of the vice-maximal cell in which this piece is contained, and conditions of types **1**, ..., **5**, $\bar{\mathbf{2}}\mathbf{a}$, $\bar{\mathbf{2}}\mathbf{b}$, drawn at or under it.

But additionally it can contain one geometrical condition more. Consider a vice-maximal cell of **4T** type. Its notation consists of $i-2$ chords and one tripod with a marked leg; see (25). Then the condition $\triangle$ means that the convex span of four rays in $\mathbb{R}^3$, three of which are the tangent directions of f at the feet of the tripod, and the fourth is the direction "up", is a wedge with three sides (i.e., one of these four vectors lies in the octant spanned by the other three); the condition $\bigtriangledown$ means that this convex span is a wedge with four sides or the whole $\mathbb{R}^3$ (or, which is the same, that the similar convex span of the same three tangent directions and the direction "down" is a wedge with

three sides). These two conditions are always accompanied by a condition 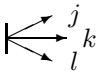 or 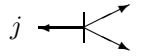 described in paragraphs $\bar{\mathbf{2}}\mathbf{a}$ and $\bar{\mathbf{2}}\mathbf{b}$ of §2.4, respectively. These conditions $\triangle$ and $\triangledown$ appear at the degenerations of type $\breve{\mathbf{R}}\mathbf{3}$, at which the endpoints of some broken line collide with the free endpoints of two chords participating in the degeneration. For illustrations, see the last two terms in any of equations (71)–(79).

3.7. **Boundary in the lower term of the filtration.** Suppose we have an $\mathcal{F}$-block in some maximal cell of $\sigma_i \setminus \sigma_{i-1}$. Its $\mathcal{F}$-picture contains i chords. Then its boundary in $\sigma_{i-1} \setminus \sigma_{i-2}$ consists of i $\mathcal{B}$-blocks of degree $i-1$. These blocks correspond to all chords of the initial $\mathcal{F}$-picture; the notation of any such block is obtained from this picture by replacing the corresponding chord by a nonoriented noncrossed broken line.

4. Description of the algorithm

4.1. **Hierarchy of subvarieties of codimension 1.** Our algorithm uses the induction over the *complexity* of $\mathcal{B}$-blocks, i.e., over some partial order on the set of such blocks in an arbitrary maximal cell of $\sigma_i \setminus \sigma_{i-1}$. Let us describe this partial order.

First of all, we order these $\mathcal{B}$-blocks by the quantities of active points in the corresponding $\mathcal{B}$-pictures. If these numbers of some two pictures are equal, then we order these pictures by the type of the (unique) equality-type condition described in items $\bar{\mathbf{1}}$, $\bar{\mathbf{2}}$, $\bar{\mathbf{3}}$, $\bar{\mathbf{4}}$, $\bar{\mathbf{5}}$, or $\bar{\mathbf{6}}$ of §2.4 and participating in the definition of this block: the $\mathcal{B}$-block with condition $\bar{\mathbf{1}}$ is older than that with condition $\bar{\mathbf{2}}$, etc. If these types also are equal for some two $\mathcal{B}$-blocks with equally many active points, then we subordinate these blocks by the lexicographic order (in the Wilson line, counting from the left to the right) of the collection of active points participating in this condition.

This is still not a linear order of the set of all possible $\mathcal{B}$-pictures. For instance, two pictures that differ only by the orientations of several broken lines or by the signs in certain conditions of inequality type (described in §2.2) will be incomparable to one another.

A similar partial order can be defined on the set of subalgebraic chains of codimension 2 forming irreducible pieces of boundaries of $\mathcal{B}$-blocks. These chains will occur below in relation with homological conditions on the linear combinations of $\mathcal{B}$-blocks defining differentials $d^r(\gamma)$ of the spectral sequence: any such linear combination should be a cycle in the corresponding term $\sigma_i \setminus \sigma_{i-1}$, $i = k - r$.

Definition 14. A $\mathcal{B}$-picture or $\mathcal{F}$-picture is called *regular* if all conditions participating in it have all properties listed in Remarks 5–7, 12, and 13. A $\mathcal{B}$-block (respectively, $\mathcal{F}$-block) is called *regular* if it is specified by a regular $\mathcal{B}$- (respectively, $\mathcal{F}$-) picture.

Proposition 7. *All $\mathcal{B}$-blocks constituting the boundary of a regular $\mathcal{F}$-block in accordance with Proposition* 5 *are also regular.*

The proof is immediate. □

4.2. **How does the algorithm work.** It starts from a weight system of a certain rank k, i.e., from a cycle γ in $\sigma_k \setminus \sigma_{k-1}$ given by a linear combination of several maximal cells corresponding to k-chord diagrams. Then we calculate its first boundary $d^1(\gamma)$, which is the sum of several $\mathcal{B}$-blocks in maximal cells of $\sigma_{k-1} \setminus \sigma_{k-2}$; see § 3.7 and also formulas (8) and (51). This boundary is the initial data of the first step of the algorithm. Similarly, the initial data of the rth step of the algorithm, $r = k - i$, is some subalgebraic cycle $d^r(\gamma) \subset \sigma_i \setminus \sigma_{i-1}$ constructed on the $(r-1)$st step.

On this r-th step we try to span the cycle $d^r(\gamma)$ by a relative chain γ_r in $\sigma_i \setminus \sigma_{i-1}$. We do it in any maximal open cell of $\sigma_i \setminus \sigma_{i-1}$ separately. Namely, we fix such a cell M,

consider the chain $d^r(\gamma)\cap M$ of codimension 1, and try to span it by a chain $\gamma_r^M\subset M$ of full dimension such that $\partial\gamma_r^M+(d^r(\gamma)\cap M)\subset\partial M$. The union of these chains over all cells M provides a homology between $d^r(\gamma)$ and some cycle in the union of vice-maximal cells; the latter cycle can be only a linear combination of these cells, and we shall overcome it later.

Denote by Δ this chain $d^r(\gamma)\cap M$ which we should kill by the chain γ_r^M. It is obviously a cycle in M, i.e., $\partial\Delta\subset\partial M$.

Inductive conjecture. *The cycle Δ can be represented by a finite linear combination of* regular *$\mathcal{B}$-blocks in the cell M, any of which is distinguished by at most $r-1$ conditions of inequality type described in items* **1**–**5** *of* §2.2*, and exactly one condition as in item* $\bar{\mathbf{1}}$ *of* §2.4 (*i.e., a noncrossed nonoriented broken line* $\sqcap$). *The $\mathcal{B}$-picture of any such $\mathcal{B}$-block contains no more than $2k$ active points.*

Define the group $\widetilde{\mathcal{B}_r(M)}$ as the group of formal $\mathbb{Z}_2$-linear combinations of all *regular* $\mathcal{B}$-blocks in our cell M, distinguished by at most $r-1$ conditions of inequality type as in items **1**–**5** of §2.2 or items $\bar{\mathbf{2}}$**a,** $\bar{\mathbf{2}}$**b,** $\bar{\mathbf{3}}$**a/**$\bar{\mathbf{3}}$**b,** $\bar{\mathbf{4}}$**!!,** $\bar{\mathbf{5}}$**a,** $\bar{\mathbf{5}}$**b** of §2.4, and one *arbitrary* condition of equality type (i.e., as in paragraphs $\bar{\mathbf{1}}$**,** $\bar{\mathbf{2}}$**,** $\bar{\mathbf{2}}$**!,** $\bar{\mathbf{3}}$**,** $\bar{\mathbf{4}}$**,** $\bar{\mathbf{4}}$**!a,** $\bar{\mathbf{4}}$**!b,** $\bar{\mathbf{5}}$**,** $\bar{\mathbf{5}}$**!,** $\bar{\mathbf{6}}$**a,** $\bar{\mathbf{6}}$**b,** or $\bar{\mathbf{6}}$**!** of §2.4).

Denote by $\mathcal{B}_r(M)$ the quotient of this group by all relations such as those in Remarks 10 and 15 (pages 28 and 35): two formal linear combinations are equivalent (i.e., define one and the same element of the group $\mathcal{B}_r(M)$), if they define equal subalgebraic chains in M in the sense of Definition 2.

The partial order of $\mathcal{B}$-blocks described in §4.1 defines an increasing filtration in the group $\widetilde{\mathcal{B}_r(M)}$ and hence also in $\mathcal{B}_r(M)$.

Definition 15. The filtration of an element of the group $\widetilde{\mathcal{B}_r(M)}$ is equal to the maximal order of $\mathcal{B}$-blocks participating with a nonzero coefficient in the corresponding linear combination.

The filtration of an element of the group $\mathcal{B}_r(M)$ is equal to the minimal filtration of elements of $\widetilde{\mathcal{B}_r(M)}$ representing it.

A *minimal representative* of an element of the quotient group $\mathcal{B}_r(M)$ is an arbitrary element of $\widetilde{\mathcal{B}_r(M)}$ representing it and having the minimal possible filtration among all its representatives.

We kill the cycle Δ by an inductive process, any step of which decreases the filtration of elements of $\mathcal{B}_r(M)$.

First, we choose an arbitrary minimal representative $\tilde{\Delta}\in\widetilde{\mathcal{B}_r(M)}$ of Δ. We select those $\mathcal{B}$-blocks in $\tilde{\Delta}$ that have the greatest number of active points. Denote this number by N. Among $\mathcal{B}$-blocks in $\tilde{\Delta}$ having N active points we select those that contain a nonoriented noncrossed broken line $\sqcap$ as in condition $\bar{\mathbf{1}}$ of §2.4.[3] Among all such $\mathcal{B}$-blocks we choose the ones for which this broken line is (lexicographically) as left as possible in $\mathbb{R}^1_w$; denote by A the sum of all such $\mathcal{B}$-blocks in $\tilde{\Delta}$. Denote by $A^\uparrow$ the sum of $\mathcal{F}$-blocks whose $\mathcal{F}$-pictures are obtained from $\mathcal{B}$-pictures of $\mathcal{B}$-blocks participating in A by replacing the nonoriented noncrossed broken line by a broken line oriented to the right; cf. formula (38).

Example 5. If Δ is given by the sum (8), then the chain A is the first summand in (8), and $A^\uparrow$ is indicated in the left-hand side of (9). The filtration of the chain $A-\partial A^\uparrow$ is then strictly lower than that of A. The leading (of highest filtration) term of the latter

[3]At the very beginning it will be *all* our $\mathcal{B}$-blocks; however, we are going to proceed by induction over N, and in the next steps of induction other equality-type conditions can also appear.

chain is equal to the second summand in (8). We kill it by the left-hand side of (10). The remaining sum consists of $\mathcal{B}$-blocks with no more than 3 active points in each; in particular, its filtration is even lower.

A similar situation holds also in the general case. Namely, we have the following general fact.

Proposition 8. *If the class of the chain A in $\mathcal{B}_r(M)$ is not equal to 0, then the filtration of the cycle $\tilde{\Delta} - \partial A^{\uparrow}$ is strictly smaller than that of Δ.*

Proof. Let W be one of the $\mathcal{F}$-blocks constituting $A^{\uparrow}$. By Proposition 3 its boundary ∂W is the sum of several $\mathcal{B}$-blocks whose $\mathcal{B}$-pictures have no more than N active points. For any such bounding $\mathcal{B}$-block obtained from W by any degeneration of type other than **X** (see §2.3), its filtration is strictly lower than that of all components of A. Thus the unique reason by which the filtration of the chain $\tilde{\Delta} - \partial A^{\uparrow}$ could be greater than or equal to that of $\tilde{\Delta}$ is as follows: the left-hand endpoints of some nonoriented broken lines ⊓ in pictures of components of $\partial A^{\uparrow}$ arising as degenerations of some oriented noncrossed broken lines ⊓↾ of $A^{\uparrow}$ can be further to the left (i.e., have smaller orders in $\mathbb{R}^1_w$) than the left-hand endpoints of similar broken lines from the description of summands of the chain A.

For instance, consider equation (105). Suppose that A contains the $\mathcal{B}$-block given by the *second* summand of the right-hand side of (105) and try to kill it by the $\mathcal{F}$-block W shown in the left-hand side of (105). Then, aside from our killed $\mathcal{B}$-block, ∂W contains the first summand in (105), whose filtration is strictly higher. Fortunately, as we shall see now, this situation cannot occur in our algorithm: e.g. the second summand in (105) cannot be the leading term of $\tilde{\Delta}$ because otherwise $\tilde{\Delta}$ is not a cycle in M.

In the general case, let j be the minimal value of orders in $\mathbb{R}^1_w$ of left-hand endpoints of noncrossed oriented broken lines ⊓↾ participating in $\mathcal{B}$-pictures of all $\mathcal{B}$-blocks of the linear combination A. If j is greater than the order of the left-hand endpoint of the nonoriented noncrossed broken line ⊓ participating in all these pictures, then the assertion of Proposition 8 is satisfied for A. If j is smaller than this order, let us denote by A_+ the sum of all $\mathcal{B}$-blocks, participating in the linear combination A, such that the $\mathcal{B}$-picture of each of them contains a noncrossed oriented broken line ⊓↾ whose left-hand endpoint has order j (i.e., is called a_j).

Lemma 1. *The chain A_+ is equal to zero in $\mathcal{B}_r(M)$.*

Proof of the lemma. The boundary of the chain A_+ contains some components defined by pictures that include two nonoriented noncrossed broken lines ⊓ : one of these broken lines is inherited from the common such broken line participating in $\mathcal{B}$-pictures of all blocks constituting A, and the other occurs at the degeneration of type **X**, i.e., by forgetting the orientation of some oriented broken line ⊓↾. Let us choose those of such components of A_+ that occur by such a degeneration of oriented broken lines whose left-hand endpoints have the number j (i.e., are denoted by a_j). Denote by $A^{\downarrow}_+$ the sum of these components. The condition $\partial\tilde{\Delta} = 0$ implies that this chain $A^{\downarrow}_+$ is equal to 0. Indeed, by the definition of the chain A none of its summands can coincide with any other piece of boundaries of $\mathcal{B}$-blocks participating in the cycle $\tilde{\Delta}$: all these pieces either have a smaller number of active points, or their equality-type conditions are not of type $\bar{\mathbf{1}}$, or they are of type $\bar{\mathbf{1}}$, but the endpoints of the corresponding nonoriented broken lines ⊓ are lexicographically further to the right than in our chain.

On the other hand, the chain A_+ is swept out by a one-parameter family of chains similar to $A^{\downarrow}_+$ and depending on a parameter $\tau \in \mathbb{R}_+$. Any chain of this family is defined in the same way as $A^{\downarrow}_+$, only with the following difference. The condition $f(a_j) = f(a_l)$

(expressed by our nonoriented broken line ⊓) is replaced in this definition by the following one: $f_1(a_j) = f_1(a_l)$ (i.e., the projections of points $f(a_j)$ and $f(a_l)$ to $\mathbb{R}^2$ still coincide), but the difference of projections of $f(a_j)$ and $f(a_l)$ to the "vertical" line in $\mathbb{R}^3$ is equal to τ. Therefore the chain A_+ also is equal to 0. □

Proposition 8 follows immediately from this lemma. □

So, the $\mathcal{F}$-chain $A^\uparrow$ provides a homology between the cycle Δ and a cycle of strictly smaller filtration. Applying this trick several times we kill all the summands in $\tilde{\Delta}$ whose $\mathcal{B}$-pictures contain N active points and a nonoriented broken line ⊓ as in paragraph $\bar{\mathbf{1}}$ of §2.2. Denote by Δ_1 the class in $\mathcal{B}_r(M)$ of the resulting linear combination of $\mathcal{B}$-blocks in M. Let $\tilde{\Delta}_1 \in \widetilde{\mathcal{B}_r(M)}$ be an arbitrary minimal representative of the chain Δ_1. By construction, it is a cycle in M, its class in $\mathcal{B}_r(M)$ is homologous to Δ, and $\tilde{\Delta}_1$ has no summands with N active points and a degeneration of type $\bar{\mathbf{1}}$.

Consider all the $\mathcal{B}$-blocks in $\tilde{\Delta}_1$ with the equality-type condition of type $\bar{\mathbf{2}}$ (⌒). Denote by $\tilde{B} \in \widetilde{\mathcal{B}_r(M)}$ the formal sum of them, and by B the corresponding element of the group $\mathcal{B}_r(M)$.

Let us divide the formal chain $\tilde{B}$ into two parts $\tilde{B}_+$ and $\tilde{B}_-$ consisting of $\mathcal{B}$-blocks such that the noncrossed oriented broken line participating in the notation of the degeneration of type $\bar{\mathbf{2}}$ in any of them is directed from (respectively, to) the center of the chord to (respectively, from) a point of the Wilson line.

Proposition 9. *If we reverse the orientations of these noncrossed oriented broken lines participating in the notation of degenerations of type* $\bar{\mathbf{2}}$ *in all summands of the formal chain* $\tilde{B}_+$*, then we obtain an element of* $\widetilde{\mathcal{B}_r(M)}$*, whose class in* $\mathcal{B}_r(M)$ *is equal to* $\tilde{B}_-$*, and vice versa.*

Proof. The proof follows immediately from the condition $\partial\Delta_1 \cap M = \varnothing$. □

Corollary 1. 1. *The sum of all B-blocks in* $\tilde{B}$*, such that the free (i.e., lying on the Wilson line) endpoint of the oriented noncrossed broken line, participating in the corresponding degeneration of type* $\bar{\mathbf{2}}$*, does* not *lie between the endpoints of the corresponding chord (also participating in this degeneration) is equal to* 0 *in* $\mathcal{B}_r(M)$*.*

2. *The chain B can be described by a linear combination of* $\mathcal{B}$*-blocks, for any of which the following holds:*

a) this block is regular (see Definition 14*, page 49),*

b) its $\mathcal{B}$*-picture contains no more than N active points,*

c) its filtration is not greater than that of the chain B, and

d) the unique equality-type condition participating in its definition is of type $\bar{\mathbf{2}}$**!**, *i.e., is expressed by a once crossed nonoriented broken line* ⌒ *, one of whose endpoints lies in the center of a chord and the second on the Wilson loop between the endpoints of this chord.*

For illustrations of this corollary; see formula (11) and also Lemmas 7, 8, and 9 on page 75.

Proof. Statement 1 follows from the previous proposition and from the fact that all broken lines considered in this statement are oriented to the right (see Definition 14 and especially its assertion about Remark 12).

Therefore we can remove from the linear combination $\tilde{B}$ all $\mathcal{B}$-blocks, described in statement 1, and replace in the remaining linear combination the remainder of $\tilde{B}_-$ by the chain obtained from the remainder of $\tilde{B}_+$ by the switch of orientations of broken lines as described in Proposition 9. By this proposition and Statement 1 the resulting linear combination defines the same chain B and satisfies statement 2 of our Corollary. □

Let us choose the minimal formal chain $\tilde{B}$ representing B in exactly this way.

Proposition 10. *None of the $\mathcal{B}$-blocks constituting $\tilde{B}$ contains conditions of type* $\bar{\mathbf{2}}\mathbf{a}$ *or* $\bar{\mathbf{2}}\mathbf{b}$.

Proof. All $\mathcal{B}$-blocks, constituting the chain $\tilde{B}_+$, occur as components of boundaries of regular $\mathcal{F}$-blocks. Conditions of type $\bar{\mathbf{2}}\mathbf{a}$ or $\bar{\mathbf{2}}\mathbf{b}$ can occur only at the complete collision of three $\times$-pairs. Such a degeneration can provide a chord connected by an oriented noncrossed broken line with a point between the endpoints of this chord only if this triple of $\times$-pairs consists of one chord and two broken lines, and the corresponding easy contraction turns them to a chord and two broken lines, connecting the endpoints of this chord with a point lying *between* these endpoints. Since the original $\mathcal{F}$-block was regular, both these broken lines should be directed to one and the same side in $\mathbb{R}^1_w$, and hence this easy contraction is contradictory; see the left-side column of Figure 20a. The assertion of the proposition is proved for the $\tilde{B}_+$ part of the chain $\tilde{B}$, and the part $\tilde{B}_-$ is symmetric to it. □

Lemma 2. *The sum of all $\mathcal{B}$-blocks participating in the formal linear combination $\tilde{B}$, whose $\mathcal{B}$-pictures contain at least one oriented (to the right) noncrossed broken line, both endpoints of which are on the Wilson line, is equal to* 0 *in $\mathcal{B}_r(M)$.*

Proof. The proof is almost the same as for Lemma 1. Namely, let $\{j < l\}$ be the lexicographically smallest pair of indices such that there exists a $\mathcal{B}$-block participating in $\tilde{B}$, containing an oriented noncrossed broken line ⊓ with endpoints a_j and a_l. Denote by β the sum of all $\mathcal{B}$-blocks in $\tilde{B}$ that contain such a broken line ⊓ with endpoints a_j and a_l. The boundary of any of these blocks contains a subalgebraic chain of codimension 2, whose notation is obtained from that of this block by forgetting the orientation of this broken line. The sum of these chains of codimension 2 should be equal to 0, since none of them can be killed by any other component of the boundary of some block participating in the *cycle* $\tilde{B}$. From this (repeating almost literally the last paragraph of the proof of Lemma 1) we obtain that the entire chain β also is equal to 0. □

Therefore we can just remove all $\mathcal{B}$-blocks containing such broken lines from the linear combination $\tilde{B}$: the chain B defined by it will be the same, and the maximal filtration of blocks participating in it will not be increased.

Let us rename by $\tilde{\Delta}_1$ and $\tilde{B}$ the linear combinations of $\mathcal{B}$-blocks, obtained by this removal from the previous linear combinations with the same names.

Proposition 11. *The representative $\tilde{\Delta}_1$ of the chain Δ_1, obtained in the previous steps, can be replaced by another minimal representative of Δ_1 such that any $\mathcal{B}$-block constituting its principal part $\tilde{B}$ does not have subscripts of type*

(46) 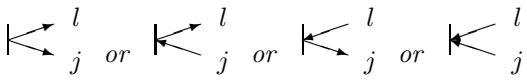

(*see* (30)) *where l is the number of the "free" (i.e., lying on the Wilson line) endpoint of the once crossed nonoriented broken line participating in the condition of type* $\bar{\mathbf{2}}$**!** (⌒∓) *in the definition of this block, and j is the number of an arbitrary endpoint of the chord, whose center coincides with the other endpoint of this broken line.*

Lemma 3. *Let $\beta^<$ (respectively, $\beta^>$, respectively, $\beta^\vee$, respectively, $\beta^\wedge$) be the sum of all $\mathcal{B}$-blocks participating in the linear combination $\tilde{B}$, whose pictures contain both a once crossed nonoriented broken line, one of whose endpoints is the center of a chord, and a subscript* 

(respectively, 

, respectively, 

, respectively,

 *where l is the number of the "free" endpoint of this broken line and j is the number of an arbitrary endpoint of the corresponding chord. Then, replacing these subscripts*  *by*  *in all $\mathcal{B}$-pictures of $\beta^<$, we obtain a chain whose class in $\mathcal{B}_r(M)$ is equal to that of $\beta^>$; replacing similar subscripts*  *by*  *in all $\mathcal{B}$-pictures of $\beta^\vee$ we obtain a chain whose class in $\mathcal{B}_r(M)$ is equal to that of $\beta^\wedge$.*

Proof of the lemma. The proof follows again from the condition $\partial\Delta_1 = 0$. Indeed, the boundary of $\beta^<$ (respectively, $\beta^>$) contains a chain consisting of all subalgebraic chains of codimension 2 in M, whose notation is obtained from that of $\mathcal{B}$-blocks in $\beta^<$ (respectively, $\beta^>$) by replacing the subscript  (respectively, ) by  . These two chains should coincide because no nonsingular piece of the supports of the latter chains of codimension 2 can occur in the boundaries of any $\mathcal{B}$-blocks *with N active points* in $\tilde{\Delta}_1$ not from $\beta^<$ or $\beta^>$.

The proof of the statement concerning the comparison of $\beta^\vee$ and $\beta^\wedge$ is almost the same, referring to the pieces of the boundary with the condition  instead of  . □

Proof of Proposition 11. By Lemma 3, we can choose the minimal representative $\tilde{\Delta}_1$ of Δ_1 in such a way that the chain $\beta^>$ is equal to that obtained from $\beta^<$ by such a switch in all its summands, and $\beta^\wedge$ is equal to that obtained from $\beta^\vee$. Then by two identities (32) we can replace the chain $\beta^> + \beta^< + \beta^\wedge + \beta^\vee$ by a sum of similar $\mathcal{B}$-blocks with all subscripts of type (46) described in Proposition 11 replaced by certain conditions $\|_l^j$ or $\nparallel_l^j$ of type **4a**. □

We can and shall assume that $\tilde{\Delta}_1$ and $\tilde{B}$ are chosen in exactly this way.

Denote by B' the sum of all $\mathcal{B}$-blocks in $\tilde{B}$ having N active points and the maximal possible filtration in the sense of §4.1, in particular with equality-type conditions of type **$\bar{2}$!** (). Let $B^\uparrow$ be the sum of similar $\mathcal{F}$-blocks, whose pictures are obtained from all the pictures of $\mathcal{B}$-blocks in B' by replacing any once crossed nonoriented broken line, connecting the center of a chord with some point of the Wilson line, by the similar once crossed broken line *oriented from the center of the chord to this point of the Wilson line*:

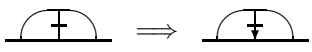

Proposition 12. *If the class of the chain B in $\mathcal{B}_r(M)$ is not equal to* 0*, then the filtration of the cycle $\Delta_1 - \partial B^\uparrow$ is strictly smaller than that of Δ_1.*

Proof. The proof almost repeats that of Proposition 8. Indeed, with the chain B' three numbers $j < l < k$ are related: j and k are the numbers of the endpoints a_j, a_k of the chord participating in the condition of type **$\bar{2}$!** in any of its $\mathcal{B}$-blocks, and l is the number of the noncrossed nonoriented broken line participating in the same condition. By definition of B', these numbers are the same for all $\mathcal{B}$-blocks in B'.

The unique obstruction to the assertion of our proposition could consist in the fact that the pictures of some $\mathcal{B}$-blocks, participating in B', contain a chord connecting some points $a_{j'}, a_{k'}$, and an *oriented* noncrossed broken line connecting the center of this chord with some point $a_{l'}$ of the Wilson line, such that the triple (j', l', k') is lexicographically smaller than the triple (j, l, k). For instance, it could happen that this chord is the same as the one participating in the degeneration of type **$\bar{2}$!**, i.e., $j' = j$ and $k' = k$, but $l' < l$. (Say, it would be so if the chain B' would consist of only the first summand of formula

(134).) However the obstruction, expressed by the sum of such $\mathcal{B}$-blocks, necessarily should be equal to zero in $\mathcal{B}_r(M)$; otherwise the homological condition $\partial\tilde{\Delta}=0$ would fail at the subset of codimension 2 specified by almost the same pictures with two nonoriented broken lines: this can be proved in exactly the same way as Proposition 8. □

So, we can kill all the summands in $\tilde{\Delta}_1$ with N active points and a condition of type $\bar{\mathbf{2}}$ or $\bar{\mathbf{2}}$**!**. Denote by $\tilde{\Delta}_2\in\widetilde{\mathcal{B}_r(M)}$ the resulting linear combination of $\mathcal{B}$-blocks, and by Δ_2 its class in $\mathcal{B}_r(M)$. By construction, all $\mathcal{B}$-blocks in $\tilde{\Delta}_2$ have no more than N active points, and those with N active points do not have degenerations of types $\bar{\mathbf{1}}$ and $\bar{\mathbf{2}}$. Among these $\mathcal{B}$-blocks we choose the blocks with N active points and degeneration of type $\bar{\mathbf{3}}$ only. The sum of all these $\mathcal{B}$-blocks in $\tilde{\Delta}_2$ will be denoted by C.

Proposition 13. *The chain C is equal to zero in the group $\mathcal{B}_r(M)$.*

Lemma 4. *In our algorithm, only those conditions of type $\bar{\mathbf{3}}$ can occur that are described by a pair of broken lines oriented from the left to the right in $\mathbb{R}^1_w$, or are equal to a linear combination of such conditions. I.e., any such condition can be of one of the types*

(47) 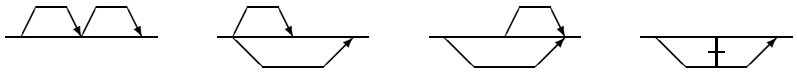

only.

Indeed, a degeneration of type $\bar{\mathbf{3}}$ can appear in our algorithm only in the partial collision of two previously created noncrossed broken lines or in the collision of three such broken lines (which are all oriented to the right in $\mathbb{R}^1_w$). □

This lemma implies immediately Proposition 13, because otherwise the condition $\partial\Delta_2=0$ will not be satisfied. □

Therefore in fact the chain Δ_2 can be realized by a linear combination $\tilde{\Delta}_2$ not containing $\mathcal{B}$-blocks with N active points and degenerations of types $\bar{\mathbf{1}}$**,** $\bar{\mathbf{2}}$ or $\bar{\mathbf{3}}$.

For any such linear combination $\tilde{\Delta}_2$, denote by $\tilde{D}$ the sum of $\mathcal{B}$-blocks in $\tilde{\Delta}_2$ with N active points and a degeneration of type $\bar{\mathbf{4}}$ or $\bar{\mathbf{4}}$**!a** or $\bar{\mathbf{4}}$**!b** (i.e., $\vee$ or $\#$ or $\#$).

Proposition 14. *A minimal formal chain $\tilde{\Delta}_2$ realizing the chain Δ_2 can be chosen so that*

a) the $\mathcal{B}$-pictures of all blocks participating in the chain $\tilde{D}$ do not contain inequality-type conditions of type **1** *or* **2***, i.e., neither the oriented noncrossed broken lines*  *connecting two points of the Wilson line, nor oriented once crossed broken lines* *connecting the center of a chord with a point of the Wilson line;*

b) the equality-type conditions participating in these pictures are of types $\bar{\mathbf{4}}$**!a** ($\#$) *or* $\bar{\mathbf{4}}$**!b** ($\#$) *only; and*

c) these conditions are not supplied with additional conditions of type $\bar{\mathbf{4}}$**!!** ( ).

Proof. The proof again follows from the homological condition checked respectively at the sets of curves,

a) having degenerations of type $\bar{\mathbf{1}}$ ( ) or $\bar{\mathbf{2}}$ (,),

b) having a self-tangency in $\mathbb{R}^3$, and

c) whose projections to $\mathbb{R}^2$ have a self-tangency of higher order. □

Let us choose $\tilde{\Delta}_2$ and $\tilde{D}$ of this form. Let D' be the sum of all $\mathcal{B}$-blocks in $\tilde{D}$ having the maximal possible order in the sense of §4.1, i.e., with the most left-hand (lexicographically) possible position of the pair of points participating in these conditions of types $\bar{\mathbf{4}}$**!a**, $\bar{\mathbf{4}}$**!b**. Denote by $D^{\uparrow}$ the sum of similar $\mathcal{B}$-blocks, whose pictures are obtained from pictures of summands of the formal chain D' by replacing all subscripts of the form $\#\ {}^{l}_{j}$ with $l<j$ by $\ {}^{l}_{j}$, and replacing all subscripts of the form $\#\ {}^{l}_{j}$ by $\ {}^{l}_{j}$.

Proposition 15. *If the class of the chain $\tilde{D}$ in $\mathcal{B}_r(M)$ is not equal to 0, then the filtration of the cycle $\Delta_2 - \partial D^{\uparrow}$ is strictly smaller than that of Δ_2.*

Proof. The proof is the same as that of Proposition 12. □

Repeating this reduction, we obtain a cycle Δ_3 which is homologous to Δ in M and can be represented by a sum of $\mathcal{B}$-blocks whose $\mathcal{B}$-pictures have no more than N active points, and those of them which have exactly N points do not have degenerations of types $\bar{\mathbf{1}}$, $\bar{\mathbf{2}}$, $\bar{\mathbf{3}}$, or $\bar{\mathbf{4}}$. Let $\tilde{\Delta}_3$ be a minimal representative of Δ_3. Denote by $\tilde{E}$ the sum of all $\mathcal{B}$-blocks in $\tilde{\Delta}_3$ whose pictures have exactly N active points and a degeneration of type $\bar{\mathbf{5}}$ ($\mapsto$) or $\bar{\mathbf{5}}$**!** ($\leftrightarrow$).

Proposition 16. *The minimal representative $\tilde{\Delta}_3$ of the cycle Δ_3 can be chosen so that all $\mathcal{B}$-pictures of $\mathcal{B}$-blocks constituting its principal part $\tilde{E}$,*

a) do not contain conditions of types **1**, **2** *or* **3** *from* §2.2,

b) have equality-type conditions of type $\bar{\mathbf{5}}$**!** *only, and*

c) do not have additional conditions of types $\bar{\mathbf{5}}$**a** (⇑) *and* $\bar{\mathbf{5}}$**b** ( ).

Proof. The proof follows from the homological condition at the points having respectively

a) degenerations of types $\bar{\mathbf{1}}$, $\bar{\mathbf{2}}$ or $\bar{\mathbf{4}}$**!**,

b) a vertical tangent direction (i.e., the condition $f_1' = 0$) at an endpoint of some chord,

c) the condition $f_2' = f_2'' = 0$ at an endpoint of some chord. □

Let us choose $\tilde{\Delta}_3$ and $\tilde{E}$ in this way. Subordinate the $\mathcal{B}$-pictures of $\tilde{E}$ with respect to the order (among all active points in $\mathbb{R}^1_w$) of the point at which the condition of type $\bar{\mathbf{5}}$**!** ($\leftrightarrow$) occurs and denote by E' the sum of $\mathcal{B}$-blocks in $\tilde{E}$ with the minimal value j of this order. Let $E^{\uparrow}$ be the sum of similar $\mathcal{F}$-blocks obtained from $\mathcal{B}$-blocks of E' by replacing these conditions $\overset{J}{\leftrightarrow}$ by $\Uparrow^j$.

Proposition 17. *If the class of the chain $\tilde{E}$ in $\mathcal{B}_r(M)$ is not equal to 0, then the filtration of the cycle $\Delta_3 - \partial E^{\uparrow}$ is strictly smaller than that of Δ_3.*

Proof. The proof is the same as that of Proposition 15. □

Repeating this reduction, we obtain a cycle Δ_4, whose minimal representative $\tilde{\Delta}_4$ is a sum of $\mathcal{B}$-blocks, all of whose pictures have no more than N active points, and those with exactly N points have degenerations of type $\bar{\mathbf{6}}$ or $\bar{\mathbf{6}}$**!** only.

Denote by F the chain equal to the sum of all $\mathcal{B}$-blocks in $\tilde{\Delta}_4$ with N active points.

Proposition 18. *The chain F can be represented by a sum of $\mathcal{B}$-blocks such that*

a) their pictures do not contain conditions of types **1**, **2**, **3**, *and* **4**;

b) all their equality-type conditions are the normal *pairs* *of clinching bridges; see paragraph* $\bar{\mathbf{6}}$**!** *of* §2.4.

Proof. The proof again consists in checking the homological condition $\partial\Delta_4 = 0$ at some points of M which lie in the boundary of $\mathcal{B}$-blocks constituting the chain F. Namely, for the assertion a) they are respectively the sets of points satisfying conditions $\bar{\mathbf{1}}$, $\bar{\mathbf{2}}$, $\bar{\mathbf{4}}$**!**, and $\bar{\mathbf{5}}$**!**. Conditions b) and c) from the definition of a normal pair follow immediately from this assertion a) concerning conditions **2** and **1**. The remaining conditions from the definition of normal pairs follow from the homological condition at the set of curves having two self-intersection points (corresponding to our two chords) with one and the same projection to $\mathbb{R}^2$. □

Let us represent the chain F by a formal chain of the form described in Proposition 18, and select those $\mathcal{B}$-blocks constituting it that have the greatest order in the hierarchy of

FIGURE 26. Spanning a $\mathcal{B}$-block of type $\bar{\mathbf{6}}$**!**

§4.1 (i.e., with the lexicographically most left-hand position of the four points participating in this degeneration of type $\bar{\mathbf{6}}$**!**). Denote by F' the sum of these selected summands. Let $F^{\uparrow}$ be the sum of similar $\mathcal{F}$-blocks, in whose pictures the clinching bridges of $\mathcal{B}$-pictures of summands of F' are divorced in the following way (see Figure 26): the $\times$-pair which is lexicographically more to the left in $\mathbb{R}^1_w$ than the other one becomes *more southern* in $\mathbb{R}^2$ than it; i.e., the nonoriented twice crossed broken line joining these $\times$-pairs becomes oriented from the former $\times$-pair to the latter one.

Proposition 19. *If $F \neq 0$, then the filtration of the cycle $\Delta_4 - \partial F^{\uparrow}$ is strictly smaller than that of Δ_4.*

Proof. The proof coincides with that of Proposition 17. □

Repeating, we finally kill all the $\mathcal{B}$-blocks with N active points, i.e., construct a homology between the cycle Δ and a sum of $\mathcal{B}$-blocks with $\leq N-1$ such points. Continuing by induction over N, we eliminate all the $\mathcal{B}$-blocks in our cell $M \subset \sigma_i \setminus \sigma_{i-1}$. The sum of all $\mathcal{F}$-chains $A^{\uparrow}, B^{\uparrow}, D^{\uparrow}, E^{\uparrow}$, and $F^{\uparrow}$, participating in this inductive process on all its steps, is the desired chain γ_r^M in the cell M.

Remark 19. In fact, on any step of the algorithm we have alternative choices of $\mathcal{F}$-blocks, killing the leading (of highest filtration) summands of a cycle of codimension 1 in M: we can orient broken lines to different sides, or kill the condition  by $\Downarrow^j$ and not by $\Uparrow^j$, or kill the condition 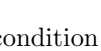 (respectively, ) by  (respectively, ) and not by  (respectively, ), etc.

In our *direct* algorithm, one of these choices is fixed. A more smart algorithm (working faster and providing more compact answers) should choose these killing blocks using some other criteria which are not clear to me yet: informally, it seems that different choices should be alternated as much as possible.

So, we can construct such spanning chains γ_r^M in all the cells M of maximal dimension in $\sigma_i \setminus \sigma_{i-1}$ (i.e., in the cells corresponding to the i-chord diagrams). Suppose that we have done it. The sum of these chains γ_r^M over all cells M provides a homology in $\sigma_i \setminus \sigma_{i-1}$ between our cycle $d^r(\gamma)$ of codimension 1 and a cycle in the union of all other cells. By dimensional reasons, the latter cycle is a linear combination of some cells of vice-maximal dimension. Furthermore, we have two possibilities.

A. *This cycle is homologous to zero in $\sigma_i \setminus \sigma_{i-1}$.*[4]

Then this linear combination of vice-maximal cells is equal to the boundary of a linear combination of maximal cells (corresponding to chord diagrams). It remains only to subtract the latter linear combination from the chain $\sum_M \gamma_r^M$ constructed previously. The obtained difference is the desired chain $\gamma_r \subset \sigma_i \setminus \sigma_{i-1}$ such that $\partial\gamma_r = -d^r(\gamma)$ in $\sigma_i \setminus \sigma_{i-1}$.

Proposition 20 (step of induction, cf. the inductive conjecture on page 50)**.** *If all the chains $\gamma \subset \sigma_k \setminus \sigma_{k-1}$, $\gamma_1 \subset \sigma_{k-1} \setminus \sigma_{k-2}$, ..., $\gamma_r \subset \sigma_i \setminus \sigma_{i-1}$ (where $i = k - r$) were*

[4]By the Kontsevich realization theorem [11], this surely will happen in similar calculations of rational knot invariants; the correctness of the homotopy splitting conjecture for knot discriminants (see e.g. §5.1 in [22]) would imply the same for homology with arbitrary coefficients.

constructed as above, then the next boundary $d^{r+1}(\gamma)$ *of their sum* $\gamma+\gamma_1+\cdots+\gamma_r$ *in* $\sigma_{i-1}\setminus\sigma_{i-2}$ *is a subalgebraic cycle, whose intersection with any maximal cell of* $\sigma_{i-1}\setminus\sigma_{i-2}$ *consists of finitely many* regular $\mathcal{B}$*-blocks, any of which is distinguished by no more than* r *conditions of inequality type as in items* **1**–**5** *of* §2.2*, and exactly one condition of equality type as in item* $\bar{\mathbf{1}}$ *of* §2.4*. The number of active points in any of these* $\mathcal{B}$*-blocks does not exceed* $2k$*.*

More precisely, the sum $\gamma+\gamma_1+\cdots+\gamma_{r-1}$ contributes nothing to this homological boundary (as its geometrical boundary has too small a dimension there), and any $\mathcal{F}$-block participating in γ_r contributes precisely i summands, whose $\mathcal{B}$-pictures are obtained from the $\mathcal{F}$-picture of this $\mathcal{F}$-block by replacing one of the chords by a nonoriented noncrossed broken line $\sqcap$ as in item $\bar{\mathbf{1}}$ of §2.4, cf. § 3.7. □

The step of induction will then be complete.

B. *Our linear combination of vice-maximal cells is not the boundary of either linear combination of maximal cells.* Of course, this means also that the class of our cycle $d^r(\gamma)$ in the Borel–Moore homology group of codimension 1 of the space $\sigma_i\setminus\sigma_{i-1}$ is not equal to 0. In general, one should not despair in this case. Maybe this happened since, in the previous steps of the algorithm, we have not constructed the spanning chains in the optimal way.

If a similar accident does not happen for either weight system γ' of degree smaller than k, then the situation cannot be saved: our weight system γ *cannot be integrated* to a knot invariant. However, taking care of the future, we have to remember the obtained linear combination of vice-maximal cells in $\sigma_i\setminus\sigma_{i-1}$ and especially its class in the group $\bar{H}_{3\omega-2}(\sigma_i\setminus\sigma_{i-1})$.

If however we have already met this situation previously (integrating weight systems of degree smaller than k), then we need to compare the class of this linear combination in the group $\bar{H}_{3\omega-2}(\sigma_i\setminus\sigma_{i-1})$ with similar elements of the same group, defined by similar linear combinations that occurred in the same way as obstructions to the integration. If this class belongs to the subgroup generated by such previous obstructions, then we can improve our system $\gamma+\gamma_1+\cdots+\gamma_{r-1}$, subtracting from it the corresponding sum of similar chains, arising from other weight systems of degrees $<k$, whose integration also stopped in the term $\sigma_i\setminus\sigma_{i-1}$. The obtained difference of $\mathcal{B}$-blocks is then integrable; i.e., we can accomplish at least one more step of induction.

Conjecture 1. In our algorithm, always the possibility **B** will be satisfied; moreover, the boundary cycle in the union of vice-maximal cells always will be *equal* to zero, and not only homologous to it.

Remark 20. Exactly the same algorithm will give a combinatorial formula in the case of integer-valued invariants: it remains only to specify the (co)orientations of all standard chains and conditions from §2. Such a specification will be described in a forthcoming work.

Problem. Is it always possible to choose the spanning chains (see Remark 19) in such a way that the entire sequence of spanning chains $\gamma_1,\dots,\gamma_k$ will be realized by the sums of $\mathcal{F}$-blocks with conditions of type **1** only?

5. Calculation of a combinatorial formula for the knot invariant of second degree

In this section we recall the first illustration of our algorithm, showing how it calculates a combinatorial formula for the unique degree 2 knot invariant v_2 reduced mod 2.

Theorem 1. *The value of v_2 on a generic long knot $f : \mathbb{R}^1 \to \mathbb{R}^3$ is equal* (mod 2) *to the sum of three numbers* (*see three summands in* (48))*:*

a) the number of configurations $(a < b < c < d) \subset \mathbb{R}^1$ such that $f(c)$ is above $f(a)$ in $\mathbb{R}^3$ and $f(d)$ is above $f(b)$;

b) the number of configurations $(a < b < c)$ such that $f(c)$ is above $f(a)$ and the projection of $f(b)$ to $\mathbb{R}^2$ lies to the east from the (*common*) *projection of $f(a)$ and $f(c)$;*

c) the number of configurations $(a < b)$ such that $f(b)$ is above $f(a)$ and the direction "to the east" in $\mathbb{R}^2$ is a linear combination of projections of derivatives $f'(a)$ and $f'(b)$, such that the first of these projections participates in this linear combination with a positive coefficient, and the second with a negative one.

(48)

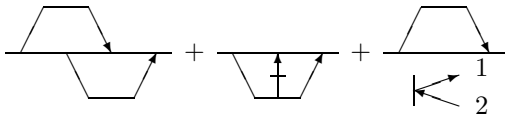

Proof. The proof is essentially done in the Introduction; let us identify its steps in the terms of our algorithm.

The principal part of v_2 in $\sigma_2 \setminus \sigma_1$ is expressed by the chord diagram (7); see e.g. [17].

The boundary of the principal part (7) in σ_1 is equal to (8).

Let us span this boundary by a chain in the maximal cell of σ_1. The direct algorithm associates to the elements of (8) the $\mathcal{F}$-blocks shown in the left-hand sides of equalities (9), (10). According to these equalities, the sum of these two $\mathcal{F}$-blocks provides a homology between the cycle (8) and the chain (10).

The direct algorithm transforms the latter two pictures to the left-hand parts of equalities (12) and (13) respectively. According to these equations, the cycle (11) is equal to the boundary of the sum of the varieties indicated in their left-hand sides.

Remark 21. The same will necessarily hold also in a similar calculation over the integers (if we put proper signs before all participating terms) because of the homological conditions: all right-hand sides of our equations and also the cycle which we are going to kill have no boundaries.

Finally, we get that the sum of four $\mathcal{F}$-blocks indicated in the left-hand sides of equalities (10), (9), (12), and (13) provides a homology in σ_1 between the cycle (8) and the vice-maximal cell of σ_1 taken with some coefficient $\lambda \in \mathbb{Z}_2$. Denote this sum by γ_1.

Lemma 5. *The latter coefficient λ is equal to zero, so that the cycle* (8) *is equal to $\partial\gamma_1$ in σ_1.*

This lemma is a direct corollary of Proposition 6 (see page 48); let us give a direct proof of the lemma for the illustration of this proposition.

The boundary of the chain γ_1 in the vice-maximal cell of σ_1 can be calculated in the following way. For any of the four $\mathcal{F}$-blocks constituting γ_1 we let the endpoints of the unique chord of the $\mathcal{F}$-picture tend to one another in $\mathbb{R}^1_w$ and consider the subvariety in the vice-maximal cell swept out by all the limit positions of singular knots from this block after the collision of these points. In all four cases this limit variety consists of pairs of the form (a point $* \in \mathbb{R}^1$, a map $f \in \mathcal{K}$ such that $f'(*) = 0$) satisfying one condition more. Namely, for the picture in the left-hand side of (9) (respectively, of (10)) this condition is as follows: there exists a point $a < *$ (respectively, $a > *$) in $\mathbb{R}^1_w$ such that $f(a)$ lies below (respectively, above) $f(*)$ in $\mathbb{R}^3$. For both blocks indicated in the left-hand sides of (12) and (13) the limit condition claims that the second derivative $f_1''(*)$ is directed "to the west" in $\mathbb{R}^2$.

All these additional conditions specify subvarieties of codimension one in the vice-maximal cell of σ_1, and the lemma is proved. □

End of the proof of Theorem 1. The projection of the chain γ_1 to Σ is indicated in (14). The direct algorithm transforms the $\mathcal{B}$-blocks, forming this projection, to the $\mathcal{F}$-blocks indicated in the left-hand sides of equalities (15)–(17). The sum of right-hand sides of these three equalities is equal to the cycle (14); therefore the sum of the $\mathcal{F}$-blocks indicated in their left-hand sides is the desired combinatorial formula.

This sum coincides with formula (48), and Theorem 1 is proved. □

6. Calculation of a combinatorial formula for v_3

This is the second demonstration of the algorithm: the calculation of a combinatorial formula for the unique degree 3 invariant v_3 reduced mod 2.

Theorem 2. *A combinatorial formula for the third degree invariant* (mod 2) *is given by the sum of fifteen $\mathcal{F}$-blocks indicated in* (49).

(49)

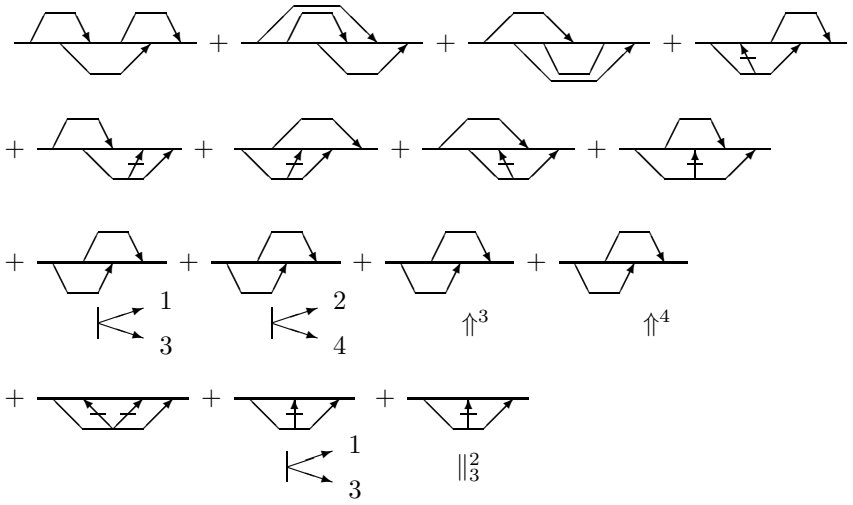

A proof of this theorem (done by our algorithm) occupies the rest of §6.

6.1. **Principal part.** The principal part γ of v_3 in $\sigma_3 \setminus \sigma_2$ is equal to the sum of three chord diagrams

(50)

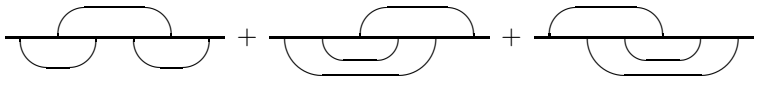

It is essential here that we consider the mod 2 homology: a similar formula with integral coefficients should contain one term more with coefficient 2; see [17]. On the other hand the very formula (50) expresses the principal part of a certain integer cohomology class of degree 3 of the space of knots in $\mathbb{R}^n$ with any *even* $n \geq 4$.

6.2. **First differential and its homology to zero.** The boundary $d^1(\gamma)$ of this principal part in $\sigma_2 \setminus \sigma_1$ is equal to the sum of nine $\mathcal{B}$-blocks

(51)

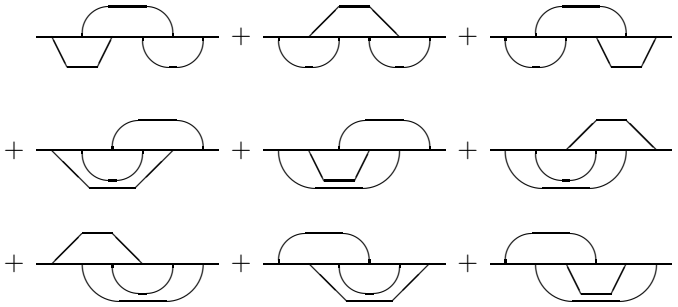

These $\mathcal{B}$-blocks lie in all three maximal cells of $\sigma_2 \setminus \sigma_1$: the second block is contained in the second cell of (24), the 6th and 7th blocks in the third one, and all six remaining blocks in the first cell of (24).

Let us span this sum by a chain in $\sigma_2 \setminus \sigma_1$. The direct algorithm associates to elements of (51) the $\mathcal{F}$-blocks indicated in the left-hand sides of equalities (52)–(60).

(52)

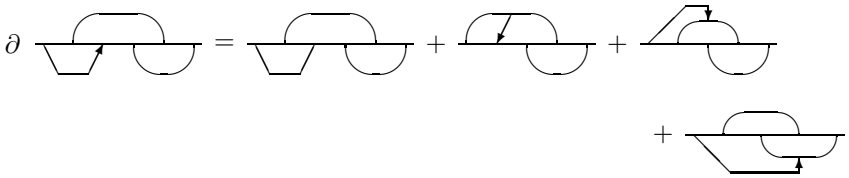

(53)

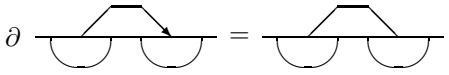

(54)

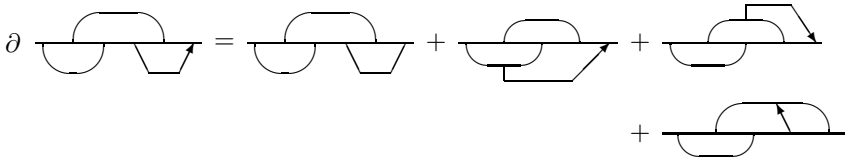

(55)

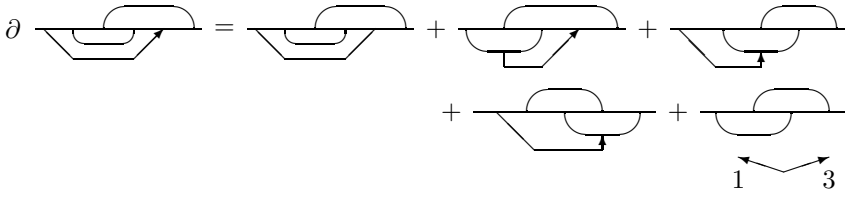

(56)

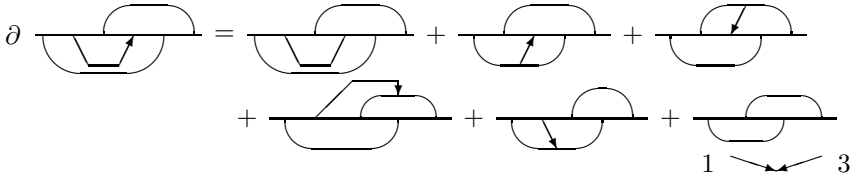

(57)

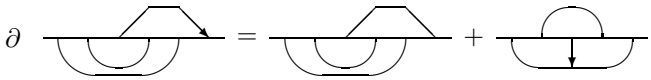

(58)

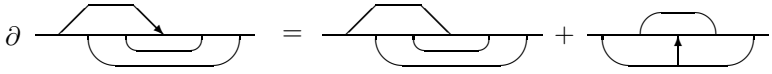

(59)

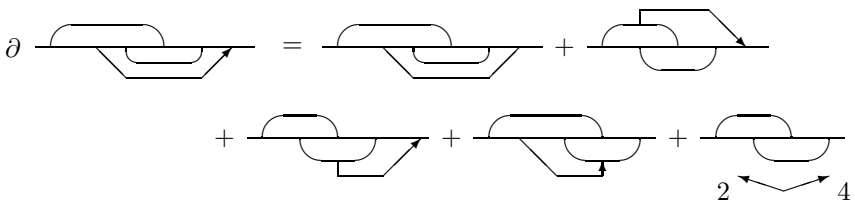

(60)

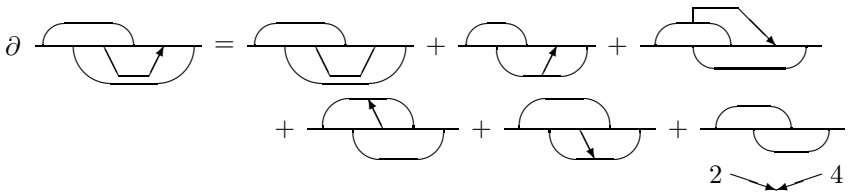

These equalities imply easily the following statement.

Proposition 21. *The cycle* (51) *is homologous to the chain* (61) *in the union of maximal cells of* $\sigma_2 \setminus \sigma_1$. *This homology is provided by nine* $\mathcal{F}$*-blocks indicated in left-hand sides of equalities* (52)–(60).

(61)

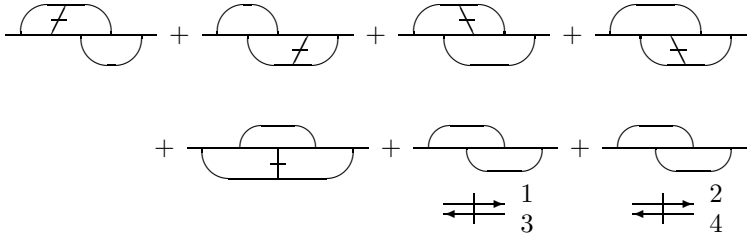

Indeed, the summands of (51) coincide with the first summands in the right-hand sides of equalities (52)–(60). The remaining terms of these equalities satisfy the following relations (where $(a;b)$ denotes the bth component of the right-hand side of the equality (a)):

$(52;3) = (55;3)$, $(52;4) = (55;4)$, $(54;2) = (59;2)$, $(54;3) = (59;3)$,
$(55;2) = (60;3)$, $(56;4) = (59;4)$, $(52;2) + (56;5) = (61;1)$,
$(54;4) + (60;2) = (61;2)$, $(55;5) + (56;6) = (61;6)$, $(56;3) + (60;5) = (61;4)$,
$(56;2) + (60;4) = (61;3)$, $(57;2) + (58;2) = (61;5)$, $(59;5) + (60;6) = (61;7)$. □

The direct algorithm transforms the chain (61) into the sum of the left-hand sides of equalities (62)–(68).

(62)

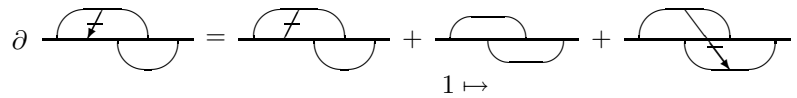

(63)

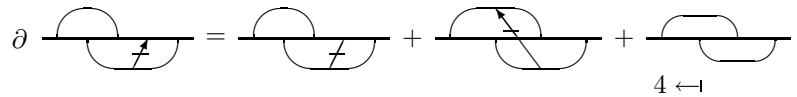

(64)

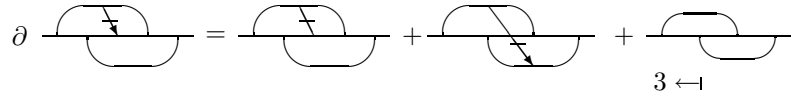

(65)

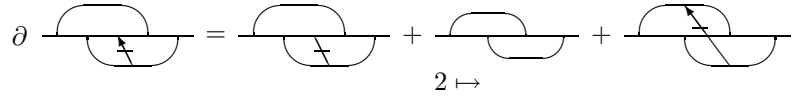

(66)

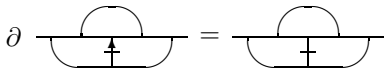

(67)

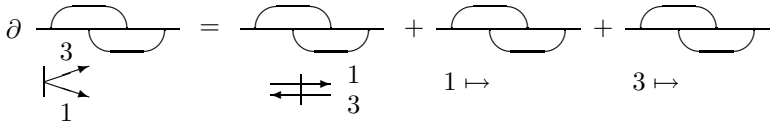

(68)

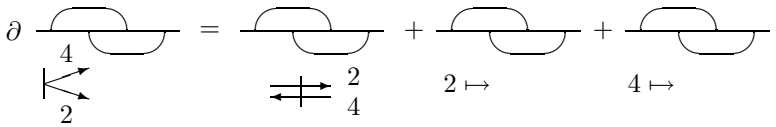

These equalities imply that the cycle (61) is homologous to the chain

(69)

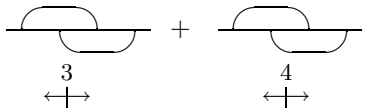

in some maximal open cell of the term $\sigma_2 \setminus \sigma_1$.

Indeed, the summands of the cycle (61) coincide with the first summands in the right-hand sides of these equalities; moreover, we have $(62;2) = (67;2)$, $(65;2) = (68;2)$, $(62;3) = (64;2)$, $(63;2) = (65;3)$, $(64;3)+(67;3) = (69;1)$, and $(63;3)+(68;3) = (69;2)$.

The blocks indicated in (69) coincide in the same cell with the boundaries of two $\mathcal{F}$-blocks indicated in (70).

(70)

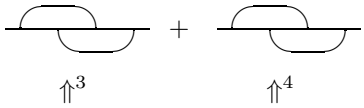

Finally, we get the following statement.

Proposition 22. *The cycle* (51) *is homologous in the term* $\sigma_2 \setminus \sigma_1$ *to some linear combination of vice-maximal cells of the canonical cell decomposition of this term. This homology is provided by the sum of eighteen* $\mathcal{F}$*-blocks indicated in the left-hand sides of equalities* (52)–(60) *and* (62)–(68)*, and in formula* (70)*.* □

Proposition 23. *The linear combination of vice-maximal cells mentioned in the previous proposition is equal to zero. In particular the cycle* (51) *is equal to the boundary in* $\sigma_2 \setminus \sigma_1$ *of the sum of these eighteen* $\mathcal{F}$*-blocks.*

Proof. Denote by $\bar{\partial}$ the part of the boundary operator associating to any $\mathcal{F}$-block the intersection of its full homological boundary with the union of vice-maximal cells of the same term $\sigma_i \setminus \sigma_{i-1}$ of the resolved discriminant (see the beginning of §3). According to §3.6 this operator $\bar{\partial}$ acts on our eighteen $\mathcal{F}$-blocks as is shown in the next equations (71)–(88):

(71)

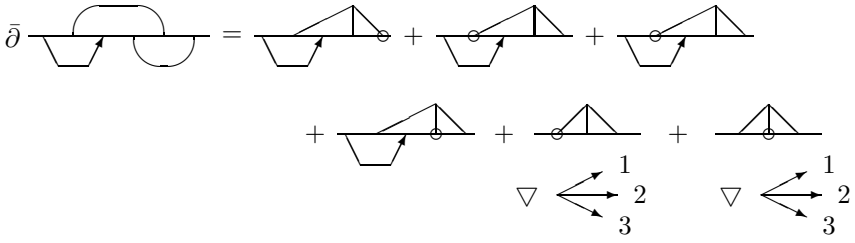

(72)

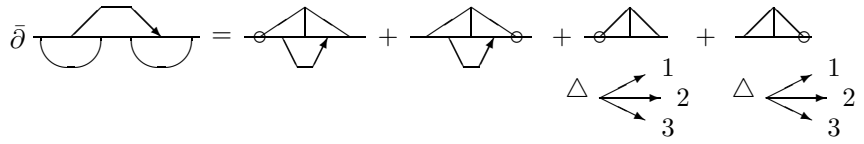

(73)

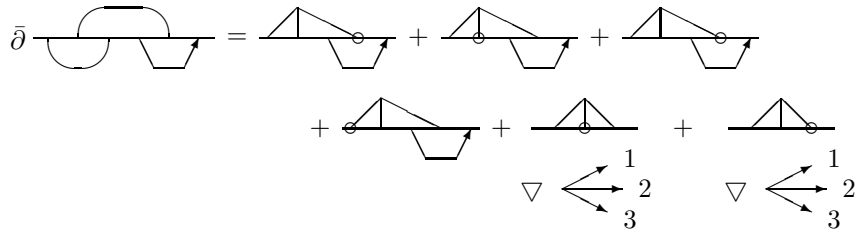

(74)

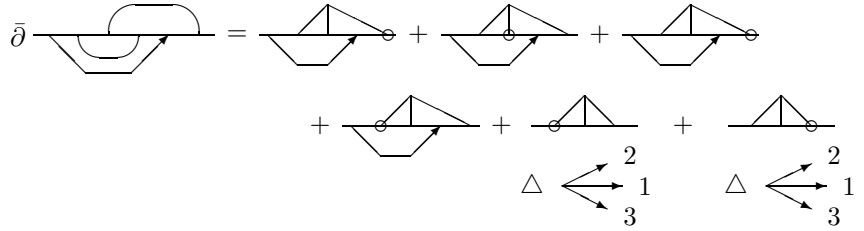

(75)

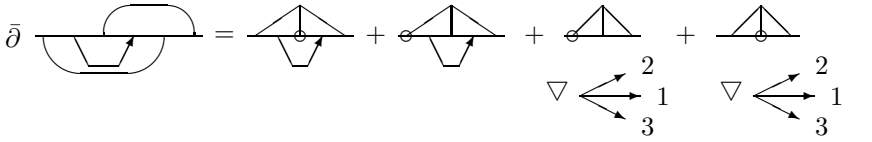

(76)

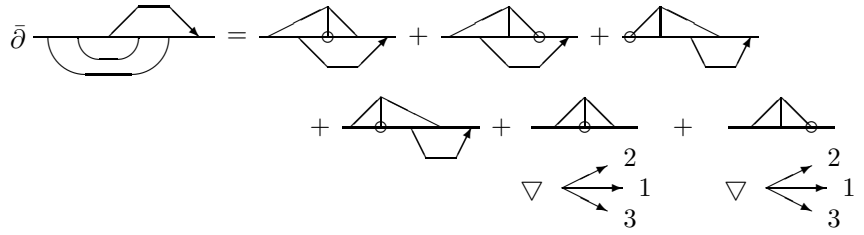

(77)

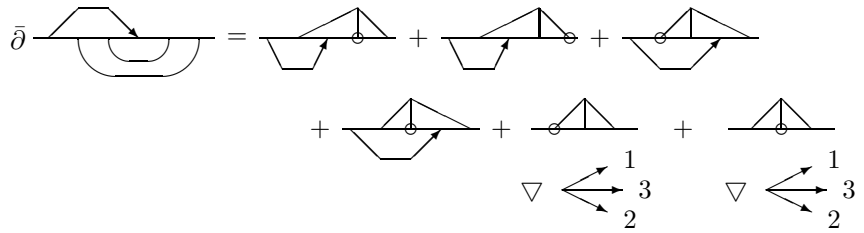

(78)

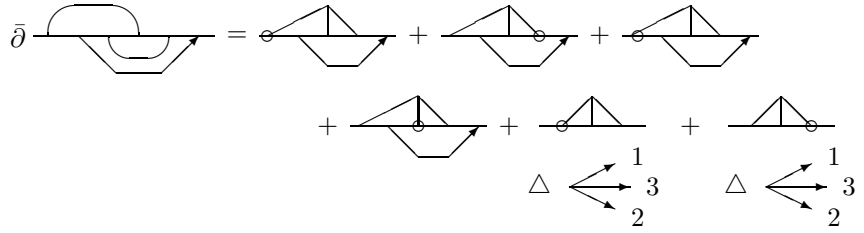

(79)
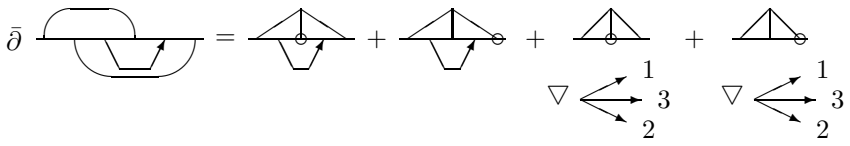

(80)
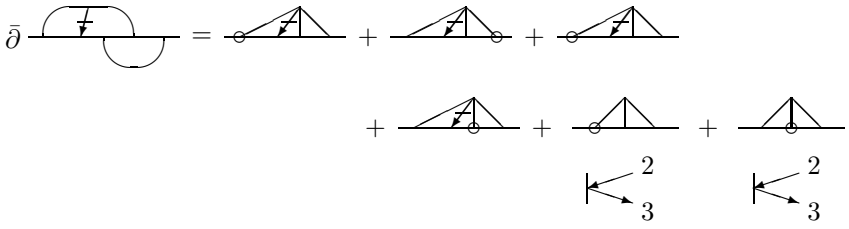

(81)
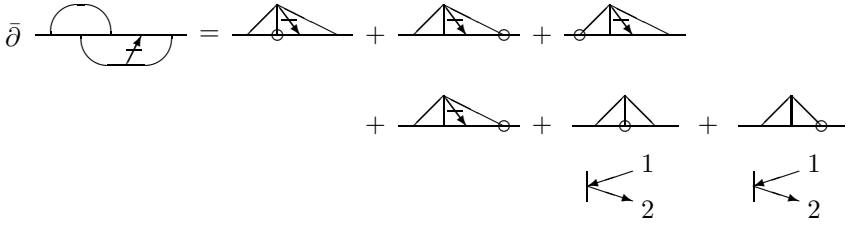

(82)
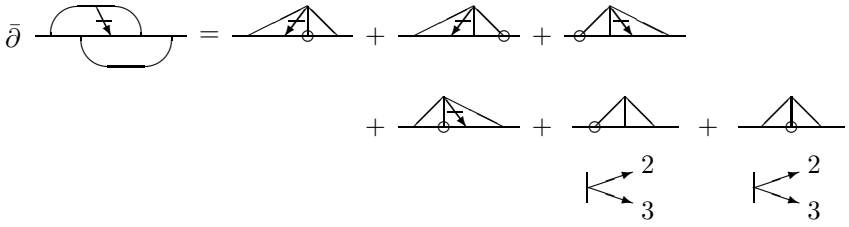

(83)
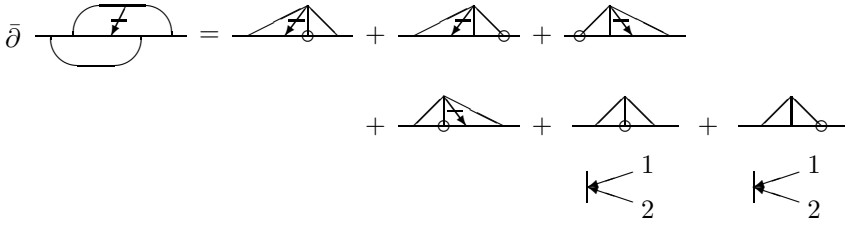

(84)
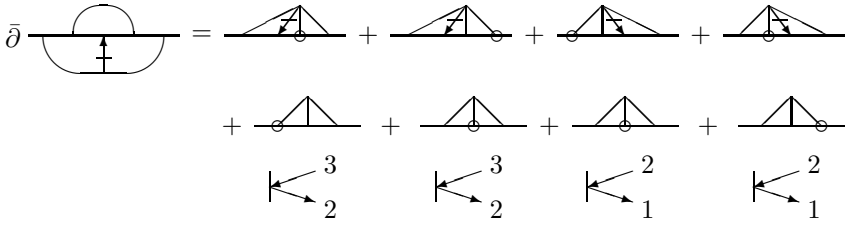

(85)
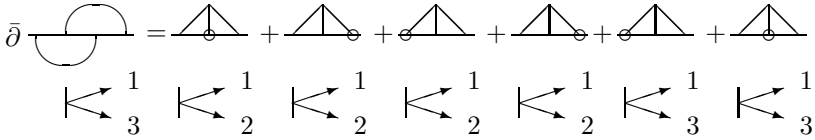

(86) 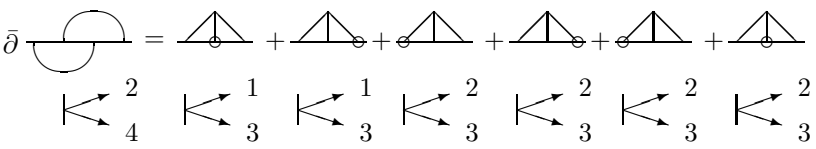

(87) 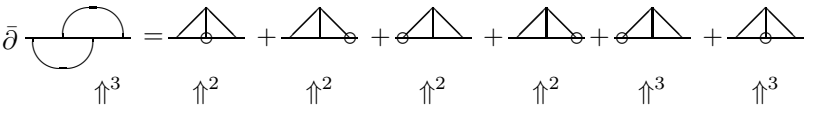

(88) 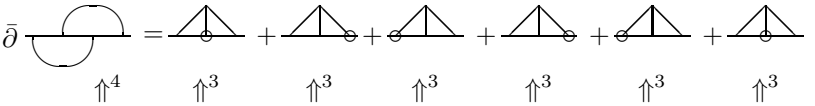

It remains to prove that the sum of the right-hand sides of all these equalities is equal to zero. Its terms satisfy the following relations, reducing this sum. Denote by $(a;b)$ the bth summand of the right-hand part of the equality (a). Then we have

$(71;1)=(77;2)$, $(71;2)=(71;3)$, $(71;4)=(77;1)$, $(71;6)=(73;5)$,
$(72;1)=(75;2)$, $(72;2)=(79;2)$, $(73;1)=(73;3)$, $(73;2)=(76;4)$,
$(73;4)=(76;3)$, $(74;1)=(74;3)$, $(74;2)=(77;4)$, $(74;4)=(77;3)$,
$(75;1)=(79;3)$, $(75;4)=(76;5)$, $(76;1)=(78;4)$, $(76;2)=(78;2)$,
$(77;6)=(79;3)$, $(78;1)=(78;3)$, $(80;1)=(80;3)$, $(81;2)=(81;4)$,
$(80;2)=(82;2)$, $(80;4)=(82;1)$, $(81;1)=(82;4)$, $(81;3)=(82;3)$,
$(82;6)=(86;6)$, $(83;1)=(84;1)$, $(83;2)=(84;2)$, $(83;3)=(84;3)$,
$(83;4)=(84;4)$, $(85;2)=(85;4)$, $(85;6)=(86;1)$, $(86;3)=(86;5)$,
$(87;2)=(87;4)$, $(87;5)=(88;3)$, $(87;6)=(88;1)$, $(88;2)=(88;4)$.

Any remaining summand containing the condition $\triangle$ is matched by a similar summand with this condition replaced by $\bigtriangledown$, and their sum is equal to a similar term without these conditions. The summands remaining after all these reductions can be combined in the sum shown in next three formulas (89)–(91); here a formula consisting of a picture and a sum in the cartouche below it denotes the sum of $\mathcal{F}$-blocks defined by pictures with one and the same main part but with different subscripts listed in the cartouche.

(89) 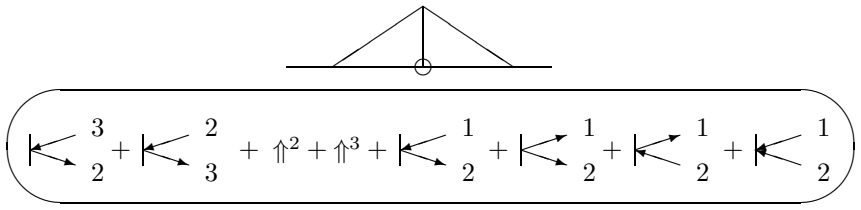

(90) 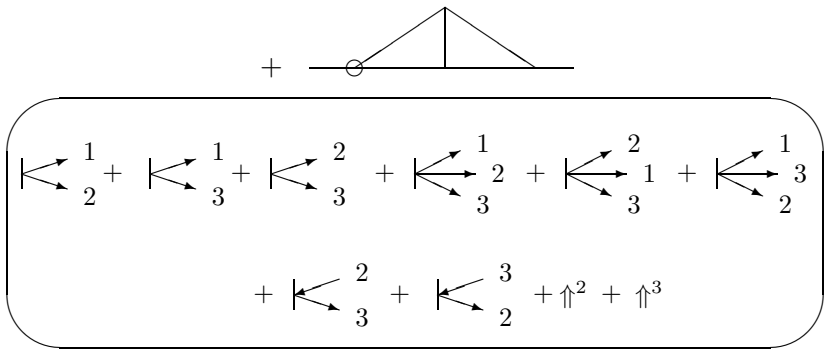

(91)

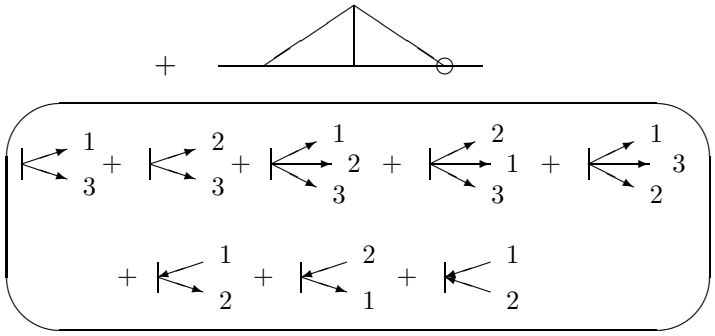

Lemma 6. *The sum indicated in either of the three cartouches in formulas* (89), (90), *and* (91) *is identically equal to zero on all generic singular knots respecting the picture over this cartouche* (*i.e., having a triple point*).

Proof. A. The sum of the first four terms in the cartouche of (89) is identically equal to $1 \in \mathbb{Z}_2$. Indeed, the sum of the first two terms (respectively, of the 3rd and 4th terms) is equal to 1 if and only if the vectors $f_2'(a_2)$ and $f_2'(a_3)$ are directed into equal (respectively, different) sides in $\mathbb{R}^1$. The sum of the remaining four terms in (89) obviously is also equal to 1, and the entire line (89) vanishes.

B. The sum of the six terms in the upper line of the cartouche of (90) also is identically equal to 1. Indeed, if all three vectors $f_1'(a_1)$, $f_1'(a_2)$, $f_1'(a_3)$ are directed into some half-plane in $\mathbb{R}^2$, then exactly one of the last three conditions of this line is satisfied and none or two of the first three conditions are satisfied. If these three vectors do not lie in one half-plane, then exactly one of the first three conditions and none of the last three conditions is satisfied.

The lower four terms in (90) coincide with the first four terms in (89) and also form a tautology.

C. Adding the term  to both levels of the cartouche (91) we obtain two functions identically equal to 1. Lemma 6 and Proposition 23 are completely proved. □

Therefore we can take the sum of the eighteen $\mathcal{F}$-blocks mentioned in Proposition 23 for the chain γ_1 spanning the cycle $d^1(\gamma)$ in all of $\sigma_2 \setminus \sigma_1$.

6.3. **Second differential and its homology to zero.** The boundary of this chain γ_1 in σ_1 (see §3.7) is equal to the sum of the thirty-six $\mathcal{B}$-blocks indicated in the next nine lines (92)–(100).

(92) 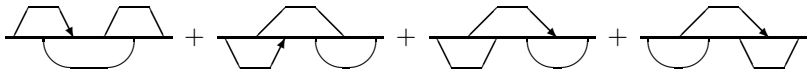

(93) 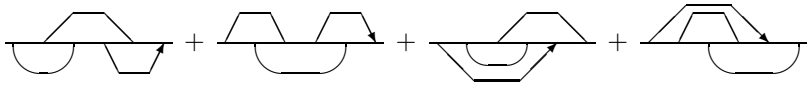

(94) 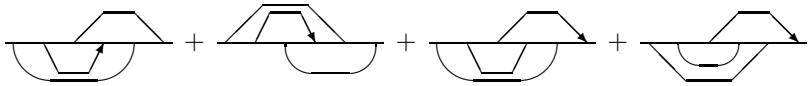

(95) 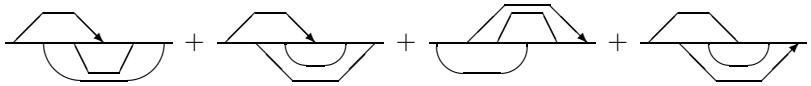

(96)

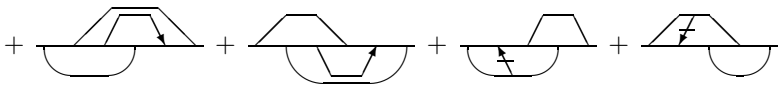

(97)

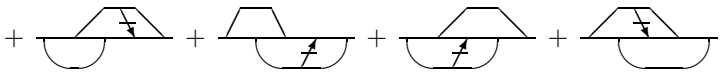

(98)

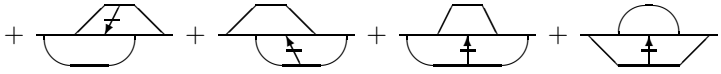

(99)

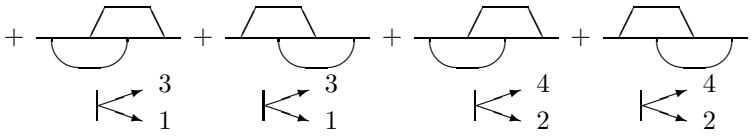

(100)

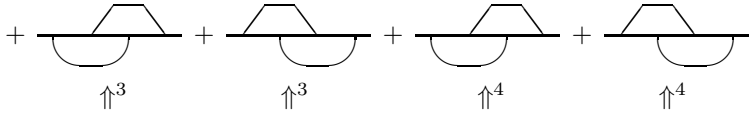

To span this cycle, the direct algorithm supplies us with the $\mathcal{F}$-blocks indicated in the left-hand sides of the next equalities (101)–(127); note that any of the first nine of them kills some two of our 36 summands in (92)–(100).

(101)

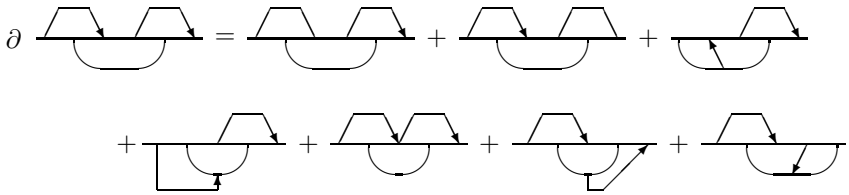

(102)

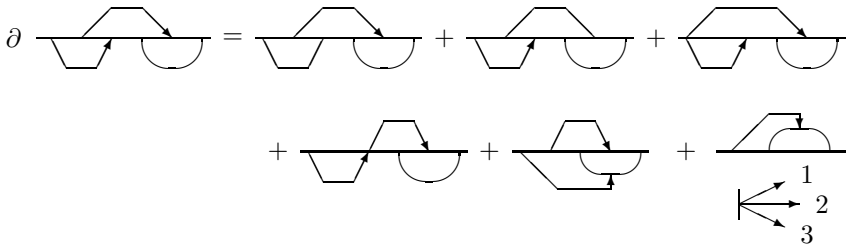

(103)

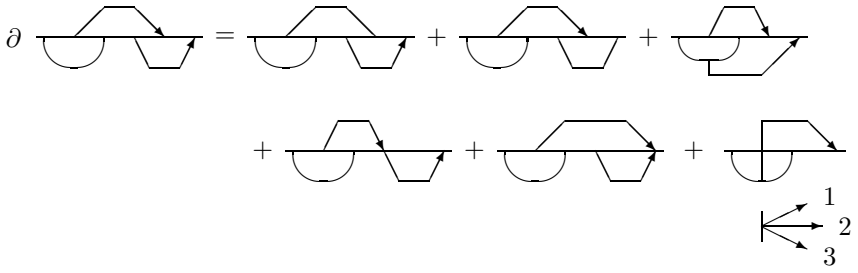

(104)

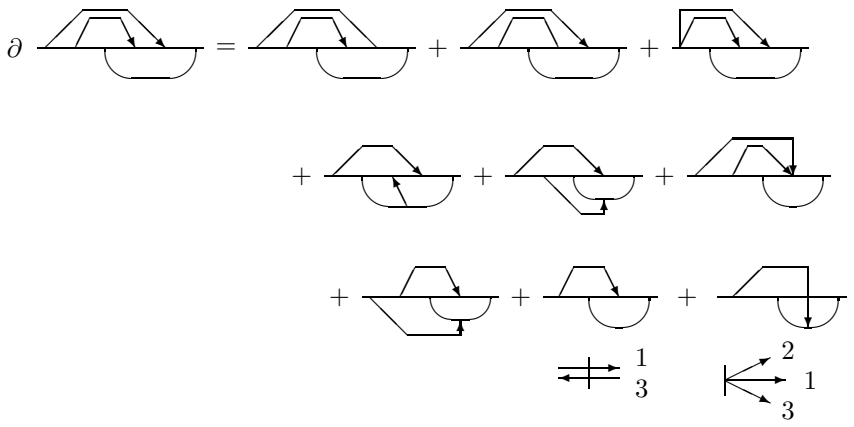

(105)

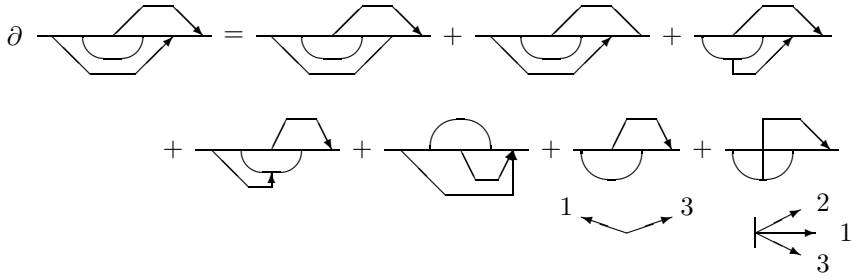

(106)

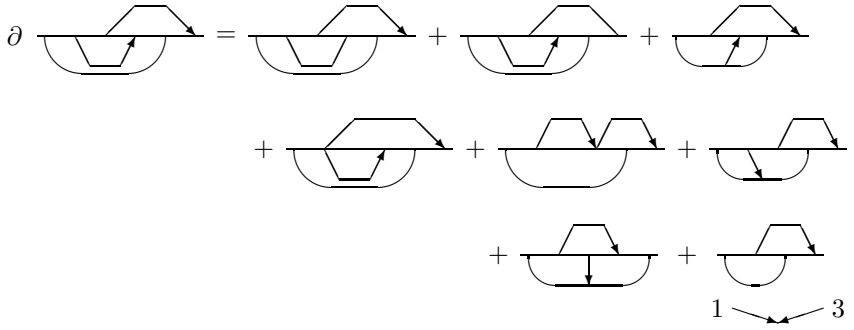

(107)

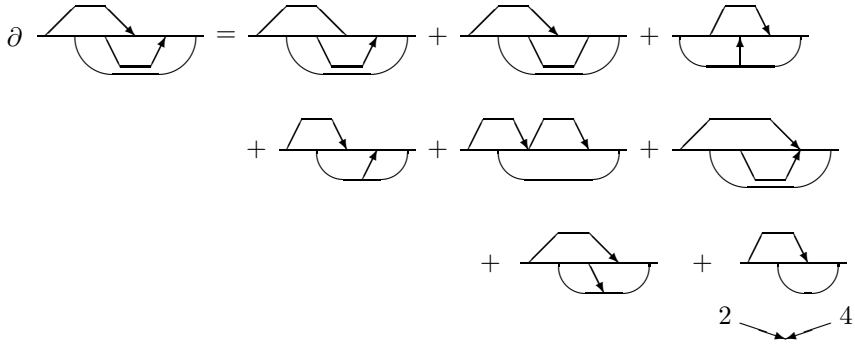

(108)

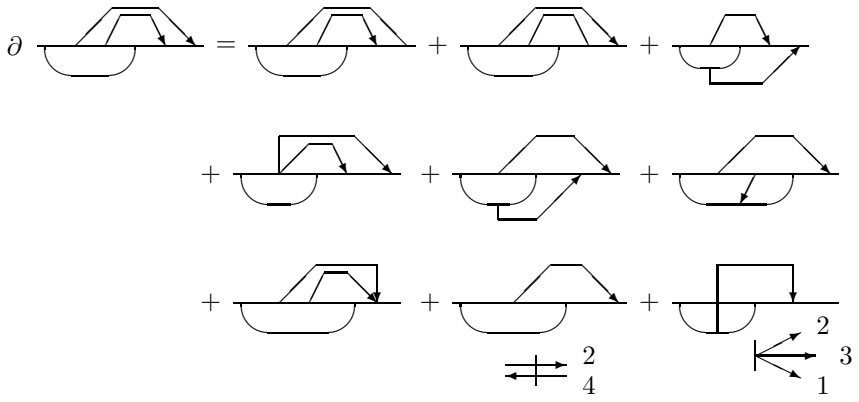

(109)

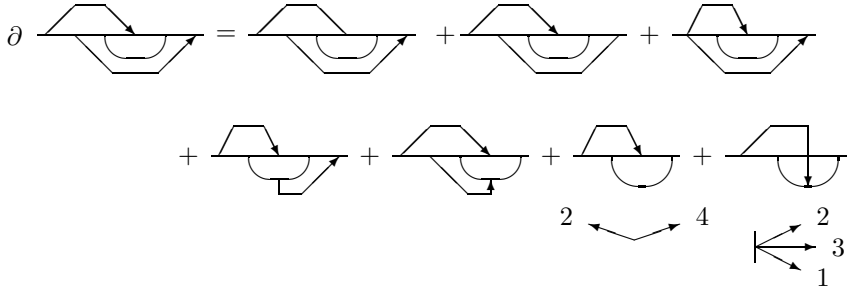

(110)

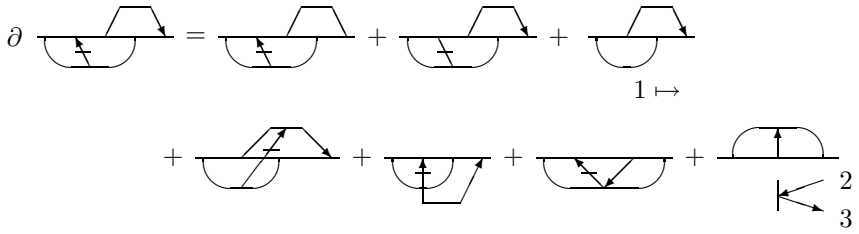

(111)

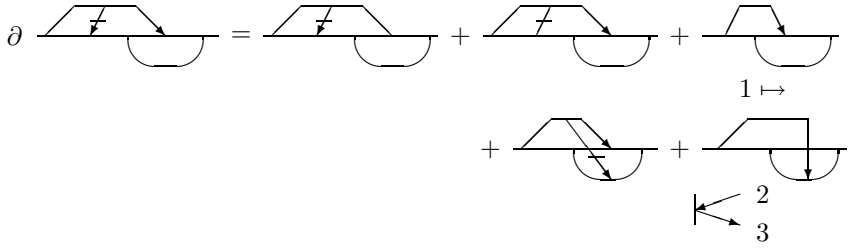

(112)

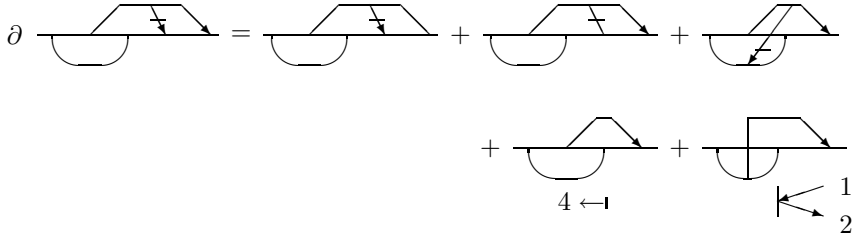

(113)

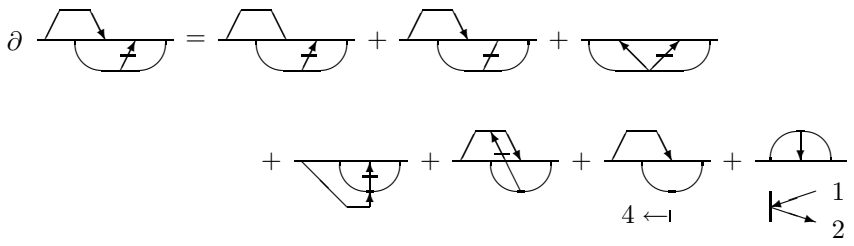

(114)

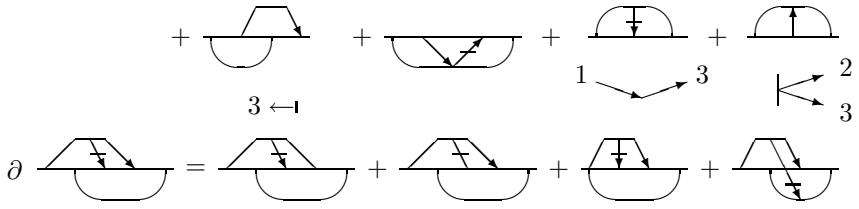

(115)

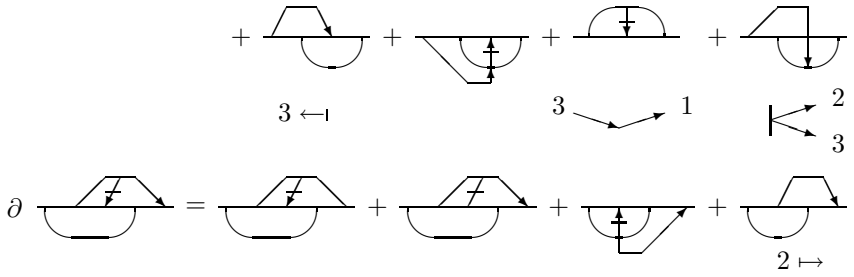

(116)

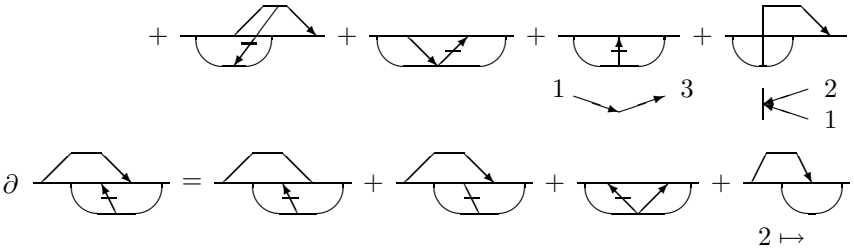

(117)

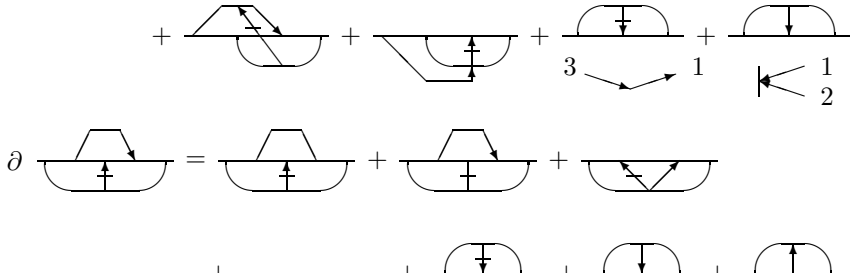

(118)

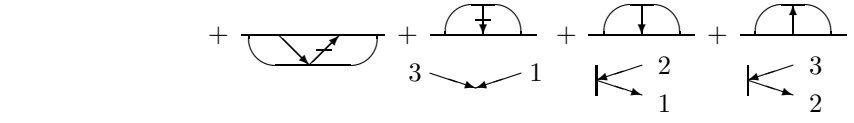

(119)

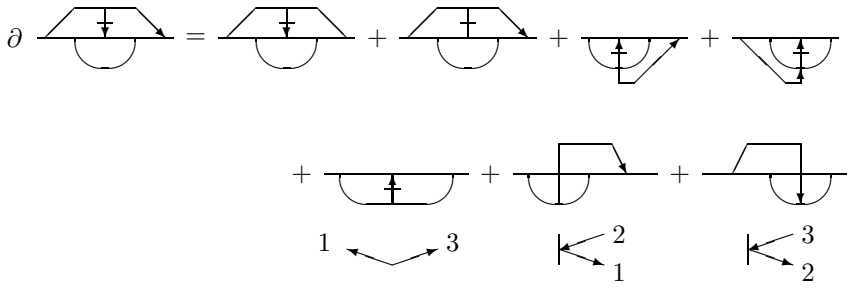

(120)

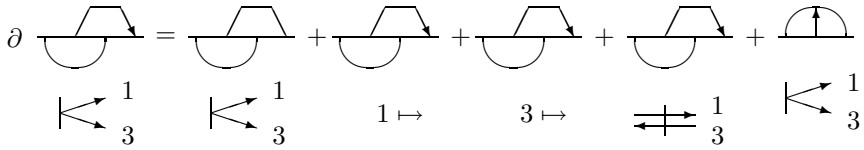

(121)

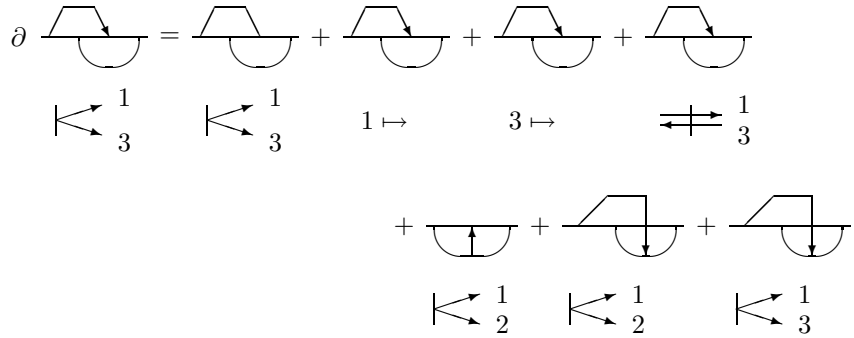

(122)

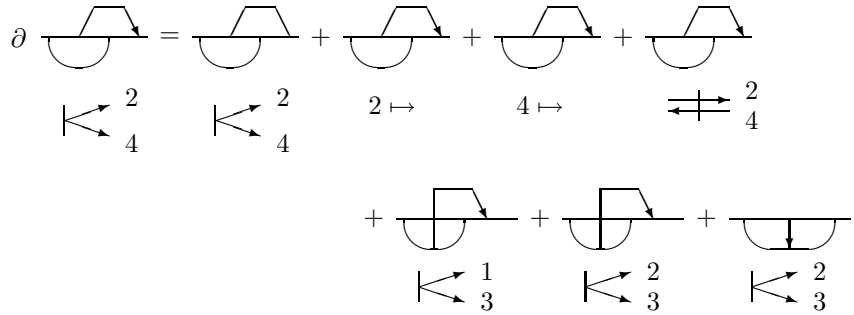

(123)

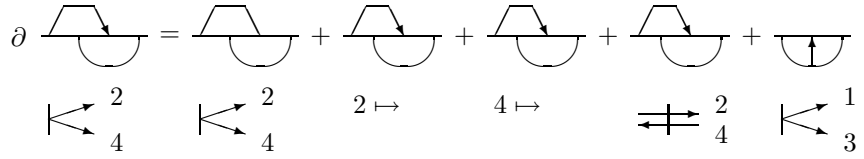

(124)

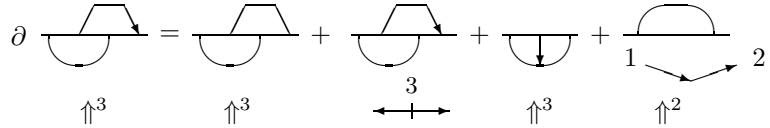

(125)

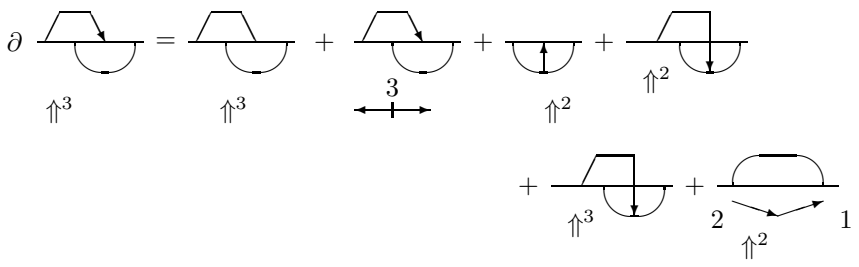

(126)

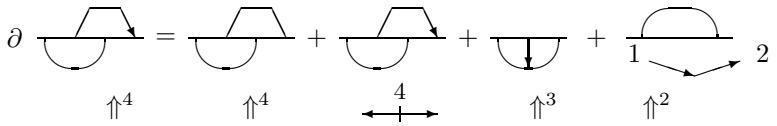

(127)

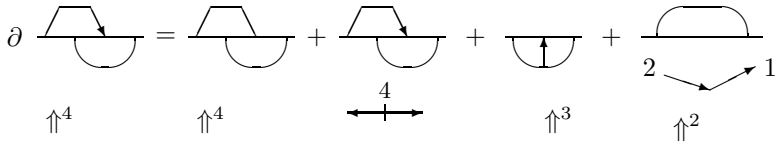

All terms of the sum (92)–(100) are contained in the right-hand sides of equalities (101)–(127). Indeed, let us denote by (a;b) the bth component of the right-hand side of the equality (a). Then we have

$$
\begin{array}{l}
(92;1)=(101;2),(92;2)=(102;2),(92;3)=(102;1),(92;4)=(103;2),\\
(93;1)=(103;1),(93;2)=(101;1),(93;3)=(105;2),(93;4)=(104;2),\\
(94;1)=(106;2),(94;2)=(104;1),(94;3)=(106;1),(94;4)=(105;1),\\
(95;1)=(107;2),(95;2)=(109;2),(95;3)=(108;2),(95;4)=(109;1),\\
(96;1)=(108;1),(96;2)=(107;1),(96;3)=(110;1),(96;4)=(111;1),\\
(97;1)=(112;1),(97;2)=(113;1),(97;3)=(114;1),(97;4)=(115;1),\\
(98;1)=(116;1),(98;2)=(117;1),(98;3)=(118;1),(98;4)=(119;1),\\
(99;1)=(120;1),(99;2)=(121;1),(99;3)=(122;1),(99;4)=(123;1),\\
(100;1)=(124;1),(100;2)=(125;1),(100;3)=(126;1),(100;4)=(127;1).
\end{array}
\tag{128}
$$

Therefore the equations (101)–(127) provide a mod 2 homology in the maximal cell of σ_1 between the cycle (92)–(100) and the sum of all remaining terms of right-hand sides of these equations. These terms satisfy many relations which very much reduce this sum. Namely, we have:

$(101;3)+(106;6)=(110;2)$, $(101;4)=(105;4)$, $(101;5)+(105;5)+(109;3)=(119;2)$, $(101;6)=(109;4)$, $(101;7)+(107;4)=(113;2)$, $(102;3)+(102;4)+(104;6)=(111;2)$, $(102;5)=(104;7)$, $(103;3)=(108;3)$, $(103;4)+(103;5)+(108;4)=(112;2)$, $(104;5)=(109;5)$, $(104;3)+(107;5)+(107;6)=(115;2)$, $(104;4)+(107;7)=(117;2)$, $(104;8)=(121;4)$, $(105;3)=(108;5)$, $(105;6)+(106;8)=(120;4)$, $(106;3)+(108;6)=(114;2)$, $(106;4)+(106;5)+(108;7)=(116;2)$, $(106;7)+(107;3)=(118;2)$, $(107;8)+(109;6)=(123;4)$, $(108;8)=(122;4)$, $(110;3)=(120;2)$, $(110;4)=(114;4)$, $(110;5)=(116;3)$, $(111;3)=(121;2)$, $(111;4)=(115;4)$, $(112;3)=(116;5)$, $(112;4)+(122;3)=(126;2)$, $(113;4)=(117;6)$, $(113;5)=(117;5)$, $(113;6)+(123;3)=(127;2)$, $(114;3)=(119;3)$, $(114;5)+(120;3)=(124;2)$, $(114;7)=(116;7)$, $(114;8)=(122;7)$, $(115;3)=(117;3)$, $(115;5)+(121;3)=(125;2)$, $(115;6)=(119;4)$, $(115;7)=(117;7)$, $(116;4)=(122;2)$, $(116;6)=(118;4)$, $(117;4)=(123;2)$, $(124;3)=(126;3)$, $(124;4)=(126;4)$, $(125;6)=(127;4)$.

Therefore the cycle (92)–(100) is homologous in the maximal cell of σ_1 to the chain consisting of all elements of right-hand sides of equalities (101)–(127) not mentioned in (128) nor in the previous relations. Namely, these are the following terms:

(102; 6), (103; 6), (104; 9), (105; 7), (108; 9), (109; 7), (110; 6), (110; 7), (111; 5), (112; 5), (113; 3), (113; 7), (114; 6), (115; 8), (116; 8), (117; 8), (118; 3), (118; 5), (118; 6), (118; 7), (119; 5), (119; 6), (119; 7), (120; 5), (121; 5), (121; 6), (121; 7), (122; 5), (122; 6), (123; 5), (125; 3), (125; 4), (125; 5), (127; 3).

It is convenient to combine these terms in the following five lines (129)–(133). Here the picture (129;5) stays for the sum (118;5)+(119;5), and any of lines (130)–(133) represents the sum of several $\mathcal{B}$-blocks, whose pictures consist of one and the same main part and different subscripts listed in the cartouche under the line.

(129)

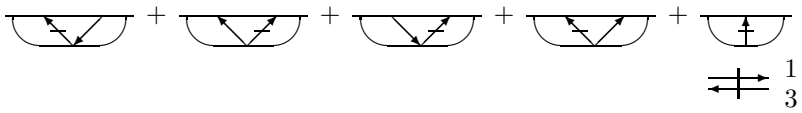

(130)

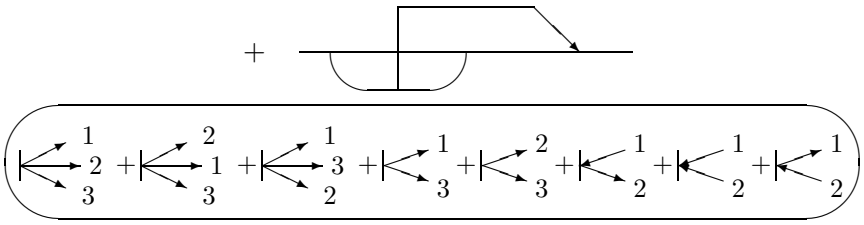

(131)

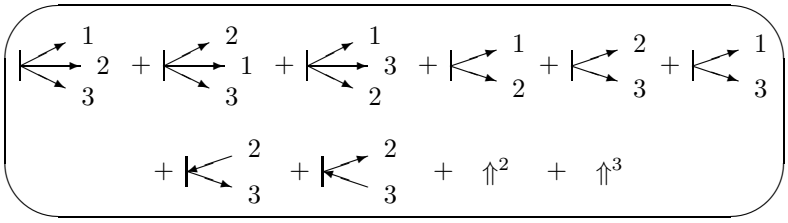

(132)

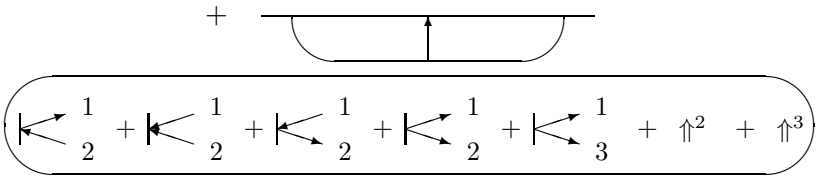

(133)

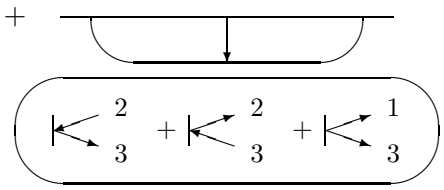

It is convenient to think of the subscripts (i.e., of the contents of cartouches) under the last four formulas as of the characteristic functions (mod 2) of certain chains in the manifolds distinguished by the pictures above these subscripts.

This cycle (129) + ⋯ + (133) can be reduced very much.

Proposition 24. *The chain* (129)–(133) *is equal in* σ_1 *to the chain*

(134) 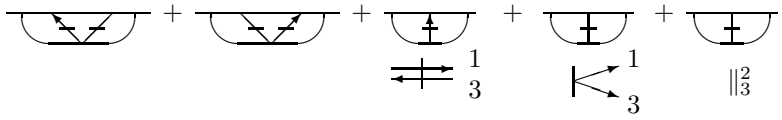

The proof is based on Lemmas 7–9 below.

Lemma 7. *The chain* (130) *is equal to zero.*

First proof. This proof is just an illustration of statement 1 of Corollary 1 of Proposition 9 (see page 52). Indeed, the boundary of this chain contains a similar chain defined by the picture with the same expression in the cartouche but in whose main part the orientation of the broken line is omitted. This part of the boundary cannot be killed by the boundaries of any other chains (129) or (131)–(133). Thus the whole chain (129)–(133) has the chance to be a cycle (which it is by its construction) only if the expression in the cartouche defines an identically zero function mod 2. □

Second proof. The sum of the conditions listed in the cartouche (130) coincides with that of formula (91). Therefore it is equal to 0 at any generic curve respecting the main picture of (130): a proof of this coincides with the corresponding part of the proof of Lemma 6 on page 67.

Lemma 8. *The chain* (131) *is equal to zero.*

The first proof of this lemma almost repeats that of Lemma 7, and the second one refers to the triviality of the line (90); see Lemma 6. □

Lemma 9. *The sums contained in two cartouches under the lines* (132), (133) *define one and the same function on the union of subalgebraic subsets in* σ_1 *defined by the main parts of pictures shown in these lines.*

The first proof is an illustration of the second statement of Corollary 1 of Proposition 9. The direct proof is as follows. The sum of the first four subscripts under the line (132) defines the function identically equal to 1. The sum of the last two subscripts of this line and the first two subscripts of the line (133) also is equal to this function. Finally, the remaining terms number 5 under (132) and number 3 under (133) coincide and Lemma 9 is again proved. □

These three lemmas imply that we can just erase both lines (130) and (131) and replace the contents of the cartouche under (132) by that under (133). Using additionally the first identity (32) we reduce the sum of all lines (130)–(133) to the sum of the last two summands of formula (134).

The sum of the first three summands of (134) is obviously equal to (129) (indeed, (129;1) + (129;4) = (134;1) and (129;2) + (129;3) = (134;2)), and Proposition 24 is proved. □

The direct algorithm transforms the chain (134) into the left-hand sides of the next three equalities:

(135) 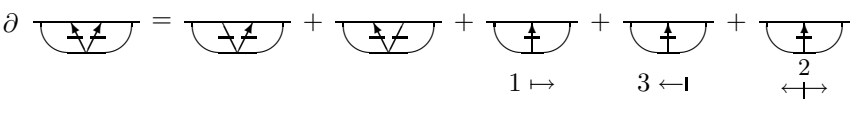

(136) 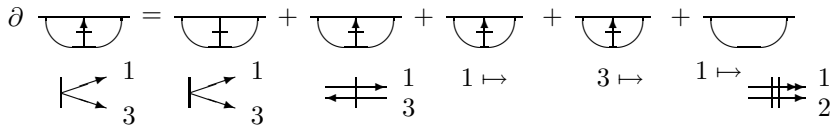

(137) 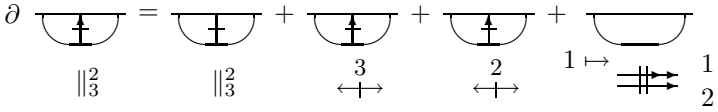

Here the (coinciding) second subscripts under the last pictures of the last two equalities are explained in paragraph **5!** of Subsection 2.4.

It is easy to see that the sum of the right-hand sides of these three equalities is equal to the cycle (134).

We have proved the following statement.

Proposition 25. *The chain representing the second differential $d^2(v_3) \subset \sigma_1$ (and expressed by the formulas* (92)–(100)*) is homologous in σ_1 to the unique vice-maximal cell of σ_1 taken with some coefficient. This homology is provided by the sum of thirty $\mathcal{F}$-blocks in σ_1 indicated in the left-hand sides of equalities* (101)–(127) *and* (135)–(137). □

Proposition 26. *The coefficient mentioned in the first assertion of Proposition* 25 *is equal to zero. In particular, the chain representing the second differential $d^2(v_3) \subset \sigma_1$ is equal to the homological boundary of the sum of thirty $\mathcal{F}$-blocks in σ_1 indicated in the left-hand sides of equalities* (101)–(127) *and* (135)–(137).

This proposition is an immediate corollary of Proposition 6. Let us give a direct proof. This proof is very similar to that of Lemma 5. Indeed, for almost all of our thirty $\mathcal{F}$-blocks the interval bounded by the endpoints of the arc contains an endpoint of at least one noncrossed arrow. Therefore the limit variety contains only the singular knots having a stationary point and one point strictly above or below it: this is a situation of codimension 2 in σ_1 or codimension 1 in the vice-maximal cell. The remaining terms for which it is not the case are shown in the left-hand sides of equalities (119) and (135)–(137). The limit variety for (119) consists of singular knots having a crossing point strictly to the right of the stationary point. The limit varieties for chains indicated in (135)–(137) can be ignored by the same reasons as the limit variety from the formula (12) in the proof of Lemma 5. □

6.4. **Third differential and the chain spanning it.** The third differential $d^3(v_3) \in \bar{H}_{\omega-1}(\Sigma)$ is represented by the image under the canonical projection $\pi : \sigma_1 \to \Sigma$ of the spanning chain mentioned in the previous proposition. It consists of thirty $\mathcal{B}$-blocks, whose pictures can be obtained from the pictures in the left-hand sides of equalities (101)–(127) and (135)–(137) by replacing the unique arc of either picture by a nonoriented broken line ⊓ .

By the construction, the sum of these thirty varieties is a cycle in Σ.

It remains to *span* this cycle by a relative chain in $\mathcal{K}$ (i.e., to represent it as a boundary of such a chain). The direct algorithm gives us immediately the left-hand sides of the

following equalities (138)–(152).

(138)

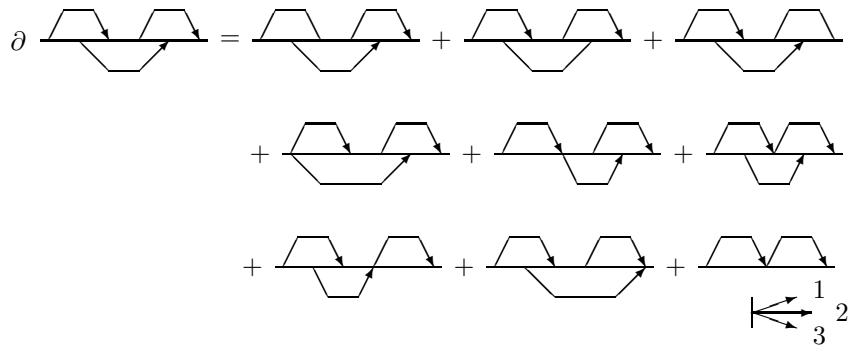

(139)

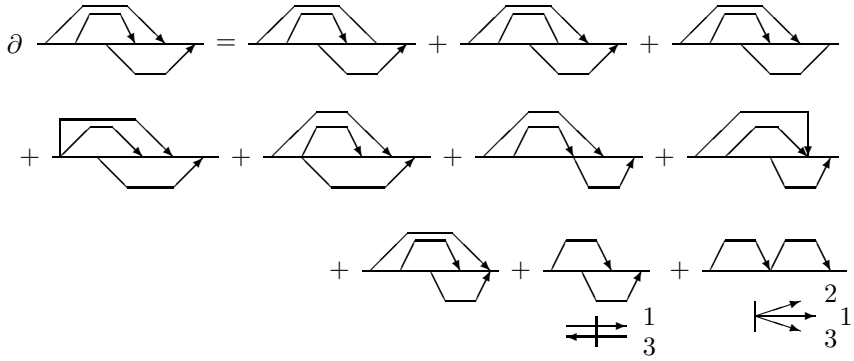

(140)

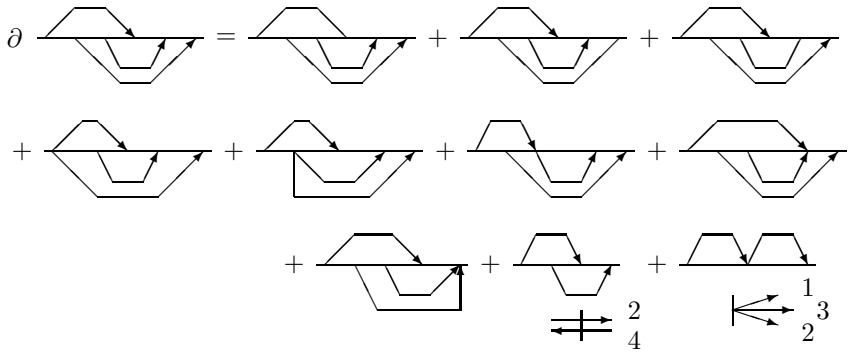

(141)

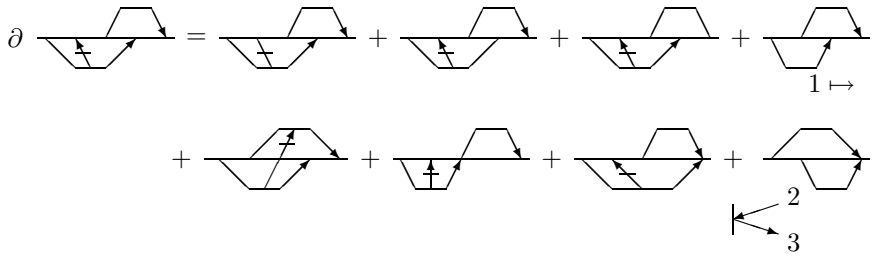

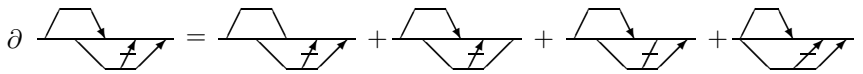

(142)

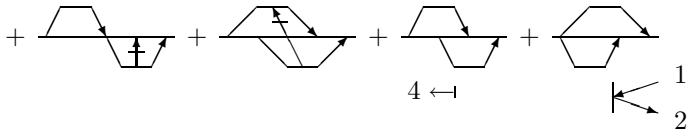

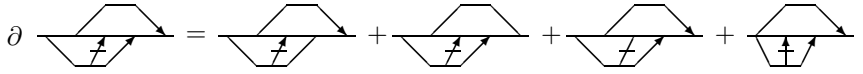

(143)

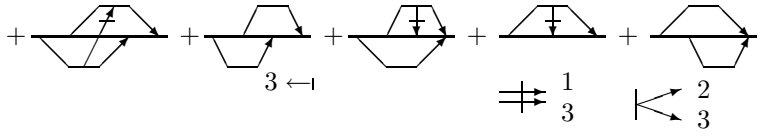

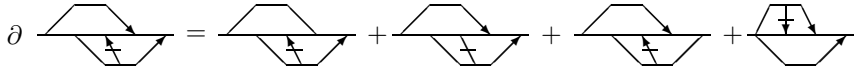

(144)

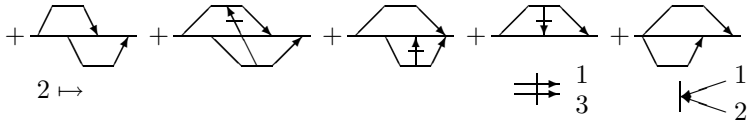

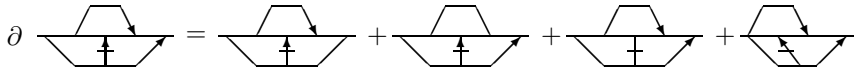

(145)

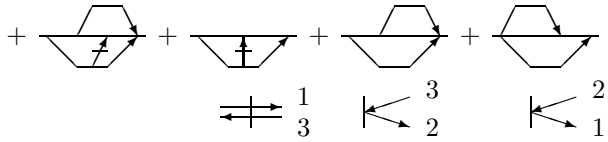

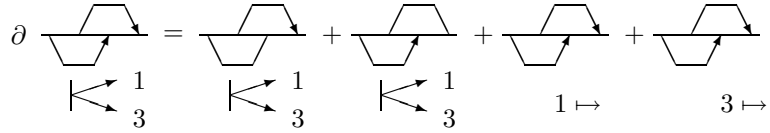

(146)

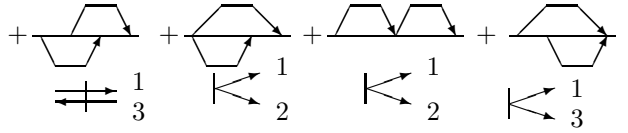

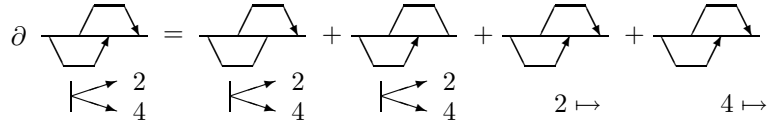

(147)

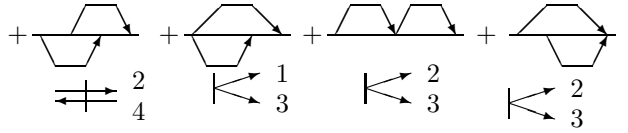

(148)

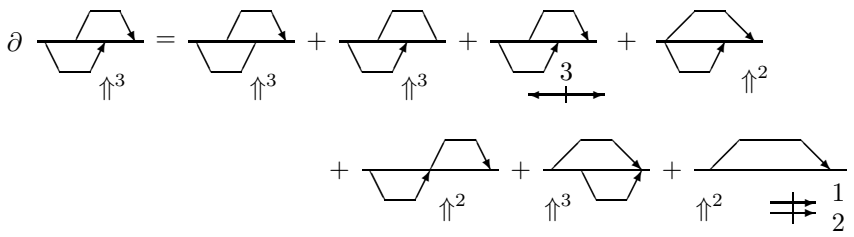

(149)

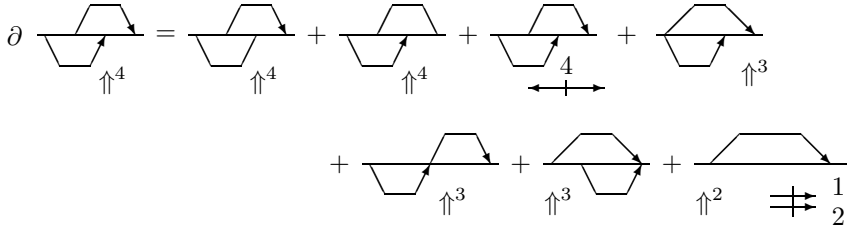

(150)

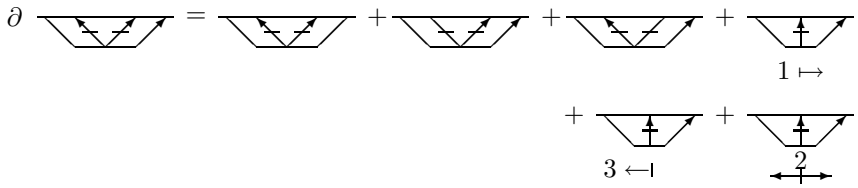

(151)

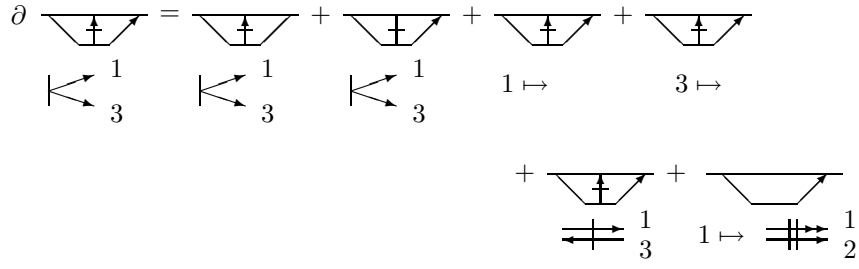

(152)

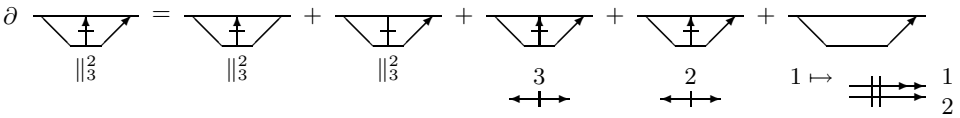

Proposition 27. *The sum of the right-hand sides of fifteen equalities* (138)–(152) *is equal to the chain* $d^3(v_3)$*, i.e., to the sum of projections to* Σ *of subalgebraic chains in* σ_1 *encoded in the left-hand sides of equalities* (101)–(127) *and* (135)–(137)*.*

Theorem 2 follows immediately from this proposition, because formula (49) consists of pictures given in the left-hand sides of these fifteen equalities.

Proof of Proposition 27. All these projections participate in the right-hand sides of formulas (138)–(152). Namely, for any a equal to one of the numbers 101, ..., 127 or 135, 136, 137, let us denote by $[a]$ the $\mathcal{B}$-block in Σ obtained by projecting the $\mathcal{F}$-block in σ_1

encoded in the left-hand part of the equality (a). Then we have

$$
\begin{array}{llll}
(138;1)=[103], & (138;2)=[101], & (138;3)=[102], & (139;1)=[106],\\
(139;2)=[105], & (139;3)=[104], & (140;1)=[108], & (140;2)=[107],\\
(140;3)=[109], & (141;2)=[110], & (141;3)=[111], & (142;1)=[112],\\
(142;2)=[113], & (143;1)=[114], & (143;2)=[115], & (144;1)=[116],\\
(144;3)=[117], & (145;1)=[118], & (145;2)=[119], & (146;1)=[120],\\
(146;2)=[121], & (147;1)=[122], & (147;2)=[123], & (148;1)=[124],\\
(148;2)=[125], & (149;1)=[126], & (149;2)=[127], & (150;1)=[135],\\
(151;1)=[136], & (152;1)=[137]. & &
\end{array}
\tag{153}
$$

So we need only to prove that the sum of the remaining terms of the right-hand parts of equalities (138)–(152) is equal to zero. These terms satisfy many obvious relations, which reduce very much this sum. Namely, we have

$(138;4)+(138;5)+(139;7)=(141;1)$, $(138;6)+(139;8)+(140;4)=(145;3)$,
$(138;7)+(138;8)+(140;5)=(142;3)$, $(139;4)+(140;6)+(140;7)=(143;3)$,
$(139;5)+(139;6)+(140;8)=(144;2)$, $(141;6)+(141;7)+(143;4)=(150;3)$,
$(142;7)+(147;4)=(149;3)$, $(143;6)+(146;4)=(148;3)$, $(150;4)=(151;3)$,
$(139;9)=(146;5)$, $(140;9)=(147;5)$, $(141;5)=(143;5)$, $(141;4)=(146;3)$,
$(142;6)=(144;6)$, $(143;8)=(144;8)$, $(143;9)=(147;8)$, $(144;4)=(145;4)$,
$(144;5)=(147;3)$, $(144;7)=(145;5)$, $(145;6)=(151;5)$, $(148;6)=(149;6)$,
$(148;7)=(149;7)$, $(150;6)=(152;4)$, $(151;6)=(152;5)$,
$(150;5)+(151;4)=(152;3)$, $(142;4)+(142;5)+(143;7)=(150;2)$.

The remaining summands are the following ones: $(138;9)$, $(139;10)$, $(140;10)$, $(141;8)$, $(142;8)$, $(144;9)$, $(145;7)$, $(145;8)$, $(146;6)$, $(146;7)$, $(146;8)$, $(147;6)$, $(147;7)$, $(148;4)$, $(148;5)$, $(149;4)$, $(149;5)$, $(151;2)$, $(152;2)$.

They can be combined as shown in the following four formulas (154)–(157):

(154)

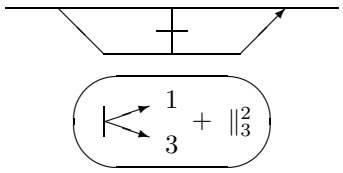

(155)

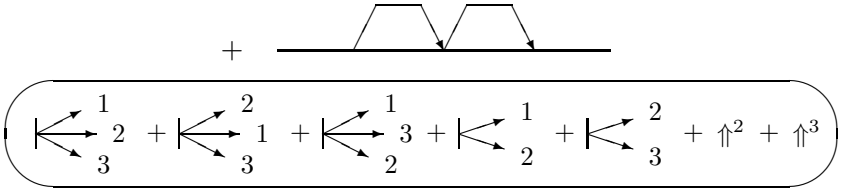

(156)

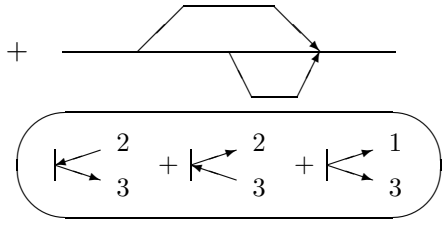

(157)

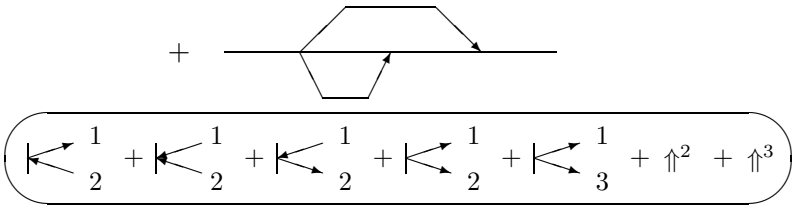

By Remark 10 on page 28, the subscripts under lines (154) and (156) define equal functions. Similarly to the direct proofs of Lemmas 7, 8, 9, it is easy to show that the expressions in subscripts under the other two lines, (155) and (157), also are equal to this subscript. But the varieties given by the main parts (without subscripts) of pictures (155)–(157) and (154) satisfy condition (34).

Proposition 27 is proved, and the proof of Theorem 2 is complete. □

7. Another algorithm

Let a knot invariant of degree k be defined by a linear combination of Polyak–Viro arrow diagrams with $\leq k$ arrows each. The weight system of this invariant can then be easily reconstructed from these diagrams: we take the part of this linear combination consisting of diagrams with exactly k arrows, forget the orientation of arrows in any of these diagrams (so that they become chord diagrams) and additionally multiply these diagrams by appropriate signs 1 or -1 (if we calculate the integer-valued invariants); see [15].

This implies an easy algebraic method of computing sums of arrow diagrams representing an invariant with a given k-weight system. Indeed, there are only $\sum_{j=0}^{k}(2j)!/j!$ arrow diagrams with $\leq k$ arrows. Consider the space of all linear combinations of these diagrams. Then we have a system of linear equations on these combinations. The first $(2k)!/(2^k k!)$ equations are, generally, nonhomogeneous and ensure that the weight system of our invariant is the given one. The remaining equations are homogeneous and reflect the fact that our linear combination actually is an invariant. Namely, we consider these arrow diagrams as $\mathcal{F}$-pictures (with all arrows expressed by oriented noncrossed broken lines; see Remark 4 on page 25) and calculate the boundaries of corresponding $\mathcal{F}$-blocks as indicated in Section 3 above (and in the future analog of this section "with integer coefficients"). Then the corresponding linear combination of these boundaries should vanish.

Goussarov's theorem implies that this system of linear equations always can be resolved.

This algorithm is more elementary than the one described in Section 4, but the systems of linear equations arising in its execution are greater (approximately by the factor 2^k).

References

[1] Bar-Natan, D. (1994–) Bibliography of Vassiliev Invariants. Web publication `http://www.math.toronto.edu/~drorbn/VasBib/index.html`

[2] Bar-Natan, D. (1995) On the Vassiliev knot invariants, *Topology*, Vol. 34, 423–472. MR1318886 (97d:57004)

[3] Birman, J. (1993) New points of view in knot theory. *Bull. AMS (N.S.)*, **28**:3, 253–287. MR1191478 (94b:57007)

[4] Budney, R., Conant, J., Scannell, K., and Sinha, D. (2003) *New perspectives of self-linking*, Web publication `math.GT/0303034`.

[5] Fiedler, T. (2001) Gauss diagram invariants for knots and links, Mathematics and its Applications, Vol. 532, Kluwer Academic Publishers, Dordrecht. MR1948012 (2003m:57031)

[6] Golubitsky, M., Guillemin, V. (1973) Stable Mappings and Their Singularities. Grad. Texts Math., vol. 14, Springer-Verlag, New York-Heidelberg-Berlin. MR0341518 (49:6269)
[7] Goresky, M. and MacPherson, R., *Stratified Morse Theory,* Springer, Berlin, 1988 MR0932724 (90d:57039)
[8] Goussarov, M., Polyak, M., and Viro, O. (2000) Finite-type invariants of classical and virtual knots, *Topology* **39**:5, 1045–1068. MR1763963 (2001i:57017)
[9] Hatcher, A., Spaces of knots, `http://math.cornell.edu/~hatcher`
[10] Kauffman, L.H. (1999) Virtual Knot Theory, *European Journal of Combinatorics,* **20**:7, 663–690. MR1721925 (2000i:57011)
[11] Kontsevich, M., Vassiliev's knot invariants, in *Adv. in Sov. Math.,* **16:2,** (1993) AMS, Providence RI, 137–150. MR1237836 (94k:57014)
[12] Lannes, J. (1993) Sur les invariants de Vassiliev de degré inférieur ou égal à 3. *L'Enseignement Mathématique* **39** (3–4), 295–316. MR1252070 (94i:57015)
[13] Merkov, A.B. (2003) Vassiliev invariants classify plane curves and doodles, *Math. Sbornik*, **194**:9-10, 1301–1330. MR2037502 (2005c:57013)
[14] Merkov, A.B. (2000) Segment–arrow diagrams and invariants of ornaments, *Mat. Sbornik*, **191**:11, 47–78. MR1827512 (2001m:57013)
[15] Polyak, M. and Viro, O. (1994) Gauss diagram formulas for Vassiliev invariants, *Internat. Math. Res. Notes* **11**, 445–453. MR1316972 (95k:57012)
[16] Tyurina, S.D. (1999) On the Lannes and Viro-Polyak type formulas for finite type invariants, *Matem. Zametki* **66:**4, 635–640; Engl. transl. in Math. Notes, **66**, No.3–4, 525–530. MR1747094 (2001b:57031)
[17] Vassiliev, V.A. (1990) Cohomology of knot spaces, in: *Theory of Singularities and its Applications* (V. I. Arnold, ed.), Advances in Soviet Math. Vol. 1, 23–69 (AMS, Providence, RI). MR1089670 (92a:57016)
[18] Vassiliev, V.A. (1999) Topological order complexes and resolutions of discriminant sets, *Publications de l'Institut Mathématique Belgrade, Nouvelle série* **66(80)**, 165–185. MR1765045 (2002f:55040)
[19] Vassiliev, V.A., Complexes of connected graphs, in: L. Corvin, I. Gel′fand, J. Lepovsky (eds.), *The I. M. Gel′fands mathematical seminars 1990–1992,* 1993, Birkhäuser, Basel, 223–235. MR1247293 (94h:55032)
[20] Vassiliev, V.A. (1994) *Complements of discriminants of smooth maps: topology and applications, Revised ed.*, Translations of Math. Monographs 98, AMS, Providence, RI. MR1168473 (94i:57020)
[21] Vassiliev, V.A. (1997) *Topology of complements of discriminants,* FAZIS, Moscow. (Russian) MR1642095 (99m:57011)
[22] Vassiliev, V.A. (1999) Homology of i-connected graphs and invariants of knots, plane arrangements, etc. *Proc. of the Arnoldfest Conference, Fields Inst. Communications*, Vol. **24**, AMS, Providence, RI, pp. 451–469. MR1733588 (2000j:57005)
[23] Vassiliev, V.A. (1993) *Lagrange and Legendre Characteristic classes,* 2nd edition. Gordon and Breach Publ., New York, 265 pp. MR1065996 (91k:57034)
[24] Vassiliev, V.A. (2001) On combinatorial formulas for cohomology of spaces of knots, *Moscow Math. J.* **1**:1, 91–123. MR1852936 (2002g:55028)
[25] Vassiliev V.A. (2001) Homology of spaces of knots in any dimensions. Philos. Transact. of the London Royal Society, **359**:1784, 1343–1364 (Proceedings of the Discussion Meeting of the London Royal Society "Topological Methods in the Physical Sciences"). MR1853624 (2002g:55029)
[26] Vassiliev V.A. (2001) Topology of plane arrangements and their complements, *Russian Math. Surveys*, **56**:2, 167–203. MR1859709 (2002g:55030)
[27] Vassiliev, V.A., Combinatorial formulas for cohomology of spaces of knots, in: Advances in Topological Quantum Field Theory (J. Bryden, ed.), Kluwer, Dordrecht, 2004, MR2147414
[28] Ziegler, G.M., Živaljević, R.T. (1993) Homotopy types of subspace arrangements via diagrams of spaces. *Math. Ann.*, **295**, 527–548. MR1204836 (94c:55018)

Index

Steklov Mathematical Institute and Poncelet Laboratory (UMI 2615 of CNRS and Independent University of Moscow)

Translated by THE AUTHOR